

LOCAL – URBAN SCALE STUDIES SESSIONS

FLOW AROUND STRUCTURES

Vladimír Fuka, Josef Brechler - Department of Meteorology and Environment Protection, Faculty of Mathematics and Physics, Charles University Prague, V Holesovickach 2, 180 00 Prague 8, Czech Republic

ANALYSIS OF CFD AND GAUSSIAN-TYPE MODEL SIMULATIONS OF FLOW AND POLLUTANT DISPERSION IN VARIOUS URBAN CONFIGURATIONS

Silvana Di Sabatino¹, Riccardo Buccolieri¹, Beatrice Pulvirenti² and Rex Britter³ - ¹Dipartimento di Scienza dei Materiali, University of Lecce, Italy, ²Dipartimento di Ingegneria Energetica, Nucleare e del Controllo Ambientale, University of Bologna, Italy, ³Department of Engineering, University of Cambridge, U.K.

VALIDATION OF OML, AERMOD/PRIME AND MISKAM USING THE THOMPSON WIND TUNNEL DATA SET FOR SIMPLE STACK-BUILDING CONFIGURATIONS

Helge Rørdam Olesen, Ruwim Berkowicz, Matthias Ketzler, Per Løfstrøm - National Environmental Research Institute, Aarhus University, Denmark.

THREE-DIMENSIONAL SIMULATIONS OF POLLUTANTS ATMOSPHERIC DISPERSION AROUND THE BUILDINGS OF INDUSTRIAL SITES AND URBAN AREAS COMPARISON OF MERCURE CFD APPROACH WITH MICRO-SWIFT-SPRAY SIMPLIFIED APPROACH

Patrick ARMAND¹, Julien COMMANAY², Maxime NIBART², Armand ALBERGEL², Pascal ACHIM¹ - ¹ Commissariat à l'Énergie Atomique, Département Analyse, Surveillance, Environnement – Service Radioanalyse, Chimie, Environnement, 91 680 Bruyères-le-Châtel – France, ² ARIA Technologies – 8-10, rue de la Ferme – 92 100 Boulogne-Billancourt – France

THE MODELLING OF THE VEHICULAR EXHAUST PLUMES IN A ROADSIDE ENVIRONMENT, BY COUPLING A DISPERSION MODEL AND AN AEROSOL PROCESS MODEL

Pohjola M A¹, Pirjola L^{2,3}, Kukkonen J¹, Karppinen A¹, Härkönen J¹, Ketzler M⁴, Kulmala, M³ - ¹ Finnish Meteorological Institute, Air Quality Research, Helsinki, FI-00101, Finland, ² Helsinki Polytechnic, Department of Technology, P.O. Box 4020, FIN-00099 Helsinki, Finland, ³ University of Helsinki, Department of Physical Sciences, P.O. Box 64, FI-00014 Helsinki, Finland, ⁴ National Environmental Research Institute, Department of Atmospheric Environment, Frederiksborgvej 399, DK-4000 Roskilde, Denmark

SIMULATIONS OF THE DISPERSION OF REACTIVE POLLUTANTS IN A STREET CANYON, CONSIDERING DIFFERENT CHEMICAL MECHANISMS AND MICROMIXING.

A. Garmory, I. S. Kim, R. E. Britter and E. Mastorakos - Hopkinson Laboratory, Department of Engineering, University of Cambridge, UK

AN APPLICATION OF THE THERMO-RADIATIVE SOLENE MODEL FOR THE EVALUATION OF STREET CANYON ENERGY BALANCE

Marcin Idczak^(1,2), Dominique Groleau⁽³⁾, Patrice Mestayer⁽¹⁾, Jean-Michel Rosant⁽¹⁾, Jean-Francois Sini⁽¹⁾ - ¹Laboratoire de Mécanique des Fluides, UMR 6598 CNRS, Ecole Centrale de Nantes, Nantes, France, ²Institute of Heating and Ventilation, Warsaw University of Technology, Warsaw, Poland, ³CERMA, UMR 1563, Ecole Nationale Supérieure d'Architecture de Nantes, Nantes, France

COMPUTATIONAL SIMULATION OF THE RESIDENCE OF AIRBORNE POLLUTANTS IN THE WAKE OF A 3-DIMENSIONAL CUBE

I. Mavroidis¹, S. Andronopoulos² and J.G. Bartzis^{2,3} - ¹ Hellenic Open University, Patras Greece, ² Environmental Research Laboratory/INT-RP, NCSR Demokritos, 15310 Aghia Paraskevi Attikis, Greece ³ University of Western Macedonia, Dept. of Engineering and Management of Energy Resources, Bakola & Sialvera Str., 50100, Kozani, Greece

A POTENTIAL RISKS IN INDUSTRIAL SITES – WIND TUNNEL STUDY

Z. Janour¹, K. Bezpalcova¹, M. Yassin¹, K. Brych², F. Ditttr², F. Ditttrich³ - ¹Institute of Thermomechanics AS CR, Prague +420266053273, ²Institute of Hydrodynamics, ³Regional Authority of the Pardubice Region

AIR QUALITY AT THE AIRPORT BUDAPEST AND INVERSE DISPERSION MODELLING TO DETERMINE THE STRENGTH OF DIFFERENT EMISSION SOURCES

Klaus Schäfer, Gregor Schürmann, Carsten Jahn, Herbert Hoffmann, Stefan Emeis - Forschungszentrum Karlsruhe GmbH, Institut für Meteorologie und Klimaforschung, Atmosphärische Umweltforschung
Kreuzeckbahnstr. 19, D-82467 Garmisch-Partenkirchen

RELEASE AND DISPERSION OF HARMFUL GAS MODELLING INSIDE THE UABL

Klára Bezpalcová¹, Karel Klouda², Zbyněk Jaňour¹ - ¹Institute of Thermomechanics, Academy of Sciences of the Czech Republic, Prague, ² Czech State Office for Nuclear Safety, Prague

TREES IN URBAN STREET CANYONS AND THEIR IMPACT ON THE DISPERSION OF AUTOMOBILE EXHAUSTS

Christof Gromke, Bodo Ruck - Laboratory of Building- and Environmental Aerodynamics
Institute for Hydromechanics, University of Karlsruhe, Germany

SIMULATION OF GRAVITY WAVES AND MODEL VALIDATION TO LABORATORY EXPERIMENTS

Norbert Rácz¹, Gergely Kristóf¹, Tamás Weidinger², Miklós Balogh¹ - ¹ Department of Fluid Mechanics, Budapest University of Technology and Economics, ² Department of Meteorology, Eötvös Loránd University

NUMERICAL OF STUDY OF THE WIND FLOW AND THE DISPERSION OF TRAFFIC EMITTED POLLUTION WITH RANS CFD IN THE SIR JOHN CASS PRIMARY SCHOOL AREA IN CENTRAL LONDON

F. Barmpas¹, N. Moussiopoulos¹, I. Ossanlis¹ and R. Colville² - ¹ Aristotle University of Thessaloniki, Laboratory of Heat transfer and Environmental Engineering, Box 483, Aristotle University, Gr-54124, Thessaloniki, Greece, ² Imperial London College Consultants 47 Prince's Gate, Exhibition Road London SW7 2QA, UK

EVALUATION AND INTER-COMPARISON OF OPEN ROAD LINE SOURCE MODELS CURRENTLY BEING USED IN THE NORDIC COUNTRIES: A NORPAC PROJECT

Janne Berger^a, Sam-Erik Walker^a, Bruce Denby^a, Per Løfstrøm^b, Matthias Ketzler^b, Ruwim Berkowicz^b - ^aNorwegian Institute for Air Research (NILU) P.O. BOX 100, 2027 Kjeller, Norway; ^bNational Environmental Research Institute (NERI)

CFD ANALYSIS OF WIND FLOW FIELD FOR EVALUATING NO₂, NO, AND OZONE VERTICAL DISTRIBUTION INSIDE A STREET-CANYON

Costabile, F., Sinesi, M. and Allegrini, I. - Institute for atmospheric pollution, National Research Council, Via Salaria km 29,300 C.P. 10, 00016 Monterotondo Stazione, Rome, Italy

REFINEMENT AND STATISTICAL EVALUATION OF A MODELLING SYSTEM FOR PREDICTING FINE PARTICLE CONCENTRATIONS IN URBAN AREAS

Kauhaniemi M (1), Karppinen A (1), Härkönen J (1), Kousa A (2), Koskentalo T (2), Aarnio P (2), and Kukkonen J (1) – (1) Finnish Meteorological Institute (FMI), Helsinki, Finland, (2) Helsinki Metropolitan Area Council (YTV), Helsinki, Finland

FLUID FLOW AND POLLUTANT DISPERSION WITHIN TWO-DIMENSIONAL STREET CANYONS – EVALUATION OF VARIOUS TURBULENCE MODELS AGAINST EXPERIMENTAL DATA

N. Koutsourakis¹, J. G. Bartzis², N. C. Markatos³ - ¹ Environmental Research Laboratory, Institute of Nuclear Technology-Radiation Protection, National Centre for Scientific Research 'Demokritos', Aghia Paraskevi 15310, Greece, ² Environmental Technology Laboratory, Department of Management and Engineering of Energy Resources, University of West Macedonia, Kastorias and Fleming Str., Kozani 50100, Greece, ³ Computational Fluid Dynamics Unit, School of Chemical Engineering, National Technical University of Athens, 9 Iroon Polytechniou Str., Zografou Campus, Athens 15780, Greece

ADAPTATION OF PRESSURE BASED CFD SOLVERS TO URBAN HEAT ISLAND CONVECTION PROBLEM

Gergely Kristóf, Norbert Rácz, Miklós Balogh - Department of Fluid Mechanics, Budapest University of Technology and Economics, Budapest, Hungary

COMPARISON OF HOURLY AVERAGE CO CONCENTRATION FROM MONITORING AND CFD MODELLING IN A DEEP STREET CANYON

F. Murena and G. Favale - Dipartimento di Ingegneria Chimica - Università degli studi di Napoli "Federico II"

A MEASUREMENT CAMPAIGN IN A STREET CANYON IN HELSINKI AND COMPARISON OF RESULTS WITH PREDICTIONS OF THE CFD MODEL ADREA-HF

P. Neofytou^a, M. Haakana^b, A. Venetsanos^a, A. Kousa^c, J. Bartzis^a, J. Kukkonen^b - ^aEnvironmental Research Lab., INT-RP, NCSR Demokritos, Aghia Paraskevi, 15310 Athens, Greece, ^bFinnish Meteorological Institute, Air Quality Research, Erik Palmenin aukio 1, P.O.Box 503, FI-00101 Helsinki, Finland, ^cHelsinki Metropolitan Area Council, Opastinsilta 6 A, FIN-00520 Helsinki, Finland

LOCAL SCALE NUMERICAL SIMULATION OF AN EXTREME SO₂ POLLUTION EPISODE IN BULGARIA

Prodanova M.¹⁾, Perez J.²⁾, Syrakov D.¹⁾, San Jose R.²⁾, Ganev K.³⁾, Miloshev N.³⁾ - ¹⁾ National Institute of Meteorology and Hydrology, Bulgarian Academy of Sciences, Sofia 1784, Bulgaria, ²⁾ Technical University of Madrid, Computer Science School, 28660 Madrid, Spain, ³⁾ Geophysical Institute, Bulgarian Academy of Sciences, Sofia 1111, Bulgaria

FLOW AROUND STRUCTURES

Vladimír Fuka, Josef Brechler

Department of Meteorology and Environment Protection, Faculty of Mathematics and Physics, Charles
University Prague, V Holesovickach 2, 180 00 Prague 8, Czech Republic

ABSTRACT

This paper describes the first steps of the creation of a mathematic model for describing air flow in complex geometry areas (urban areas) and results of some test experiments. At this stage the model deals with the 2D laminar incompressible flow inside cavity or around square obstacle. All methods used in the model construction allow straightforward extension to 3D problems.

1. INTRODUCTION

In this paper the newly created model of air-flow within the complicated geometry areas (e.g. urban areas) is presented. In the mentioned model all the approaches that could result in the description of air-flow that will be as exact as possible have been used. For the spatial discretization finite volume method has been applied together with the Godunov's approach (Godunov, 1959) used for the advection part of model equations. A MUSCL type of reconstruction (van Leer, 1979) is used for dependent variables together with the TVD (total variation diminishing) temporal integration scheme. For the implementation of the geometrically complicated lower boundary condition so called immersed boundary method (hereinafter abbreviated as ImBM, see Peskin, 1982) has been implemented. At this moment the model is tested as the laminar one without the appropriate turbulent model. The vertical temperature stratification is not thought at this moment, too.

The contribution is organized as follows. In the first part a description of the used numerical methods is given. The ImBM and its implementation are mentioned in the second part of this contribution. Some preliminary results are described in the third part of this contribution and conclusions together with outlooks dealing with the future developments of the describer basis of the model are contents of the final part.

2. NUMERICAL METHODS

Governing equations for unsteady incompressible viscous laminar and isothermal flow in the non-dimensional form can be written as

$$\frac{\partial u_i}{\partial t} + \frac{\partial u_i u_j}{\partial x_j} = -\frac{\partial p}{\partial x_i} + \frac{1}{\text{Re}} \frac{\partial^2 u_i}{\partial x_j \partial x_j} + f_i, \quad (1)$$

$$\frac{\partial u_j}{\partial x_j} - q = 0, \quad (2)$$

where $i, j = 1, 2, 3$, t is time, x_i are the Cartesian coordinates, u_i stand for flow velocity vector components, p is a pressure, f_i and q are artificial momentum and mass source terms that result from the immersed boundary method utilization (see Kim et al., 2001, for example, more details will be given in the subsequent sections), Re stands for the Reynolds number. All dependent and independent variables have been non-dimensionalized with a standard way (see Ferziger, Perić, 1997, for example). In the following text all variables are used in the non-dimensional form. As it has been mentioned earlier, at this moment the model deals with the laminar flow thus no turbulence parametrization has been used. The same statement is true for vertical temperature stratification – the impact of it is also not involved into the model equations and the stratification is supposed to be neutral.

Time-integration method used is based on the fractional step approach (see Brown et al., 2001, for example) where a pseudo-pressure is used to correct the velocity field so that the continuity equation is satisfied at each time step. This method uses the TVD Runge-Kutta 2nd order temporal scheme (see Shu, Osher, 1988) for advection terms of (1) and the Crank-Nicolson implicit scheme for viscous terms. Spatial discretization uses the staggered finite volume (FV) method (see Harlow and Welch, 1965). The whole domain is discretized using the non-equidistant Cartesian grid. In the staggered approach there is not a problem with the pressure gradient terms evaluation but the most problematic terms are the non-linear advection ones that can create non-physical wiggles in the areas where high gradients occur. The methods that prevent the creation of these wiggles or those that suppress them are the most advantageous and should be used. In this presented model we have used the Godunov type of central scheme proposed by Kurganov and Tadmor, 2000 (abbreviated as

KT hereinafter) with the piecewise linear reconstruction of the MUSCL type with the minmod slope limiter to obtain point-wise values u^+ and u^- on the sides of the adjacent finite volumes. In this kind of the scheme it is not necessary to solve the Riemann problems on the boundaries of finite volumes. The KT scheme is of the second order of accuracy and do not generate undesirable oscillations and wiggles in the high gradient areas.

3. IMMERSSED BOUNDARY METHOD

A possible method how a geometrically complicated lower boundary can be implemented into a model deals with application of so-called body fitted grid. This approach is frequently used but on the other hand it uses a quite complicated method of the grid generation and, moreover, if the grid is heavily distorted the order of the spatial accuracy of the used numerical method can decrease. A quite effective way how to remedy this problem is brought with the utilization of so called immersed boundary method – ImBM.

The ImBM was firstly used by Peskin, 1982 when modelled the blood flow in a human body vascular system and heart valves. The ImBM enables to use the regular orthogonal structured grid (e.g. Cartesian) even in very complicated shapes with walls moving with the velocity that differs from that of the fluid flow. There exist several methods how to implement the immersed boundary methodology into the models, in the model presented in this contribution the one described with Kim et al., 2001 has been used.

4. SOME PRELIMINARY RESULTS

As it has been mentioned in the introductory part of this contribution at this stage the presented results deal with very beginning of the constructed urban air-flow model. From some reasons (less demand on memory, less processor-time consumption) at this stage the 2D approach has been chosen - the transition to the full 3D computation is straightforward and for validation of methods used the 2D approach is sufficient enough.

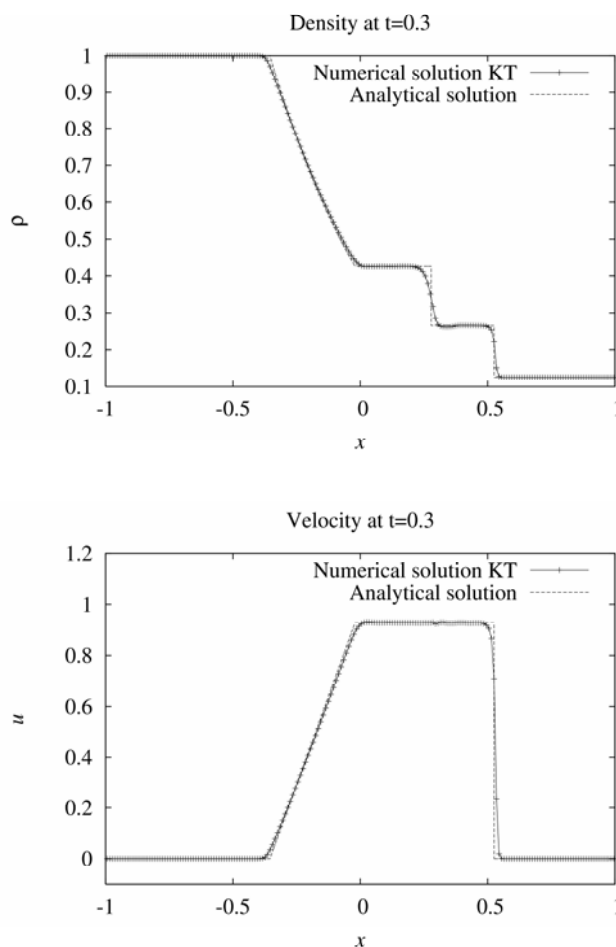


Fig.1 Sod problem compar. of analytic and numerical solution.

A standard test problem – so called Sod problem, was used to test the properties of the used KT scheme and comparison of this test results are shown on the subsequent Fig.1. For this problem an analytical solution is known and can be compared with the numerical one.

The next test problem deals with the evolution of boundary layer above a flat plate. Also in this case the analytical solution (the Blasius' solution) is known and can be compared with the numerical one.

A problem called lid driven cavity flow can be used as an example of the simplest urban canyon circulation. There are several well described results of this situation – see, for example, Ghia et al., 1982, Erturk et al., 2005.

The cavity circulation structure depends on Reynolds number $Re = UD/\nu$ of the problem where U is the upper lid dimensional velocity and D is the cavity size (in the case of the square cavity it is the length of the cavity side). The structure of circulation consists from primary vortex and, depending on the value of Re , from the secondary and tertiary vortices (when the Re is high enough). The circulation patterns are showed on the Figs. 2 ($Re = 100$) and 3

($Re = 5000$). The velocity on the upper boundary is directed from the left. In the both lower corner the secondary vortices can be seen in this case with Re being equal to 100. When the value of Re increases the axis of the primary vortex moves close to the centre of the square and in both lower corners secondary vortices intensify and tertiary vortices appear. Another secondary vortex appears on the upper right corner.

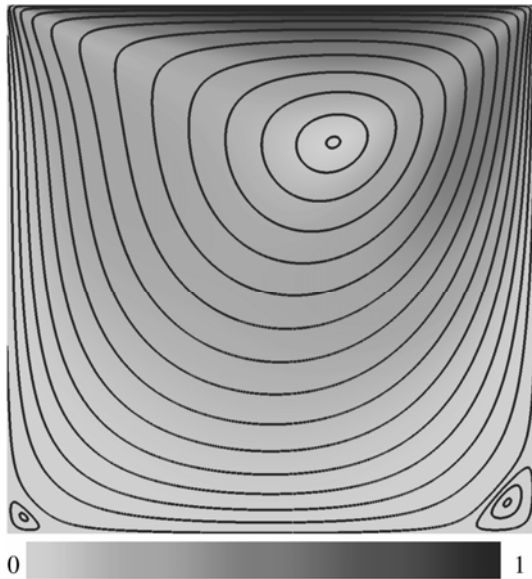


Fig.2 Cavity circulation $Re = 100$.

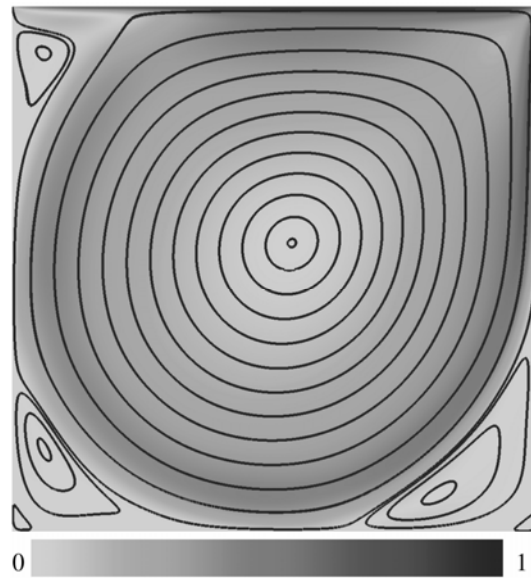


Fig.3 Cavity circulation $Re = 5000$.

Resulting flow in a cross sectional plane perpendicular to the axis of an infinitely long square cylinder is showed in this paragraph. Geometry of the problem is schematically shown on the following Fig.4. A letter H denotes the width of the area, d is the projection of the square on the plane perpendicular to the incoming flow and α is an angle of the cylinder orientation with respect to the incoming flow, L is a length of the computational domain.

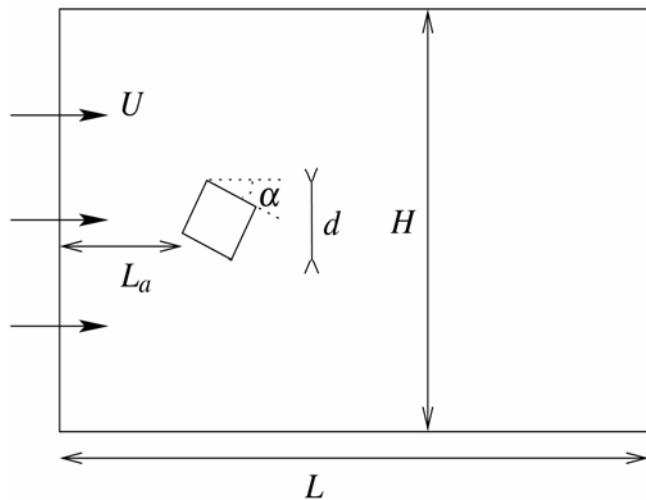


Fig.4 Geometry of the flow around square cylinder.

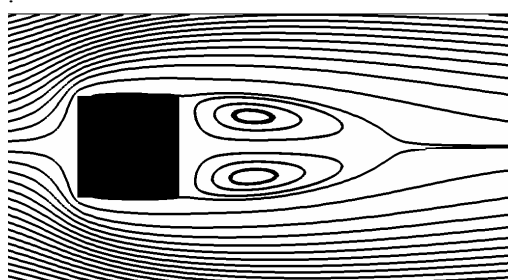


Fig.5 Flow with $Re = 30$ and $\alpha = 0^\circ$.

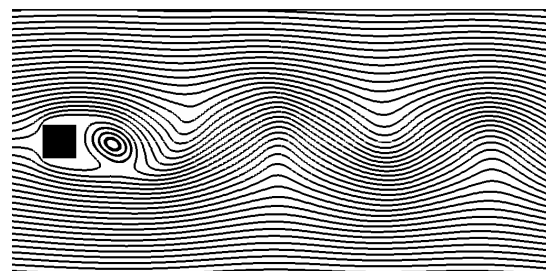


Fig.6 Flow with $Re = 200$ and $\alpha = 0^\circ$.

et al.,2003). When the value of Re is greater than 300 the flow becomes turbulent.

Flow patterns for Reynolds numbers equal to 30 and 200 and square orientation characterized with α being equal to 0° and 45° are shown on the following Figs.5 – 8. Lines are flow field streamlines. In a lower Re value a stationary recirculation zones exist in the wake of the square, when Re equals 200 the von Kármán vortex street generation in the wake of square can be seen.

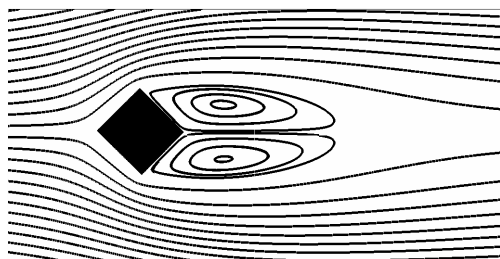


Fig.7 Flow with $Re = 30$ and $\alpha = 45^\circ$.

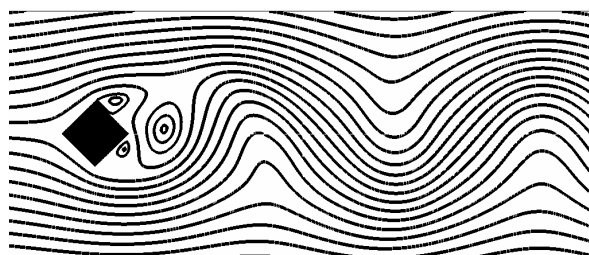


Fig.8 Flow with $Re = 200$ and $\alpha = 45^\circ$.

5. CONCLUDING REMARKS AND FUTURE OUTLOOK

This contribution shows some preliminary results of a new model of fluid flow in complex geometry (urban) areas. At this moment the 2D approach has been chosen because of time consumption limitation. But also in the 2D approach it was possible to compare the obtained results with those published earlier. The extension to full 3D approach is straightforward. The obtained results seem very promising and we will continue in creation of the presented model using the mentioned high resolution methods. In the close future the two steps are necessary to perform: The first one is to find out some more efficient pressure correction solver and to go over to the full 3D system. The second one deals with the parametrization of turbulence. It will be necessary to apply some efficient turbulence model for the case characterized with the higher values of the Reynolds number. And then also the vertical thermal stratification will be necessary to implement into the equations as now the fluid is supposed to be neutrally stratified.

6. ACKNOWLEDGEMENTS

This research has been supported by the Grant Agency of the Czech Academy of Sciences, grant no. T400300414 and by the Grant Agency of the Czech Republic, grant no. 205/06/0727.

7. REFERENCES

- Brown, D. L., Cortez, R. and Minion, M. L. (2001) Accurate Projection Methods for the Incompressible Navier-Stokes Equations. *J. Comput. Phys.*, 168: 464–499.
- Erturk, E., Corke, T. C. and Gökçöl, C. (2005) Numerical Solutions of 2-D Steady Incompressible Driven Cavity Flow at High Reynolds Numbers. *Internat. J. Numer. Methods Fluids* 48: 747–774.
- Ferziger, J. H. and Perić, M. (1997) *Computational Methods for Fluid Dynamics*. Springer Verlag, Berlin.
- Ghia, U., Ghia, K. N. and Shin, C. T. (1982) High-Re Solutions for Incompressible Flow Using the Navier-Stokes Equations and a Multigrid Method. *J. Comput. Phys.* 48: 387–411.
- Godunov, S. K. (1959) Finite difference method for numerical computation of discontinuous solutions of the equations of fluid dynamics. *Mat. Sb.* 47: 271–306.
- Harlow, F. H and E., Welch J. (1965) Numerical calculation of time-dependent viscous incompressible flow of fluid with a free surface. *Phys. Fluids* 8: 2182–2189.
- Kim, J., Kim, D. and Choi, H. (2001) An Immersed-Boundary Finite-Volume Method for Simulations of Flow in Complex Geometries. *J. Comput. Phys.* 171: 132–150.
- Kurganov, A. and Tadmor, E. (2000) New High-Resolution Central Schemes for Nonlinear Conservation Laws and Convection-Diffusion Equations. *J. Comput. Phys.*, 160: 241–282.
- Peskin, C. S. (1982) The fluid dynamics of heart valves: Experimental, theoretical, and computational methods. *Annu. Rev. Fluid Mech.* 14: 235–259.
- Saha, A. K., Biswas, G. and Muralidhar, K. (2003) Three-dimensional study of flow past a square cylinder at low Reynolds numbers. *Int. J. Heat Fluid Flow* 24: 54–66.
- Shu, C.-W., Osher, S. (1988) Efficient Implementation of Essentially Non-oscillatory Shock-Capturing Schemes. *J. Comput. Phys.* 77: 439–471.
- van Leer, B. (1979) Towards the Ultimate Conservative Difference Scheme V. A Second-Order Sequel to Godunov's Method. *J. Comput. Phys.* 32: 101–136.

ANALYSIS OF CFD AND GAUSSIAN-TYPE MODEL SIMULATIONS OF FLOW AND POLLUTANT DISPERSION IN VARIOUS URBAN CONFIGURATIONS

Silvana Di Sabatino^{1*}, Riccardo Buccolieri¹, Beatrice Pulvirenti² and Rex Britter³

¹*Dipartimento di Scienza dei Materiali, University of Lecce, Italy*

²*Dipartimento di Ingegneria Energetica, Nucleare e del Controllo Ambientale, University of Bologna, Italy*

³*Department of Engineering, University of Cambridge, U.K.*

*Corresponding author: +39 0832 297 086 - silvana.disabatino@unile.it

Abstract

The study of the effect of obstacles on flow and dispersion in the atmospheric boundary layer is one of the most important topics in dispersion research of airborne material. Computational Fluid Dynamics (CFD) methods are increasingly used to predict concentration fields near buildings in an operational context, but extensive validations are still needed. Gaussian-type modelling still is the most used tool for the prediction of pollutant concentration in urban areas. In this paper, we analyse the effect on flow and dispersion due to the presence of isolated buildings and buildings arrays placed in the atmospheric boundary layer. We compare CFD numerical simulations provided by FLUENT with wind tunnel data sets (Wang and McNamara, 2006) and with predictions from the well validated Gaussian-type model ADMS-Urban.

1. INTRODUCTION

Dispersion of pollutants in urban areas is directly affected by building arrangements. The prediction of ground-level pollutant concentrations in those areas is important for the assessment of the impact of existing sources on people health and the environment but also for the evaluation of future source scenarios on air quality. In recent years, Computational Fluid Dynamics (CFD) has become a useful tool to study atmospheric dispersion from accidental explosions, routine emissions from human activities or from the release of biological agents associated with accidents and deliberate actions. The present work is part of our current research devoted to the study of the effect of obstacles on flow and dispersion in the real urban environment using both CFD and integral-type models. During our research experience, we have compared predictions from the commercial code FLUENT with wind tunnel data and results from the commercial atmospheric dispersion model ADMS-Urban. We have investigated in some details flow and dispersion from point and line sources in different configurations from the simplest boundary layer to isolated street canyons (Di Sabatino et al., 2006, in press) and small groups of buildings (Di Sabatino et al. 2006). In particular we have found that the standard $k-\varepsilon$ model within FLUENT reproduces well the flow pattern in street canyons with the standard choice of variables. FLUENT dispersion predictions in street canyons tend to overestimate both wind tunnel measurements and ADMS-Urban concentration results. Thus, CFD calculations may require a lower turbulent Schmidt number (Sc_t) to increase plume dispersion. In this paper we extend the analysis to the effect on dispersion due to the presence of isolated buildings and buildings arrays, comparing the two models with a different wind tunnel data set (Wang and McNamara, 2006). Our broad aim being that of suggesting a best practise approach for two widely used commercial codes of different nature when applied to urban air quality.

2. METHODOLOGY

2.1 Description of wind tunnel experiments

Measurements used for our simulations refer to wind tunnel experiments (Wang and McNamara, 2006) with a boundary layer with a surface roughness $z_0=1.27$ mm and exponent of the power-law velocity profile of 0.256. The cases investigated were emissions from a point source around, above and within isolated buildings with different aspect ratios, a regular building array (with plan density of 25%) and an urban intersection with orthogonal layout. Details are summarized in Table 1. The reference wind velocity U_{ref} was 2.66 m/s at the reference height $H_{ref}=0.1$ m. The friction velocity u_* was 0.245 m/s. Passive ethane emission rate was set at 0.3 l/min for both the isolated building cases and the urban intersection case, and 0.6 l/min for the regular building array case. Measured mean concentrations are expressed as dimensionless values K which are defined as:

$$K = \frac{CU_{ref}H_{ref}^2}{Q}$$

where Q is the emission rate and C is the measured concentration.

Table 1. Summary of the simulations following Wang and McNamara (2006) wind tunnel experiments. H , W and L are the building height, width and length, respectively. $H = 0.3$ for case 4 and $H = 0.1$ for all other cases

CASE	MODEL DETAILS	SOURCE DETAILS	
1	Cube	The stack, $0.5H$ high, was installed at an upwind distance of $2H$ from the building	
2	$W/H=2, L/H=1$		
3	$W/H=1, L/H=2$		
4	$W/H=1/3, L/H=1/3$		
5	$W/H=6, L/H=1$		
6	5 by 5 regular building array	Plan density 25%	Same as above
7	Urban intersection	Four orthogonal street segments, each street segment was $5H$ long and $1H$ wide	Ground-level source, $0.1H$ high, was located at the centreline of the upwind street at $1H$ from the edge of the intersection

2.2 FLUENT flow setup

Simulations are carried out by considering a neutral boundary layer. The size of the computational domain used to simulate the boundary layer is 3.4 m by 1.9 m in the horizontal plane and 1.2 m in the vertical direction. The number of computational hexahedral cells used is about 1,000,000 for building array and urban intersection cases and 500,000 for the other cases. The smallest dimensions of the elements are equal to 0.005 m while they are about 0.025 m outside. Several grid tests were performed to ensure the independence of the solution from the grid. The standard $k-\epsilon$ model is used. Based on wind tunnel experiments the inlet wind speed is assumed to follow a power law profile with height z :

$$\frac{U(z)}{U_{ref}} = \left(\frac{z}{z_{ref}} \right)^p$$

where $U(z)$ is the average wind speed at the height z above the ground, U_{ref} the reference wind speed at the reference height z_{ref} and p is the vertical wind profile exponent. Turbulent kinetic energy and dissipation rate profiles are specified as follows:

$$k = \frac{u_*^2}{\sqrt{C_\mu}} \left(1 - \frac{z}{\delta} \right) \quad \text{and} \quad \epsilon = \frac{u_*^3}{\kappa z} \left(1 - \frac{z}{\delta} \right)$$

where δ is the boundary layer height, $C_\mu = 0.09$ is a coefficient used to define the eddy viscosity in $k-\epsilon$ models, u_* is the friction velocity and κ the von Karman's constant. The remaining boundary conditions (surface roughness representation, symmetry conditions etc.) are those specified in Di Sabatino et al. (in press).

2.3 FLUENT dispersion setup

For dispersion simulations we use the advection-diffusion (AD) module. In turbulent flows, FLUENT computes the mass diffusion which satisfies the conservation of mass as follows:

$$J = - \left(\rho D + \frac{\mu_t}{Sc_t} \right) \nabla Y$$

where D is the diffusion coefficient for ethane in the mixture, $\mu_t = 1/2(C_\mu k^2/\epsilon)$ is the turbulent viscosity, Y is the mass fraction of ethane, ρ is the mixture density. $Sc_t = \mu_t/(1/2D_t)$ is the turbulent Schmidt number, where D_t is the turbulent diffusivity. The sources have been simulated by separating a volume in the geometry at the required discharge position and by setting ethane source terms for this volume.

2.4 ADMS-Urban setup

ADMS-Urban is used to simulate Case6. The same ethane emission rate is considered. To model this case we do not explicitly model the individual buildings, but we replace the area with a single value of surface roughness. We use the same z_0 as in wind tunnel experiments in the area outside the array of buildings and $z_0 = 0.012$ m in the area occupied by the array. This value of z_0 is calculated by using the formulas proposed by Macdonald et al. (1988).

3. RESULTS AND DISCUSSIONS

We compare FLUENT results with wind tunnel data and ADMS-Urban predictions for one case. A statistical analysis is made by means of variables such as normalised mean square error (NMSE), fractional bias (FB) and correlation coefficient (R) and the Hit Rate validation test q (Schlünzen et al., 2004), using a fractional deviation $RD = 0.25$ and an absolute deviation $W = 0.06$ ($q > 66\%$ is requested for the comparison with wind tunnel data). In the figures, Profile 1 is transversal to wind direction on the ground at a distance of $0.5H$ from

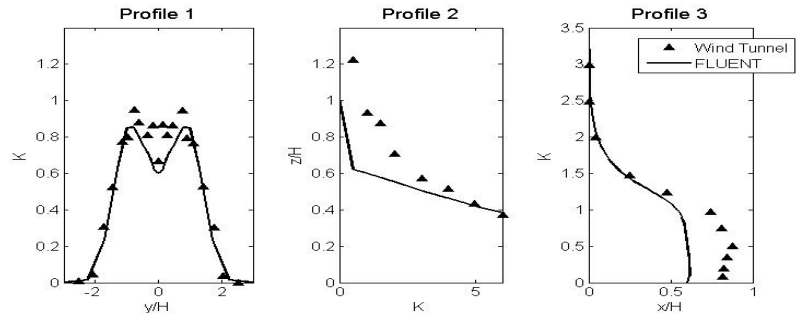
the downwind building wall; Profile 2 is along wind direction at the height of $0.5H$ starting from the downwind building wall; Profile 3 is vertical at $0.5H$ from the downwind building wall.

3.1 Dispersion around isolated buildings

Concentration profiles obtained from FLUENT predictions show a general good agreement with wind tunnel data. A summary of comparisons for all cases is discussed briefly next.

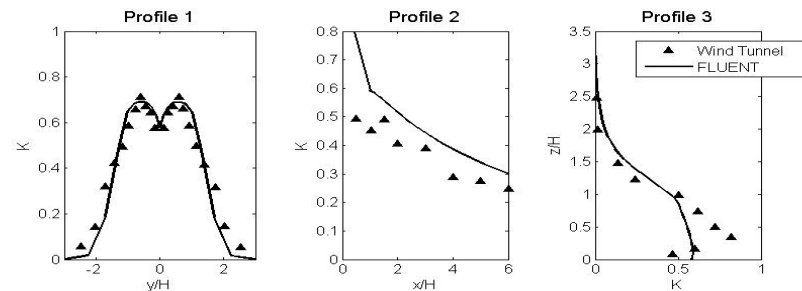
Case1. Figure 1 shows that the model under-predicts concentrations slightly. The hit rate test is $q=75\%$.

Figure 1. Concentrations profiles for Case1



Case2 (wide building) and **Case3** (long building). In these cases model predictions are in general agreement with observations from wind tunnel measurements (Figure 2). The hit rate test are $q=82\%$ (Case2) and $q=77\%$ (Case3).

Figure 2. Concentrations profiles for Case3

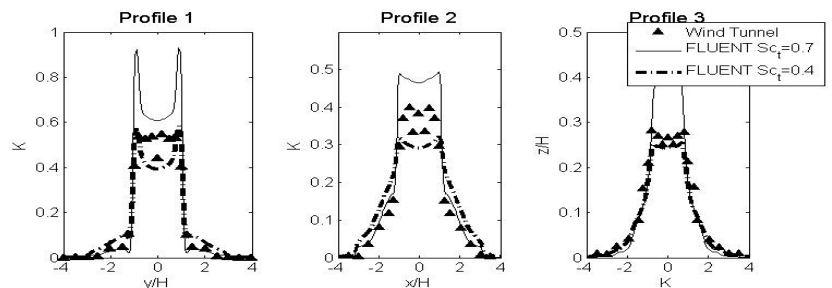


Case4 (tower-like building) and **Case5** (very wide building). Also in these cases model predictions are in general agreement with observations from wind tunnel measurements. The hit rate tests are $q=78\%$ (Case4) and $q=68\%$ (Case5).

3.2 Dispersion in a regular building array

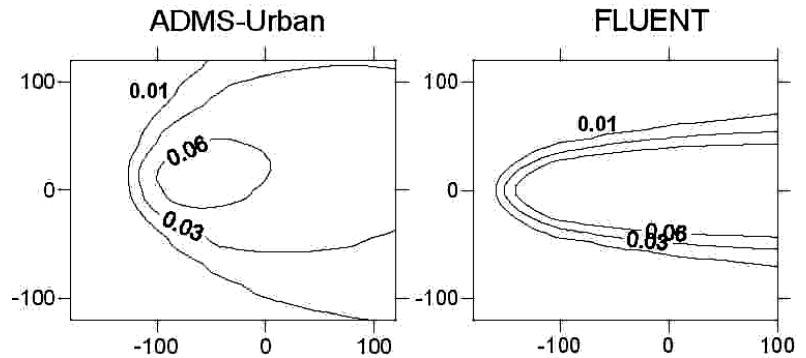
Di Sabatino et al. (2006, in press) observed that FLUENT dispersion spread from sources placed within street canyons and building arrays is smaller than that predicted by wind tunnel results and by ADMS-Urban. This is due to the lower mixing predicted within FLUENT when the simulated cases are very simple. The CFD code performs better with the standard choice of parameters for more complex building configurations. Fig. 4 shows comparison for **Case6**. Wind tunnel and FLUENT results are plotted in Figure 3 along the first three buildings rows. FLUENT results agree well with wind tunnel measurements. The hit rate test is $q=89\%$.

Figure 3. Concentrations profiles for Case6



We also analyse this case using ADMS-Urban. Figure 4 shows ADMS-Urban and FLUENT concentration contours obtained using $Sc_t = 0.4$. FLUENT plume width at $z = 1.5H$ is again smaller than the ADMS-Urban one. Even though this case is characterized by an intermediate building packing density we also need to reduce the turbulent Schmidt number.

Figure 4. Concentration contours obtained from ADMS-Urban (left) and FLUENT (right) at $z/H=1.5$ for Case6 in the area occupied by the building array



3.3 Dispersion in urban intersection

In **Case7**, FLUENT results, using $Sc_t = 0.4$, tend to under predict measured concentrations. Hit rate test is fulfilled only in some positions ($q=70\%$).

5. CONCLUSIONS

In this paper we show that, with the methodology set up in our previous works, dispersion within simple geometries such as single block buildings, street intersections and arrays of buildings, can be modelled with the CFD code FLUENT with a certain degree of reliability. Our previous results pointed out that, besides the correct choice of grid refinement near obstacles, it is important to modify some parameters such as the turbulent Schmidt number to adequately simulate dispersion within canyons. The novel aspects of this paper are, firstly, the validation of the CFD code in non-cubical buildings, secondly, the verification of the validity of general simulation criteria found for the simplest configurations in more complex conditions. We found that for dispersion within building arrays with buildings of different aspect ratios, similar criteria for grid refinement and parameters used for the single building and street canyons cases, can be adopted. For example, a grid independence solution can be obtained with a grid dimension close to the building equal to $0.06 H$. The comparison of FLUENT results with ADMS-Urban ones shows that there is a better agreement between the two models when reducing Sc_t in the CFD simulations. Averaged concentration results from ADMS-Urban compare fairly well with FLUENT in presence of arrays of building by using a surface roughness equivalent within ADMS-Urban.

6. REFERENCES

- CERC 2006. ADMS-Urban, USER Guide. Available from Cambridge Environmental Research Consultants, Cambridge, UK.
- Di Sabatino, S., Buccolieri, R., Pulvirenti, B., Britter, R. 2006. Application and validation of FLUENT flow and dispersion modelling within complex geometries. Proc. 28th NATO/CCMS International Technical Meeting on Air Pollution Modelling and its Application. Leipzig (Germany).
- Di Sabatino, S., Buccolieri, R., Pulvirenti, B., Britter, R. in press. Flow and pollutant dispersion modelling in street canyons using Fluent and ADMS-Urban. Environmental Modelling & Assessment.
- Fluent 6.2 2005. User's Manual. <http://www.fluent.com>.
- MacDonald, R.W., Griffiths, R.F., Hall, D.J., 1998. An improved method for estimation of surface roughness of obstacle arrays. Atmospheric Environment, 32, 1857-1864.
- Neofytou, P., Venetsanos, A. G., Rafailidis, S., Bartzis, J. G. 2006. Numerical investigation of the pollution dispersion in an urban street canyon. Environmental Modelling & Software 21, 525-531.
- Schlünzen, K.H., Bächlin, W., Brünger, H., Eichhorn, J., Grawe, D., Schenk, R., Winkler, C., 2004. An evaluation guideline for the prognostic microscale wind field models. Proc. 9th International Conference on Harmonisation within Atmospheric Dispersion Modelling for Regulatory Purposes, Garmisch-Partenkirchen (Germany).
- Wang, X., McNamara, K. F. 2006. Evaluation of CFD simulation using RANS turbulence models for building effects on pollutant dispersion. Env. Fluid Mech. 6, 181-202.

VALIDATION OF OML, AERMOD/PRIME AND MISKAM USING THE THOMPSON WIND TUNNEL DATA SET FOR SIMPLE STACK-BUILDING CONFIGURATIONS

Helge Rørdsdam Olesen, Ruwim Berkowicz, Matthias Ketzel, Per Løfstrøm
National Environmental Research Institute, Aarhus University, Denmark. email: hro@dmu.dk

ABSTRACT

In 1990 a comprehensive data set on dispersion behind rectangular buildings was compiled in the US EPA wind tunnel. The data set systematically describes dispersion for a variety of building shapes, stack heights and stack locations. These data were originally used to estimate so-called Building Amplification Factor, but the potential of the data set extends much beyond this application. In a recent study we have used this data set to analyse the performance of a number of dispersion models with more or less sophisticated approaches for handling building effects. The models are the Danish OML model, the US AERMOD/PRIME model, and the German MISKAM model.

1. INTRODUCTION

The Danish OML model is a Gaussian plume model, which belongs to the same family of models as AERMOD and UK-ADMS. It is based on boundary-layer theory and not on traditional stability classification. The current standard OML model became operational for regulatory purposes in Denmark already in 1990. The model has recently been reviewed in order to introduce improvements where appropriate (Olesen et al., 2007).

The OML model is equipped with a rather simple building algorithm that allows buildings to modify dispersion only through the effect of plume height and dispersion parameters. It has been considered to replace the OML building algorithm with the PRIME algorithm, which is used by the US AERMOD model. For this reason a study was performed, where the performance of 3 models was analysed for scenarios with buildings present. The models were OML, AERMOD and - for detailed exploration of a limited number of cases - the German CFD model MISKAM.

As basis for the study we used a comprehensive data set on dispersion behind rectangular buildings that was compiled in the US EPA wind tunnel by Thompson (1993). Originally, these data were used to estimate so-called Building Amplification Factor, but the potential of the data set extends much beyond this application.

2. THOMPSON'S WIND TUNNEL DATA

The experimental database of Thompson includes measurements of ground-level centreline concentration distributions for several different combinations of building shapes, stack heights, and stack location relative to the building.

The data set includes around 250 scenarios, where the following parameters vary:

- *Building shape:* Four building geometries were considered, as well as a baseline scenario without building. The buildings were a cube and rectangular buildings with a footprint which is twice or four times the size of the cube. The wind was always perpendicular to the building face. In the present paper we show only results for the cube and the widest building (the width is four times the height).
- *Stack height:* In terms of relative stack height (stack height divided by building height), emphasis was on five values ranging from 0.5 to 3. There are some scenarios for additional stack heights.
- *Stack location:* The location of the stack varied, so there are scenarios with the stack upwind of the building, on top of the building, and downwind of the building. Altogether 17 locations were considered, extending from 14 building heights upwind to 12 building heights downwind. Not all combinations of stack locations with the other parameters were considered.

The data were made available to us in the form of a large number of ASCII files and a data report. We have rearranged the data sets into a few spreadsheets with embedded graphs, so that it is easy to vary parameters and inspect concentration results according to measurement and models. We encourage readers to explore the graphs in the spreadsheets. These can be found through the atmospheric dispersion Wiki http://atmosphericdispersion.wikia.com/wiki/Thompson_Wind_Tunnel_data

The use of a Wiki in this context permits others to contribute with information in future. Many graphs are available in the report by Olesen et al. (2007).

3. THE MODELS

In the comparisons with measured data, the standard version of OML was used (OML version 5.0). Although a new, improved "Research Version" of OML has been developed (Olesen et al., 2007), it was not used in the present context as it still lacks a building algorithm. For the AERMOD computations, version 04300 (with PRIME) was used. The CFD model MISKAM (version 5.01) was used for a limited number of cases.

4. RESULTS AND DISCUSSION

Figure 1 shows measured and modelled results for four scenarios. The scenarios have been selected because they show some interesting features concerning the effect of building width on measurements and on model results. The characteristic parameters for the four scenarios are:

- The relative stack height is 1 (top row), respectively 1.5 (bottom row)
- The building is a cube (left column), respectively wide (4 times its height, right column).
- The stack is placed in the middle of the building.

Each panel shows both the geometry of the simulation and the results in terms of concentrations. The wind blows from the left to the right. Results are shown for AERMOD, for standard OML and for MISKAM, with and without building. The full drawn curves refers to scenarios with a building, and the dotted curves to scenarios without. In addition to model results, measurements are displayed as the black curves.

The physical dimensions in the wind tunnel and on the graph's x-axis are in mm, but the results can be scaled. The building height is 150 mm, and the boundary layer in the wind tunnel has been found to be 700 mm. When results are scaled, all length scales are adjusted, whereas the wind speed remains the same.

It is a useful exercise to inspect plots like those of Figure 1. As noted, a much wider variety of scenarios is available for inspection in the report previously referred to. In Figure 1, it appears (top row) that for a relative stack height of 1 measured results are not very sensitive to the building width. The standard OML model, which uses a simple building downwash algorithm, does likewise not show any sensitivity to building width, whereas AERMOD/PRIME – in contrast to reality – shows a strong dependence with building width, and overpredicts by a factor of more than two close to the building. As a contrast, it is interesting to note that with a relative stack height of 1.5 (lower row in Figure 1), building width *does* have a substantial influence on results. Maximum ground-level concentration for the wide building is more than twice of that for the cube. However, in this case, AERMOD does *not* reflect this dependence, and neither does standard OML.

The entire series of plots reveal many discrepancies between observed concentration profiles versus those modelled by AERMOD and OML. A discrepancy, which is characteristic for many cases modelled with OML is that the model predicts the maximum concentration as close to the building as the model permits (e.g. the lower left panel in Figure 1), while the maximum in reality occurs further away. Although the location of the maximum is misrepresented, the size of the maximum is often in reasonable agreement with the observed maximum.

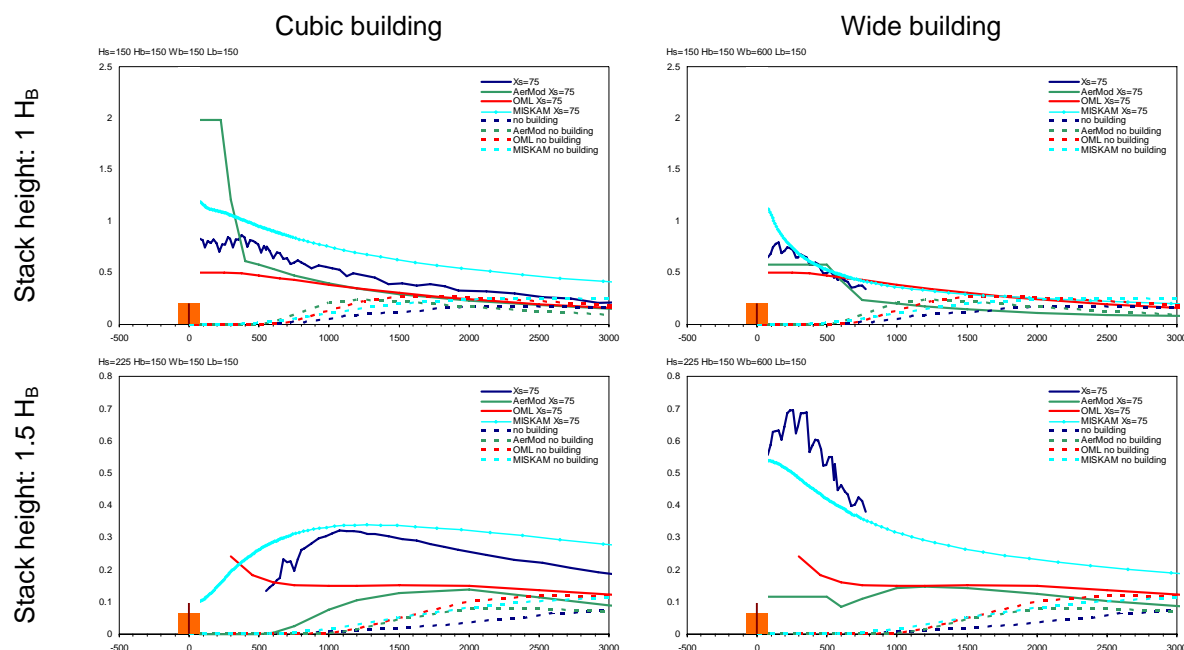


Figure 1 Along-wind concentration profiles for four scenarios, both with building (full drawn lines) and without building (dotted lines). As measured, and as modelled by AERMOD/PRIME, standard OML and MISKAM.

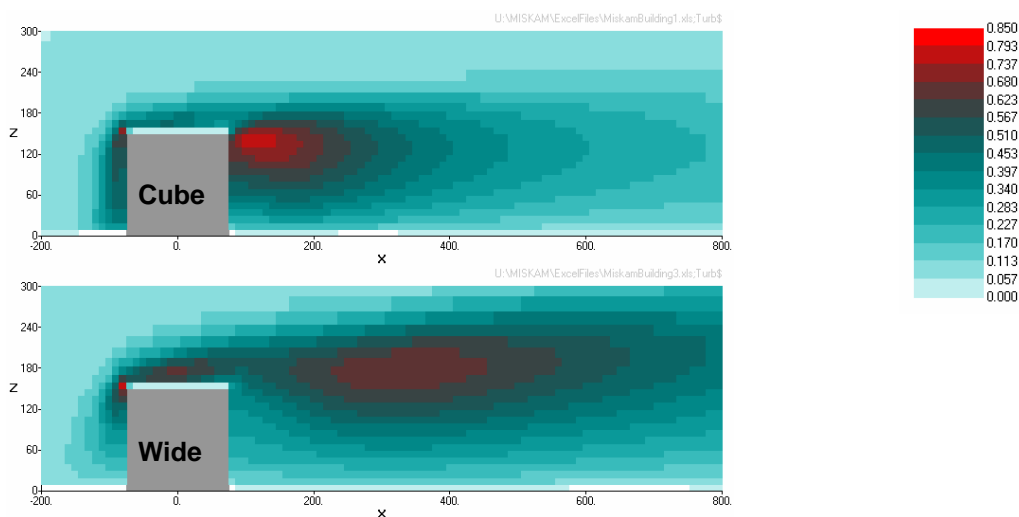


Figure 2 Turbulent kinetic energy (TKE, m^2/s^2), according to MISKAM in an x-z cross-section in the centre of the building. Top: the cube building; bottom: the very wide building.

The CFD model MISKAM has been used in an attempt to understand the different behaviour that building width has on dispersion from a stack with a relative height of 1, compared to an elevated stack. MISKAM runs were conducted for the four cases in *Figure 1*. MISKAM much more faithfully reproduces the concentration profiles than the simple models. The fact that MISKAM is a CFD model allows us to visualize the modelled distribution of the turbulent kinetic energy (TKE) in the x-z plane, as indicated in *Figure 2*.

It is interesting to compare the TKE pattern caused by the cube, respectively the wide building. A non-buoyant plume emitted at a height of 1.5 times the building height will experience very different levels of TKE, depending on whether it is released over a cube or over a wide building. If, on the other hand, the plume is released *at roof level*, it will be affected by high levels of TKE for both building shapes. This can qualitatively explain why concentration results for an elevated stack are much more sensitive to building width than results from a roof-top stack. Relatively simple models like AERMOD and OML do not account correctly for these effects.

One can gain insight into model behaviour by inspecting the more than hundred available plots like those of *Figure 1*. It is an impossible challenge to provide a synthesis of results in a way that retains *all* information from the individual graphs. Nevertheless, various types of syntheses can be produced that illustrate important features.

The original paper by Thompson (1993) presents contour plots of the so-called Building Amplification Factor, BAF. The BAF is formed by comparing two situations: a situation where a building is located near a stack, and a reference situation without a building. For both situations, the maximum ground-level concentration is determined. The ratio between these two concentrations is the BAF. The value of the BAF depends on the height and position of the stack relative to the building.

Thompson's studies of BAF allowed him to conclude that the Good Engineering Practice 2.5-times rule (according to which a stack height of 2.5 building heights is sufficient to make building effect negligible) is inadequate for wide buildings. Furthermore, the results indicated that even with a distance between stack and building of ten times building height, the buildings still has a significant effect on maximum concentrations.

We have chosen to present results for a somewhat similar parameter that carries information on model performance: We determine the maximum ground-level concentration (along the concentration profile), according to the model and according to measurements. The ratio of the modelled to the observed – one may call it the *Model Discrepancy Factor* (MDF) – is computed. A perfect model would have a MDF of 1 for every scenario. Note that a MDF of 1 certainly is no guarantee that the model is correct, as the *location* of the maximum might be misplaced. In *Figure 3* the performance of OML and AERMOD in terms of MDF is exposed.

Figure 3 contains a lot of information in a very condensed form. Each numbered label summarises information for an entire scenario. Pay attention to the fact that at a *given point in space* the degree of misprediction by a model may be more serious than the numbers in the figure indicate.

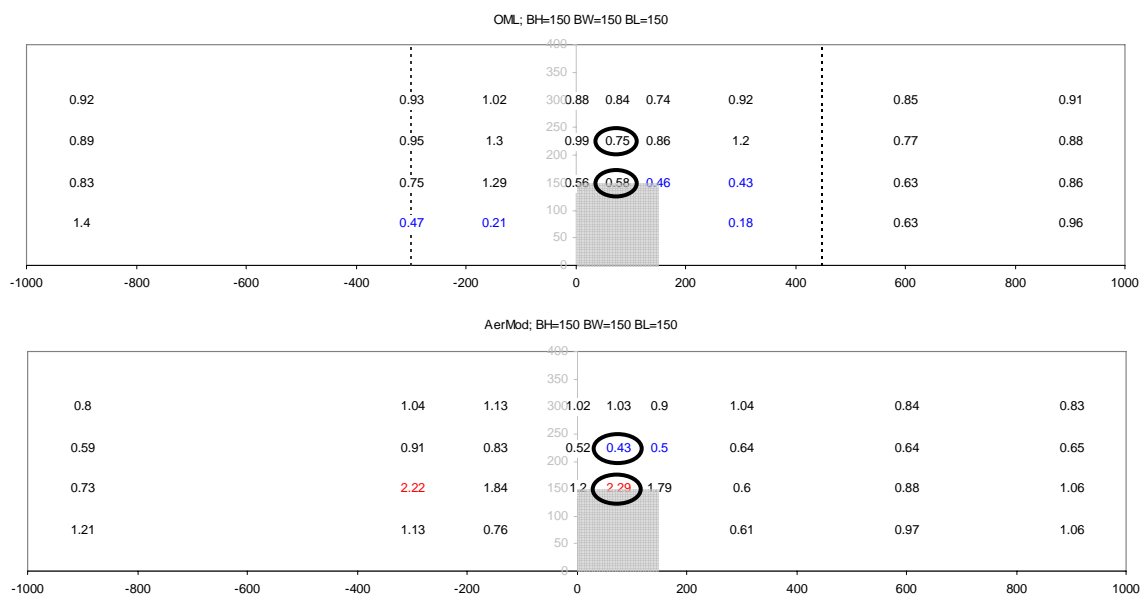


Figure 3 "Model Discrepancy Factor" for 33 scenarios with different combinations of stack height and stack location, all pertaining to the cube building. The upper plot refers to OML, the lower to AERMOD. The position of each label indicates the scenario. Results corresponding to Figure 1 are encircled. E.g., the red label of 2.29 in the lower plot indicates the MDF for AERMOD for the scenario displayed in the upper left of Figure 1. Overpredictions by more than a factor of 2 are in red, underpredictions worse than 0.5 are in blue. For OML, the dotted lines indicate how far the building effect extends according to the current, simple algorithm.

5. CONCLUSION

Thompson's data set is very comprehensive, and deserves to be used much more than it has been in the past.

The concepts of BAF and MDF are useful for obtaining an overview of results, but looking at such factors alone is not sufficient to provide an adequate synthesis of results. One can learn by inspecting plots with results for individual scenarios, like Figure 1. The data have been organised in a spreadsheet with embedded graphs, so that it is easy to vary parameters and inspect concentration results for measurement and models. With a relative stack height of 1 measured results are not very sensitive to the building width, but with a relative stack height of 1.5, building width *does* have a substantial influence on results. Measured maximum ground-level concentration for the widest building is more than twice of that for the cube building. Such dependence is reflected in neither AERMOD/PRIME nor standard OML. For the limited number of cases where we have MISKAM runs, the discrepancies are much smaller. MISKAM is clearly superior to AERMOD/PRIME and OML.

On basis of the studies it was decided not to replace the OML building algorithm with the PRIME algorithm. It is an overall impression from the results that there is not much to be gained by directly replacing the building algorithm of the standard OML model with that of PRIME. The OML model has some weaknesses, but so does AERMOD/PRIME.

From a model user's point of view, the overall conclusion of the present study is that a user of either AERMOD or OML must accept rather large deviations between model predictions and observations for many situations. Predictions in the far field, away from the stack, are reasonable, but in the near field there can easily be overpredictions or underpredictions by a factor of 2 for both models. Such are the current limitations of the models. This claim presumably applies to many other simple models. If a modeller's purpose is an accurate prediction of concentrations close to a building, he can consider using a model of an entirely different type such as MISKAM. However, MISKAM is orders of magnitude more demanding in terms of required man-power, user skill and computer resources.

6. REFERENCES

- Thompson, R.S., 1993: Building Amplification Factors for Sources Near Buildings - A Wind-Tunnel Study. Atmospheric Environment Part A, 27, 2313-2325.
- Olesen, H.R., Berkowicz, R.B., Løfstrøm, P., 2007: OML: Review of model formulation. National Environmental Research Institute, Denmark. NERI Technical Report No. 609, pp. 130, <http://www.dmu.dk/Pub/FR609>.

**THREE-DIMENSIONAL SIMULATIONS OF POLLUTANTS ATMOSPHERIC DISPERSION
AROUND THE BUILDINGS OF INDUSTRIAL SITES AND URBAN AREAS
COMPARISON OF MERCURE CFD APPROACH
WITH MICRO-SWIFT-SPRAY SIMPLIFIED APPROACH**

Patrick ARMAND¹, Julien COMMANAY², Maxime NIBART², Armand ALBERGEL², Pascal ACHIM¹

¹ Commissariat à l'Énergie Atomique

Département Analyse, Surveillance, Environnement – Service Radioanalyse, Chimie, Environnement
91 680 Bruyères-le-Châtel – France

² ARIA Technologies – 8-10, rue de la Ferme – 92 100 Boulogne-Billancourt – France

ABSTRACT

Usual Gaussian models appear of limited relevance when simulating the dispersion of pollutants on industrial complex sites or in the urban atmospheric environment. On the other hand, full 3D CFD approaches are powerful ways of investigation but require huge CPU resources. The Micro-SWIFT-SPRAY modeling system represents an alternative rapid response capability to simulate the flow field and the dispersion processes at the micro-scale. MSS has been applied in various complicated configurations including either accidental short duration or chronic long term impact releases. The simulations in case of an accident have also been carried out with EDF-MERCURE CFD code. While the 3D numerical results are quite comparable, MSS computation times are much lower than MERCURE ones. As demonstrated in the paper, MSS objective of having '90% of the solution for less than 10% of the CPU' is even greatly surpassed.

1. INTRODUCTION

Small as well as large industries are now committed to produce impact assessment studies for their facilities. This is a requirement made by the National and European regulations and meeting the societal concerns. The impact assessment relates to the normal operation or hypothetical on-site accidents. In both cases, the studies require the dispersion computation of atmospheric releases (gases or particles) and their impact evaluation on the health of the workers and populations around the facilities.

In the frame of regulatory studies, the dispersion of radiological or chemical pollutants is usually computed using Gaussian plume or puff models, the advantages of which are to be easy to handle with and give a quick answer. On the other hand, these models appear very limited when simulating the pollutants dispersion in the urban environment or around the buildings of the industrial sites. 3D meshes solving of the equations may be necessary to get realistic results of the pollutants spatiotemporal distribution and exposure consequences.

At the micro-scale, dispersion around obstacles needs a CFD model well adapted for the planetary boundary layer, like MERCURE code. It is an interesting way of investigation, although requiring heavy computational resources, especially for two important applications: emergency response or preparedness, long term impact around a source near the ground. That is why the Micro-SWIFT-SPRAY (MSS) modeling system is being developed as an alternative quick response capability to simulate the flow field and dispersion processes at the micro-scale in the presence of obstacles.

In the following, MSS, and more briefly, MERCURE codes are introduced. MSS has been used in numerous and various complicated configurations with either accidental releases of toxic materials or chronic long term releases from the stacks of facilities. Some examples are commented in the paper. For accidental releases, the 3D computations have been done with MSS and MERCURE in order to compare the results and evaluate MSS solution. In the conclusion, MSS other uses and potential promising developments are discussed.

2. DESCRIPTION OF MICRO-SWIFT-SPRAY (MSS)

Micro-SWIFT-SPRAY (MSS) is a recent modeling system developed as an alternative approach where CFD codes would need heavy computational resources. It is tagged as '90% of the solution for less than 10% of the CPU'. MSS allows an exact representation of buildings, directly generated by a GIS (as .shp files).

Micro-SWIFT is an analytically modified interpolator over complex terrain and gives the micro-scale quick solution to the flow problem. A 3D mass consistent wind field is generated by following the steps below.

- According to meteorological data, a first guess of the mean flow is computed through customisable interpolation using all available and relevant data (inside or outside the target domain).
- This first guess is modified by creating analytical zones where the flow takes account of buildings, these being isolated or not (Röckle, 1990 or Kaplan and Dinar, 1996).
- Finally, the flow is adjusted to satisfy the continuity equation and impermeability on the ground and building walls. Turbulence is diagnostically deduced considering the distance to the nearest obstacle as a mixing length and using the value of the wind field local shear.

Micro-SPRAY is a Lagrangian particle dispersion model directly derived from the SPRAY code (Tinarelli *et al.*, 1998), able to take obstacles into account. The dispersion of an airborne pollutant is simulated following the movement of a large number of fictitious particles, each representing a part of the emitted mass from sources of general shapes. This movement is obtained applying a motion equation where the particle velocity

is split into two components: a mean one defined by the local wind reconstructed by Micro-SWIFT, and a stochastic one, reproducing the atmospheric turbulence and dispersion. The stochastic component is obtained applying the scheme developed by Thomson in respect of the 'well-mixed' condition (Thomson, 1987).

3. DESCRIPTION OF MERCURE

MERCURE software has been developed by EDF (French Electricity Company) on the basis of ESTET CFD code. Many validation exercises of MERCURE have been performed through systematic comparisons with experimental data and output of other 3D codes. It has also played a major role in several European Projects with the objective to compare results *vs.* site measurements corresponding to several releases (Thorney Island experiments 1982 and 1984, German propane release 1990, FLADIS project 1994). The MERCURE results compared reasonably well with the collected measurements.

MERCURE / ESTET fully solves Navier-Stokes equations (for averaged quantities if the flow is turbulent) by the fractional step method in finite differences and finite elements, on two- or three-dimensional domains, in transient or permanent regimes. Structured monoblock meshes are created with cartesian or non orthogonal curved coordinates. ESTET uses staggered grids for the velocity and pressure variables.

MERCURE was fitted to the planetary boundary layer, using the virtual potential temperature as the thermal variable for the energy balance equation or other features making atmospheric releases easier to deal with.

4. SIMULATIONS OF AN ACCIDENTAL RELEASE

A case study was defined and carried out using both MSS and MERCURE codes. The simulation relates to a hypothetical accidental chemical release among the buildings on an industrial site. The accident scenario is built as a reference one for an emergency situation on this site.

4.1. Input conditions

Meteorological condition

The atmosphere is considered as very stable (F Pasquill-Gifford class). The north-east wind has a module of 2 m.s^{-1} (at 10 m above the ground). This common situation is often considered as a worst case for pollutants dispersion.

Atmospheric releases

Cylinders of pressurized liquid chlorine are stored outdoor on the site. The accident consists in the formation of a chlorine plume due to a breach in one cylinder. A diphasic flow occurs with a quick evaporation of the liquid phase. The source term is calculated with the ATRCOD module developed by ARIA Technologies. The mass flow rate varies with time and takes into account the chlorine vapor and liquid phases.

Toxicological reference values

In France, 'toxicological reference values' are given by the INERIS (*Institut National de l'Environnement et des Risques Industriels*) for the main toxic species. These values are concentrations, combined with exposure durations, (1) under which no irreversible effects on human health were observed or (2) leading to the death of a fraction (1 or 5%) of exposed people. In an accident, the atmospheric concentration C is time dependant ; the common practice is to calculate the dose $D = \int C^n(t) dt$ (for chlorine, n is 2.3). Introducing toxicological values in this formula, one obtains the 'irreversible effects' and 'death' doses. The computed doses are then compared to the threshold doses to determine the sanitary impact of the accident.

4.2. Computations conditions

Meshing

MSS calculation domain is a 645 m x 426 m x 250 m parallelepiped. The horizontal meshing is regular with a 3 m mesh size. The vertical meshing is refined near the ground level (28 levels, minimum size of 1.5 m).

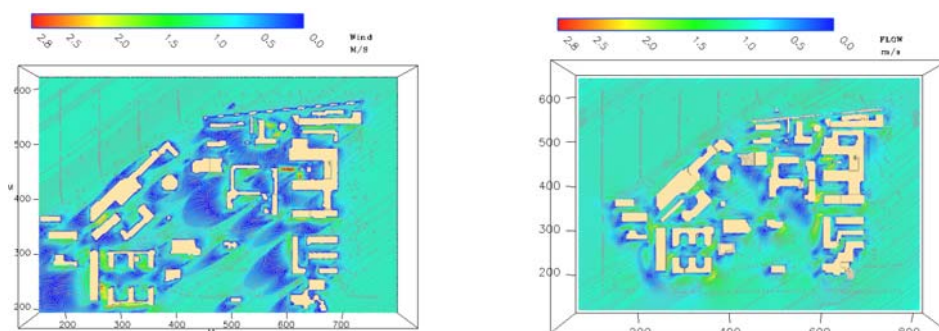
MERCURE calculation domain is slightly larger. The horizontal meshing is refined near the release location with minimum and average mesh sizes of 0.5 and 5 m. The vertical meshing is refined near the ground level (33 levels, minimum size of 0.5 m).

Numerical parameters

The simulated duration is 10 minutes in order to limit MERCURE computation time. In Micro-SPRAY, 250 particles are emitted at each time step of 1 s. In MERCURE, the time step is constant and equal to 1 s.

4.3. Wind fields results

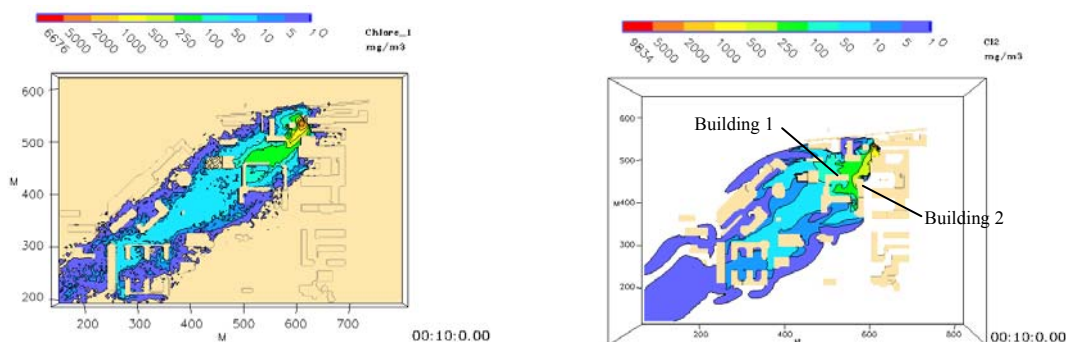
Figures 2a and 2b present the wind module and the streamlines, at 2 m above the ground level, simulated by MSS and MERCURE respectively. These figures illustrate the global behavior of the air flow around the buildings, the acceleration, deceleration or recirculation zones around the obstacles. The zones with low wind speeds are a bit larger according to MSS than for MERCURE. Close to a complex 'three-shaped' building, MSS indicates a high speed region corresponding to a canyon in MSS modeling of the buildings.



Figures 2a and 2b. Wind module and streamlines at 2 m (MSS on the left and MERCURE on the right).

4.4. Concentrations results

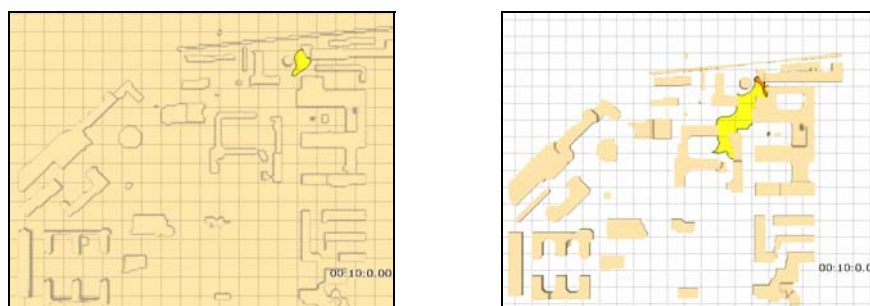
Figures 3a and 3b present sections, near the ground, of the concentration field, issued from respectively MSS and MERCURE. The figures show similar plumes with same extents of the coloured areas. Chlorine plume is advected a bit more southerly by MERCURE and farther by MSS while remaining more confined in the vicinity of the release and being slightly larger along with MERCURE. The difference is due to the method of taking the obstacles into account. While MSS does not consider the global effect of the buildings on the wind field, MERCURE channels the flow between the buildings denoted 1 and 2 on figure 3b. Moreover, turbulence modeling is different in the two models which influences the pollutants dispersion.



Figures 3a and 3b. Chlorine concentration at 2 m – t = 10 min (MSS on the left and MERCURE on the right).

4.5 Doses results

Figures 4a and 4b show the ‘irreversible health effects’ and ‘death’ zones as computed respectively by MSS and MERCURE. The lethal dose is obtained nowhere along with MSS while it is reached up to a maximum distance of 28 m with MERCURE. The irreversible effects dose is located close to the release, up to 32 m, according to MSS while it extends to 125 m for MERCURE. The shape and the extent of the doses contours are more dissimilar than the concentrations contours. This is explained by the doses calculation in which the concentrations are raised to the power 2.3 with the consequence to amplify the small discrepancies between the models. It is worth noticing the accident impact is restricted to a small area directly near the release point.



Figures 4a and 4b. ‘Irreversible effects’ and ‘death’ zones (MSS on the left and MERCURE on the right).

4.6. Computation times

Table 1 indicates the computation times for the 10 minutes simulations on one processor Intel® Xeon® 3.2 GHz with 3.2 Go RAM. While the 3D numerical results obtained with MSS and MERCURE are comparable, MSS computation times are much lower than MERCURE ones.

Table 1. MSS and MERCURE computation times.

	MSS	MERCURE	Ratio
Wind and dispersion	640 s	85 680 s	0.7%

5. LONG TERM IMPACT ASSESSMENT

For many industrial chronic atmospheric releases, a long term assessment is required. The local authorities demand to estimate air concentration or soil deposition in terms of annual mean averages and other statistical figures as percentiles. These kind of studies are generally carried out with simple Gaussian approaches doing the assumption of no building effects or using empirical and not very accurate downwash formulations. Facing the more and more severe regulations, especially for VOC or other species going through low stacks, better solutions are necessary as provided by MSS. To perform a long term assessment, the model must be driven typically with five years of hourly meteorological data. This requirement is not compatible with full CFD CPU times as MERCURE and faster algorithms are necessary.

The following application illustrates the VOC impact around an important car factory. Figure 5a shows how the plumes are affected by the wakes produced by the factory buildings. Figure 5b corresponding to the same computation with Pasquill-Gifford Gaussian approach shows that the impact is actually underestimated at the close vicinity of the plant while it is overestimated far from the buildings. These computations can be easily dispatched on several CPUs and can be carried out in one or two weeks.

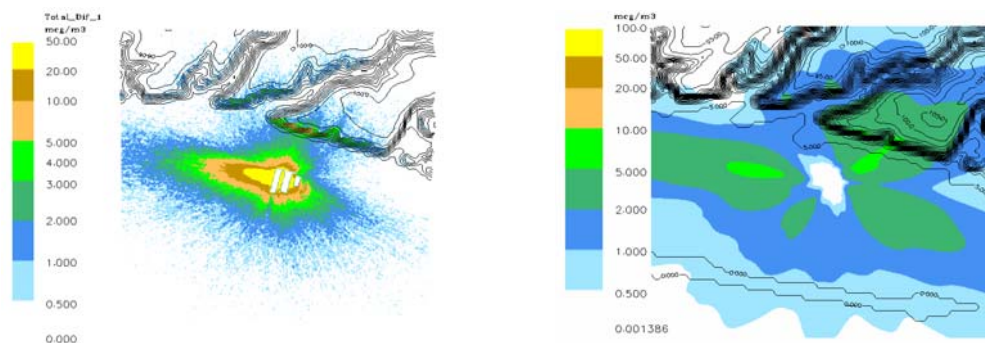


Figure 5a and 5b. Impact assessment using respectively MSS and Pasquill-Gifford Gaussian approach.

6. CONCLUSIONS

Gaussian plume or puff models have important limitations when used in the frame of dispersion and impact assessment studies for industrial sites or urban environment. On the other hand, a full CFD approach needs very important CPU resources. Micro-SWIFT-SPRAY modeling system, still under development, represents a promising compromise to quickly simulate the 3D flow field and dispersion processes at the micro-scale. Some examples of MSS computations are given and discussed in the paper.

Concerning chronic releases, MSS has been used to do statistical descriptions of the atmospheric dispersion based on numerous calculations (typically with five years of hourly meteorological data) in a limited time.

Concerning accidental releases, 3D simulations with MSS and MERCURE CFD code have been carried out for the same site in identical meteorological conditions. Wind fields, concentrations and doses results are comparable with minor explained discrepancies. While 3D numerical results are similar, MSS computation times are much lower than MERCURE ones. In this application, MSS goal of '90% of the solution for less than 10% of the CPU' is greatly reached.

Other MSS comparisons with CFD numerical results and wind tunnel or in field experimental data also give acceptable results. The implementation of MSS in operational tools such as the new version of HPAC (US-DOD) has now been completed successfully.

Finally, it is foreseen to use MSS in 'real time' or 'near real time' conditions in the framework of emergency response or preparedness to accidental or malevolent dispersal events. This would imply the development of a parallel version of MSS modeling system in order to still more decrease the CPU.

7. REFERENCES

- Kaplan, H., and Dinard, N. 1996. A Lagrangian dispersion model for calculating concentration distribution within a built-up domain. *Atmos. Environ.* 30 (24), 4197-4207.
- Röckle, R. 1990. Bestimmung der Strömungsverhältnisse im Bereich komplexer Bebauungsstrukturen. PhD Thesis, Darmstadt, Germany.
- Thomson, D.J. 1987. Criteria for the selection of stochastic models of particle trajectories in turbulent flows. *J. Fluid Mech.* 180, 529-556.
- Tinarelli, G., Anfossi, D., Bider, M., Ferrero, E., Trini Castelli, S. 1998. A new high performance version of the Lagrangian particle dispersion model SPRAY. Some case studies. *Proceedings of the 23rd CCMS-NATO Meeting, Varna.* Kluwer Academic. 28 September - 2 October 1998. 499-507.

THE MODELLING OF THE VEHICULAR EXHAUST PLUMES IN A ROADSIDE ENVIRONMENT, BY COUPLING A DISPERSION MODEL AND AN AEROSOL PROCESS MODEL

Pohjola M A¹, Pirjola L^{2,3}, Kukkonen J¹, Karppinen A¹, Härkönen J¹, Ketzel M⁴, Kulmala, M³

¹ Finnish Meteorological Institute, Air Quality Research, Helsinki, FI-00101, Finland

² Helsinki Polytechnic, Department of Technology, P.O. Box 4020, FIN-00099 Helsinki, Finland

³ University of Helsinki, Department of Physical Sciences, P.O. Box 64, FI-00014 Helsinki, Finland

⁴ National Environmental Research Institute, Department of Atmospheric Environment, Frederiksborgvej 399, DK-4000 Roskilde, Denmark

* Corresponding author: Mia.Pohjola@fmi.fi, phone: +358-9-1929 5457, fax: +358-9-1929 5403, Finnish Meteorological Institute, Air Quality Research, Erik Palménin aukio 1, FI-00101 Helsinki, Finland.

ABSTRACT

In this study we report on the analysis of fine and ultrafine particle transformation within the distance scale of 200 m (time scale of a couple of minutes) from a major road in Helsinki, and compare the model results with measurement data. Measurement data was obtained from a mobile laboratory campaign in city traffic conditions. We have developed a mathematical procedure for coupling a dispersion model and an aerosol process model. In this work the aerosol process model MONO32 is applied for the evaluation of the temporal evolution of number concentration, size distribution and chemical composition of various particle size classes, and the roadside dispersion model CAR-FMI provides the dilution rate of the particles.

1. INTRODUCTION

In this work we have modelled the transformation of fine and ultrafine particles from vehicular traffic in the vicinity of a major road in Helsinki, and compared the modelled results with measurement data. We address the evolution of the number concentrations and size distributions within the time scale of a couple of minutes (distance scale of < 300m). The monodisperse aerosol process model MONO32 (Pirjola et al., 2003) was applied for the evaluation of the aerosol processes while the atmospheric dilution rate of particles, influenced by the local meteorology, was obtained from the roadside dispersion model CAR-FMI. This work is a continuation of a previous study analysing the transformation and dilution of vehicular exhaust plumes in street environment (Pohjola et al., 2003 and 2004).

2. METHODOLOGY

The aerosol measurements by a mobile laboratory were conducted at various locations near Itäväylä, a major road in an urban area of Helsinki, during the LIPIKA campaign in February 17 – 20, 2003 (Pirjola et al., 2004, 2006). A schematic of the measurement site is presented in Figure 1.

The mobile laboratory used was constructed into a Volkswagen LT35 diesel vehicle and was operated by Helsinki Polytechnic. Particle size distribution in the size range of 7 nm – 10 µm (aerodynamic diameter) with 12 channels was measured by the Electrical Low Pressure Impactor (ELPI, Dekati Ltd). The nucleation mode particle size distribution with a high size resolution was measured by the Hauke type Scanning Mobility Particle Sizer (SMPS), where particles are first neutralised, then classified by a DMA based on their electrical mobility, and counted by a CPC 3025 (TSI, Inc.). Measurement size range was 3 – 50 nm (mobility diameter), the number of channels was 20 and the scan-up time mostly 30 s. Additionally, the total number concentration of particles larger than 3 nm was detected by an ultrafine condensation particle counter CPC 3025 (TSI, Inc.). A passive clean air dilution system was installed, with a dilution ratio of 1:3. The SMPS and CPC instruments were operated by the University of Helsinki. The particle measurement inlet was located at the height of 2.4 m. The weather station was located at the roof of the van. Temperature and relative humidity were measured (Model HMP45A, Vaisala) at the height of 3.4 m from the ground. Additionally, a global position system (GPS V, Garmin) saved the van speed and the driving route and a video camera in the cab recorded visually the traffic situations. Further wind speed and direction data was measured at 10 m height at the roof of a cabin located 9 m from the edge of the road.

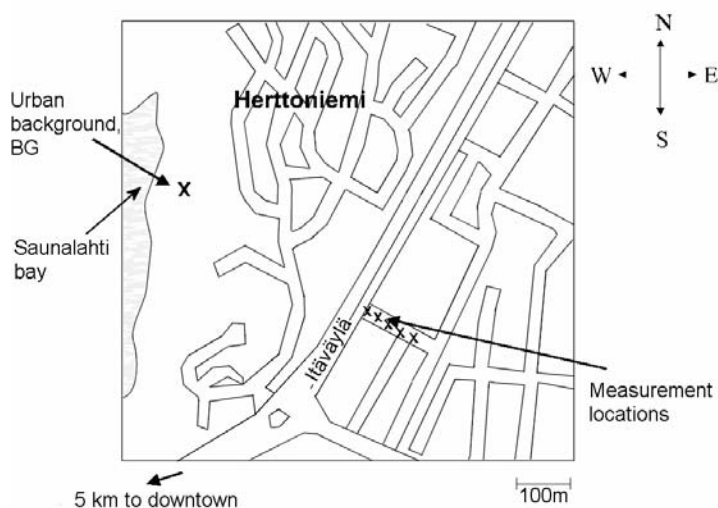


Figure 1. Schematic map of the measurement site and its surroundings (Pirjola et al., 2006).

The CAR-FMI model includes an emission model, a dispersion model and statistical analysis of the computed time series of concentrations. The CAR-FMI model utilises the meteorological input data evaluated with the meteorological pre-processing model MPP-FMI. For a more detailed description of these models, the reader is referred to Härkönen et al. (2002) and Karppinen et al. (2000 a, b).

The aerosol dynamics model MONO32 is a box model, which includes gas-phase chemistry and aerosol dynamics, and can be applied under clear sky conditions. The model uses monodisperse representation for particle size distribution with an optional number of size modes. In this work we have used six modes: nucleation1 (diameters $d < 7.5\text{nm}$), nucleation2 (diameters $7.5\text{nm} < d < 43.2\text{nm}$), Aitken ($43.2\text{nm} < d < 0.122\mu\text{m}$), accumulation1 ($0.122\mu\text{m} < d < 0.321\mu\text{m}$), accumulation2 ($0.321\mu\text{m} < d < 2.5\mu\text{m}$), and coarse ($d > 2.5\mu\text{m}$). All particles in a mode are characterised by the same size and the same composition. Particles can consist of soluble material such as sulphuric acid, ammonium sulphate, ammonium nitrate and sodium chloride, organic carbon which can be soluble, partly soluble or insoluble, and insoluble material like elemental carbon and mineral dust. Size and composition of particles in any class can change due to multicomponent condensation of sulphuric acid and organic vapours as well as due to coagulation between particles. Dry deposition can also effect particle number concentration. For a more detailed description of the MONO32 model and its evaluation against measurement data, the reader is referred to Pirjola and Kulmala (2000), Pirjola et al. (2003) and Pohjola et al. (2003).

3. RESULTS AND DISCUSSION

The studied time periods were chosen so that the wind direction was approximately perpendicular from the road towards the measurement sites. We used the particle number concentrations measured in traffic during the campaign combined with the chemical composition data combined from Kauhaniemi (2003), Norbeck et al. (1998) and Shi et al. (2000) for the input data describing the exhaust particles.

The diameters and the limits of the six modes as well as the percentile portions of the number concentrations in each mode were obtained from the average size distribution measured by the mobile laboratory at Itäväylä. These percentiles were used in calculating the modal emission factors from the emission factors of the total number concentration by Gidhagen et al. (2004) and Yli-Tuomi et al. (2004). The modal emission factors were extended to allow for the temporal variation by using the measured traffic density profiles. We evaluated an average urban background particle size number distribution based on the LIPIKA-measurements at the urban background site 600 m from the roadside site, and chemical composition of the background particles was based on the works of Pakkanen et al. (2001 a, b) and Viidanoja et al. (2002).

The width of the road Itäväylä is approximately 30 m, the width of the three lanes to each direction are 12 m altogether, and there is 6 m wide green belt (mainly grass) in the middle. We have assumed that the height of the initial dilution volume in the MONO32 model is 80 cm, and this height is increased up to 280 cm while passing the traffic lanes to take traffic induced turbulence into account. Nucleation of particles was assumed to have already occurred before start of modeling period, due to the temperature decrease immediately after the tailpipe. The functions describing dilution were obtained for $PM_{2.5}$ by the FMI-CAR model; the road was modelled as a set of two line sources that were located in the middle of the three lanes in both directions. We have assumed that the dilution rate is the same also for the particle number concentrations. The emission and dilution rates were taken into account in the aerosol process model by appropriately modifying the differential equations of the number and mass concentrations of particles.

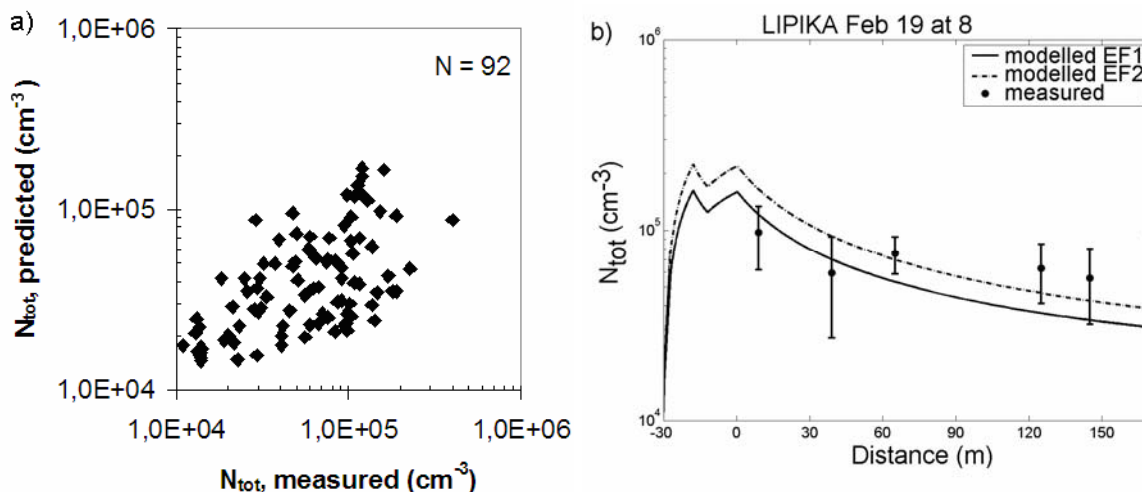


Figure 2. a) Predicted total number concentrations versus measured total number concentrations at all studied cases at all measurement distances from the edge of the road. b) The modelled and measured total number concentrations of particles as a function of distance from the edge of the road Itäväylä at 14 to 15 p.m. on February 18, 2003. EF1 and EF2 refer to emission factors based on Gidhagen et al. (2004) and Ylituomi et al. (2005.). The error bars show the estimated uncertainty of the experimental techniques. (Pohjola et al., 2007).

The correspondence of the measured total number concentrations during all modelled hour cases ($n=14$) at all measurement points (5.9 measurements per hour) is presented in Figure 2a. The agreement of the modelled total number concentrations with the measured concentrations was fairly good. An example of modelled and measured evolution of total particle number concentration is presented in Figure 2b. One reason between the discrepancy between the measurement point concentrations and the modelled concentrations may be that the measurements at the chosen distances from the edge of the road were not simultaneous but from subsequent time periods during the measurement hour, while the modelling does not take shorter term variation into account, eg. variation of wind direction and traffic density. Dilution with urban background air was shown to be the most important process affecting the evolution of the total number concentration. The concentration of condensable vapours is the main factor controlling particle growth and size distribution; its effect was found to be important for the evolution of the particle size distributions, if the concentration of the condensing vapor is sufficiently high.

4. CONCLUSIONS

A mathematical method that (i) presents the dilution of pollution as simplified equations that are based on the roadside dispersion model, and (ii) combines these equations mathematically with the set of differential equations that constitute the aerosol process model has been developed. The same or similar mathematical procedure could probably be used also for coupling other dispersion models representing various spatial scales, and aerosol process models.

5. ACKNOWLEDGEMENTS

This work has been funded by the Maj and Tor Nessling Foundation. We also wish to thank all the people in the LIPIKA project for their careful work in producing the mobile laboratory measurement data, the projects KOPRA, OSCAR and SAPPHIRE, and the CLEAR cluster of EU-funded projects.

6. REFERENCES

- Gidhagen, L. 2004. Emissions, dynamics and dispersion of particles in polluted air. Doctoral dissertation, Department of Meteorology, Stockholm University, SE-106 91 Stockholm, Sweden. 140 p.
- Härkönen, J. 2002. Regulatory dispersion modelling of traffic-originated pollution. Finnish Meteorological Institute, Contributions No. 38, FMI-CONT-38, ISSN 0782-6117, University Press, Helsinki, 103 p.
- Karppinen, A, J. Kukkonen, T. Elolähde, M. Konttinen, T. Koskentalo and E. Rantakrans 2000a. A modelling system for predicting urban air pollution, Model description and applications in the Helsinki metropolitan area. *Atmos. Environ.* 34-22, 3723-3733.
- Karppinen, A, J. Kukkonen, T. Elolähde, M. Konttinen and T. Koskentalo, 2000b. A modelling system for predicting urban air pollution, Comparison of model predictions with the data of an urban measurement network. *Atmos. Environ.* 34-22, 3735-3743.
- Kauhaniemi M. 2003. Usability of the Air Quality Model CAR-FMI in City Planning. Master's Thesis, University of Oulu, Department of Process and Environmental Engineering, Control Engineering Laboratory, 87+7 (13) p.
- Norbeck, J.M., Durbin, T.D., Truex, T.J. 1998. Measurement of Primary Particulate Matter Emissions from Light Duty Motor Vehicles. CRC Project No: E-24-2 Final Report. University of California, College of Engineering, Center for Environmental Research and Technology. 56 p.
- Pakkanen, T., Kerminen, V.-M., Korhonen, C.H., Hillamo, R., Aarnio, P., Koskentalo T. & Maenhaut, W. 2001. Urban and rural ultrafine (PM_{0.1}) particles in the Helsinki Area. *Atmos. Environ.* 35, 4593-4607.
- Pakkanen, T.A., Loukkola, K., Korhonen, C.H., Aurela, M., Mäkelä, T., Hillamo, R.E., Aarnio, P., Koskentalo, T., Kousa, A., Maenhaut, W. 2001. Sources and chemical composition of atmospheric fine and coarse particles in the Helsinki area. *Atmos. Environ.* 35, 5381-5391.
- Pirjola, L. and Kulmala, M. 2000. Aerosol dynamical model MULTIMONO. *Boreal Environment Research* 5, 361-374.
- Pirjola, L., Tsyro, S., Tarrason, L. and Kulmala, M. 2003. A monodisperse aerosol dynamics module – a promising candidate for use in the Eulerian long-range transport model. *J. Geophysical Research*, 108, (D9), p. 4258. doi:10.1029/2002JD002867.
- Pirjola, L., Parviainen, H., Hussein, T., Valli, A., Hämeri, K., Aalto, P., Virtanen, A., Keskinen, J., Pakkanen, T.A., Mäkelä, T., Hillamo, R.E. 2004. "Sniffer" – a novel tool for chasing vehicles and measuring traffic pollutants. *Atmospheric Environment*, 38, 3625-3635.
- Pirjola, L., Paasonen, P., Pfeiffer, D., Hussein, T., Hämeri, K., Koskentalo, T., Virtanen, A., Rönkkö, T., Keskinen, J., Pakkanen, T.A., Hillamo, R. 2006. Dispersion of particles and trace gases nearby a city highway: mobile laboratory measurements in Finland. *Atmospheric Environment*, 40, 0867-0879.
- Pohjola, M A, Pirjola, L, Kukkonen, J, Kulmala, M. 2003. Modelling of the influence of aerosol processes for the dispersion of vehicular exhaust plumes in street environment. *Atmos. Environ.*, 37, 3. 339-351.
- Pohjola, M., Pirjola, L., Kukkonen, J., Karppinen, A., Härkönen, J. 2004. The influence of aerosol processes in vehicular exhaust plumes: model evaluation against the data from a roadside measurement campaign. In: *Proceeding of the 9th International Conference on Harmonisation within Atmospheric Dispersion Modelling for Regulatory Purposes*, 1-4 June 2004, Garmisch-Partenkirchen, Germany. Vol. 2, 142-146.
- Pohjola, M.A., Pirjola, L., Karppinen, A., Härkönen, J., Ketzler, M., Kukkonen, J. 2007. Evaluation of a coupled dispersion and aerosol process model against measurements near a major road. Submitted to *Atmospheric Chemistry and Physics*, December 2006.
- Shi, J.P., Mark, D., Harrison, R.M. 2000. Characterization of Particles from a Current Technology Heavy-Duty Diesel Engine. *Environ. Sci. Technol.*, 34, 748-755.
- Yli-Tuomi, T., Aarnio, P., Pirjola, L., Mäkelä, T., Hillamo, R. and Jantunen, M. 2005. Emissions of fine particles, NO_x, and CO from on-road vehicles in Finland. *Atmos. Environ.*, 39, 6696-6706.
- Viidanoja, J., Sillanpää, M., Laakia, J., Kerminen, V.-M., Hillamo, R., Aarnio, P., Koskentalo, T. 2002. Organic and black carbon in PM_{2.5} and PM₁₀:1 year of data from an urban site in Helsinki, Finland. *Atmos. Environ.* 36, 3183-3193.

SIMULATIONS OF THE DISPERSION OF REACTIVE POLLUTANTS IN A STREET CANYON, CONSIDERING DIFFERENT CHEMICAL MECHANISMS AND MICROMIXING.

A. Garmory, I. S. Kim, R. E. Britter and E. Mastorakos

Hopkinson Laboratory, Department of Engineering, University of Cambridge, UK

ABSTRACT

The Field Monte Carlo (FMC) Method has been used to model the dispersion of reactive scalars in a street canyon, using a simple chemistry and the CBM-IV mechanism. FMC is a Probability Density Function (PDF) method which allows both means and variances of the scalars to be calculated as well as considering the effect of segregation on reaction rates. It was found that the variance of reactive scalars such as NO₂ was very high in the mixing region at roof top level with rms values of the order of the mean values. The effect of segregation on major species such as O₃ was found to be very small using either mechanism, however some radical species in CBM-IV showed a significant difference. These were found to be the seven species with the fastest chemical timescales. The calculated photostationary state defect was also found to be in error when segregation is neglected.

1. INTRODUCTION

Recent studies have focused on the turbulent dispersion of reactive pollutants in street canyons. Baker et al [2] have carried out a LES study of a street canyon using a simple, reversible NO, NO₂ and O₃ chemistry using a constant temperature in the canyon. Baik et al [1] on the other hand have used a RANS model to predict the flow field in the canyon while using a similar chemistry to [2]. They also consider the effect of temperature variation within the canyon on both the flow field and the chemistry. Most reactive pollutant dispersion models so far have not included the effect of turbulence on reaction rates. Due to the non-linearity of the Arrhenius term and the effect of non-zero covariances between reactants evaluating mean reaction rates as a function only of mean concentrations and temperature may not yield a correct value. The fluctuations from the mean (either spatially or temporally) may need to be considered. The presence of fluctuations from the mean is known as segregation, while their decay due to molecular diffusion at the smallest scales of turbulence is often called micromixing. Whether the segregation has a significant effect on the reaction rate will depend on how rapidly micromixing destroys the segregation compared to the reaction speed. This is characterised by the Damköhler number, Da , defined as the ratio of mixing timescale to chemical timescale $Da = T_{phys}/T_{chem}$. For further discussion of this see [4].

In this work we use the Field Monte Carlo method to simulate the dispersion of reactive pollutants within a street canyon and also to assess what effect segregation and micromixing have on the reactions. This is done using the simple NO, NO₂ & O₃ chemistry used in [1] and also using the CBM-IV mechanism, which is a more complex chemistry comprising of 28 species [5]. The Field Monte Carlo method, also called the Stochastic Fields method, is a transported PDF method first developed by Valiño [7]. Rather than using the motion of notional particles through the flow this method solves stochastic partial differential equations (spde), derived from the PDF equation, for a number of scalar fields extending across the spatial domain. A spde is solved for each scalar in each field, if the values for a particular scalar are taken at a point in space across all fields then the ensemble is statistically equivalent to the flow at that point. For further details see [4]. By doing this the effect of fluctuations on the reaction rates are calculated directly with no need for closure models. The advantage of the field based method is that it is easily coupled with existing CFD techniques and is hence straightforward to implement in practical scenarios.

2. FORMULATION

Field Monte Carlo Method

More details of the Field Monte Carlo method and our implementation of it can be found in [3], a summary is included below for completeness. The spde used here is that derived using the Ito stochastic calculus, and is akin to an unsteady advection-diffusion-reaction equation with the addition of a random forcing term and a term representing micromixing. The micromixing model employed here is the interaction by exchange with the mean (IEM) model.

$$d\tau_i^n = -\bar{u}_k \frac{\partial \tau_i^n}{\partial x_k} dt + \frac{\partial}{\partial x_k} \left(K \frac{\partial \tau_i^n}{\partial x_k} \right) + \dot{w}(\tau_1^n, \tau_2^n, \dots, \tau_N^n) dt + (2K)^{1/2} \frac{\partial \tau_i^n}{\partial x_k} dW_k^n - \frac{\tau_i^n - \bar{\phi}_i}{T_{eddy}} dt \quad (1)$$

where τ_i^n is the concentration of species i in field n . $\bar{\phi}_i$ is the mean concentration of the scalar calculated over all fields. \bar{u}_k is the mean velocity in the k direction, K is the turbulent diffusivity and T_{eddy} is the scalar mixing timescale here assumed to be equal to the velocity timescale for all scalars. The term dW_i^n is an increment of a Wiener process, i.e. a process with mean zero and variance equal to time elapsed. Eq (1) is solved on a grid

covering the domain of the flow, with information about velocity and turbulence required at each grid node. As a separate CFD calculation of the flow is required, we coupled our Field Monte Carlo method with a commercial CFD package, FLUENT. This was used not only to calculate the flow field, but also by using an operator-splitting method the advection and diffusion terms in Eq (1) for each time-step. The remaining terms are then solved by a user-defined subroutine; firstly the random forcing term is calculated using a simple explicit Euler method, secondly the chemistry and micromixing is solved for each field in turn using the VODPK backward multistep solver. The advantages of coupling with a commercial CFD package are that there is no difficulty in exporting velocity field data to the reacting flow code and also that all the grid making and post-processing tools already available in FLUENT can be used with this problem. By using only one field and switching off the random and micromixing terms we are left with a standard advection-diffusion-reaction code, which allows us to observe the effect of segregation on calculated species concentrations.

Numerical Methods

The velocity and turbulence fields were calculated using a RANS method with the $k-\varepsilon$ model in FLUENT. The domain consisted of seven identical evenly spaced street canyons each of width 20m and height 24m. The total height of the CFD domain was 100m and it extended 50m upstream of the first 'building,' a total of 79,680 cells were contained within this domain. A bulk velocity of 5ms^{-1} was specified at the upstream boundary, while the downstream boundary was set to be an outflow. The top of the domain had a symmetry boundary condition and this was sufficiently far above the canyons that its effect will be negligible.

For the reacting flow calculations only the second last of the seven canyons was used with a domain extending 20m up and downstream along the adjacent rooftops and 70m in total height. This grid had a resolution half that of the CFD grid with a total of 14700 cells in this grid. The flow field was fixed for the duration of the reactive calculations by turning off the flow and turbulence solvers. A background concentration for each species was set at the inlet (left hand edge, above the building level) and initially at all points in the grid. The emission source was defined by setting a fixed value for each species in a $0.6 \times 0.3\text{m}$ region consisting of 4 grid cells centred on a point on the centre-line of the canyon 0.45m above the ground. FLUENT was then run with the reacting flow model switched off until a steady inert solution was obtained. At this point the reacting flow model is switched on and the code run as an unsteady solution. The turbulent timescale is calculated from the $k-\varepsilon$ model by $T_{eddy} = k/\varepsilon$, a turbulent viscosity is also calculated by the $k-\varepsilon$ model and this is used for K in Eq (1) thereby assuming a turbulent Schmidt number of unity. The time-step used was 0.1s and it was found that the solution did not change appreciably after 100s. 60 fields were used with the simple Baik et al chemistry but only 14 for the CBM mechanism due to constraints of user defined memory in FLUENT.

3. RESULTS AND DISCUSSION

Simple Chemistry

For the simple chemistry [1] we used a background O_3 concentration of 30ppb, NO and NO_2 were set to 0.05ppb and 0.2ppb respectively. At the emission source the O_3 level was set to zero with NO at 1000ppb and NO_2 at 10ppb. This NO_2 level is low but it allows us to observe more clearly its production by chemical reaction in the canyon. Fig. 1 shows the mean and rms values for NO_2 in and above the canyon as calculated using these boundary conditions by the FMC method. The relatively long residence time allows the reaction of NO and O_3 to build up the NO_2 in the centre of the canyon to a level of approximately 23ppb, which is more than double the level in our source. The mixing layer at the building height introduces relatively clean air into the canyon along the windward (right hand) wall, while polluted is transported out of the domain in the downwind direction. As expected, the highest variance is observed where the scalar gradient is largest. The variance is particularly large around the source, where the chemistry produces strong gradients, and in the mixing layer. In the latter the variance is of the order of the mean concentration in this region. Further analysis of the stochastic fields in this region (not shown here for reasons of space) reveal that concentrations in this region take either 'high' or 'low' values as the gradient remains steep in each field.

Fig. 2(a) shows mean and rms O_3 concentrations along a vertical line 2.5m to the left of the right hand, or windward, wall (see Fig. 1). Again we see the variance increasing to a maximum in the mixing layer at roof height. The FMC calculation does not differ from the plain advection-diffusion-reaction (ADR) by more than statistical noise seen in a similar comparison for results for a passive scalar (not shown). The same is true for results for NO and NO_2 indicating that segregation effects do not play a significant role in this situation for this chemistry. This conclusion is supported by consideration of the Damköhler number. By writing the reaction term for each species, X, in terms of production and loss, $dX/dt = P - LX$, we can define a chemical

timescale for each species based on the rate at which it will decay to its equilibrium value, hence $T_{chem}=1/L$ [6]. By using T_{eddy} as defined above we can then calculate a value for Da at each grid point. When this was done it was found that the highest Da was found for O_3 reaching a maximum of around 3 in the centre of the canyon where there is variance is low. Previous work [6] found that significant segregation effects were only observed for $Da \geq 5$, as such we would not expect a large segregation effect here.

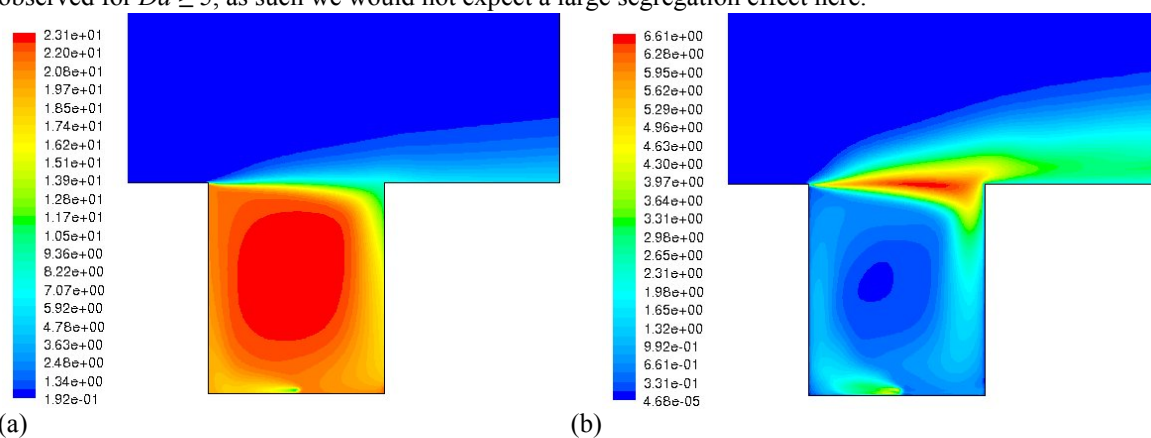


Figure 1. Contours of mean, (a), and rms, (b), NO₂ volume fraction (ppb), using simple chemistry [1]. Canyon height is 24m, width 20m.

Fig. 2(b) shows the profile of photostationary state defect along the vertical 2.5m line. This is calculated as defined by [1] and [2]:

$$\delta_{ph} = (k_1[NO][O_3]/J_{NO_2}[NO_2] - 1) \times 100 \quad (2)$$

As was found by [1] and [2], δ_{ph} is small within the canyon and in the free stream above indicating that the chemistry is close to equilibrium in these regions. However in the mixing region above the street very large values are seen indicating that the chemistry is far from equilibrium here where polluted air and fresh, O_3 rich air are mixed. Shown on the same figure are δ_{ph} calculated using results from the plain ADR model, values calculated using mean concentrations from the FMC model (defect of means) and the mean of δ_{ph} calculated using concentrations from each field (mean defect). We see that the FMC defect of mean values is slightly higher than when fluctuations are ignored, suggesting that there are small differences in calculated values of means that are not apparent when considered individually. The peak true mean defect is significantly smaller and narrower than those using mean quantities, indicating that the chemistry is closer to equilibrium. The covariance of O_3 and NO caused by their opposite gradients in the mixing region will have an effect on mean δ_{ph} which, unlike reaction rate, will be unaffected by micromixing.

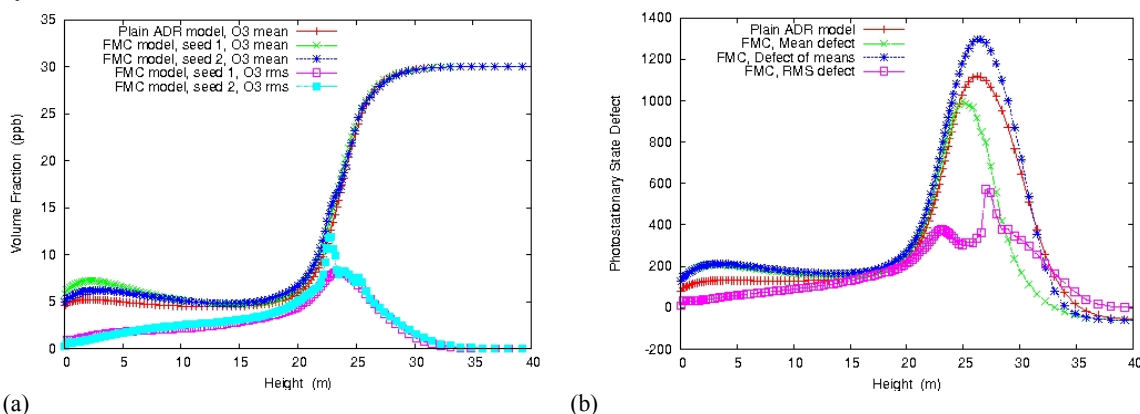
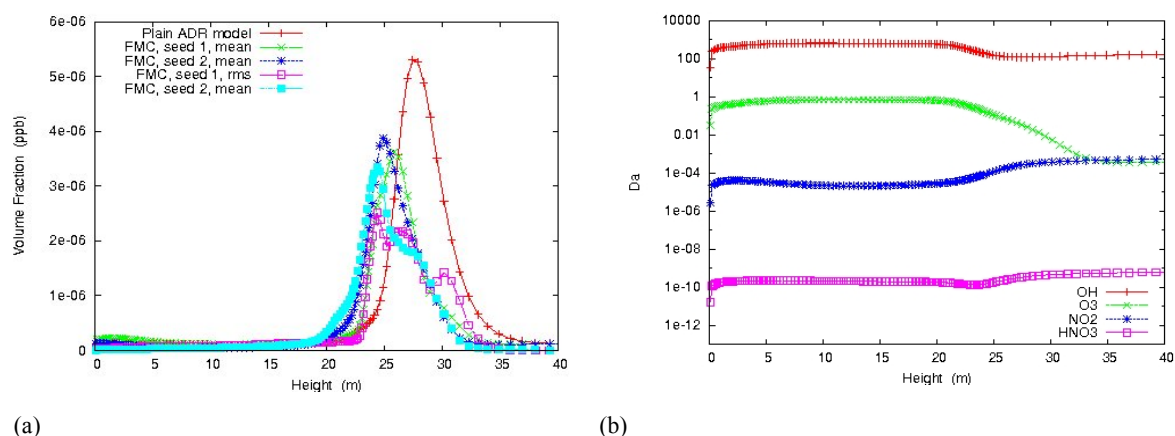


Figure 2. Profiles taken along line 2.5m from windward (right) wall using simple chemistry data. Shown are (a) O_3 mean and rms volume fraction and (b) photostationary state defect. Results from plain advection-diffusion-reaction model and the Field Monte Carlo model.

CBM-IV Mechanism

For the simulations with the CBM-IV chemistry NO , NO_2 and O_3 levels for both background and source were kept the same as for the simple chemistry. A VOC/ NO_x ratio of 35 was used for the background and a ratio of 1.0 for the source, the VOC's comprised 70% PAR and 5% each of ETH, OLE, ALD, FORM, XYL and TOL. CO was set to 1000ppb in the background and 40ppb at the source, OH and HO_2 were set to 4×10^{-6} ppb and 4×10^{-5} ppb respectively for both source and background. All other species were set to small values and allowed to achieve equilibrium levels.

It was found that predicted levels of O_3 and NO_2 using this chemistry were close to those predicted by the simple chemistry. The peak NO_2 level in the centre of the canyon was slightly higher at 25ppb compared to 23ppb. Again we saw no significant difference in the predicted levels of these species when using the FMC model as compared with neglecting segregation. No significant difference was observed for VOC's or for secondary pollutants such as HNO_2 and HNO_3 . However, significant differences were observed for NO_3 , OH, HO_2 , C_2O_3 , XO_2 , XO_2N and PHO. The variation of mean and rms volume fraction with height along the 2.5m line for OH is shown in Fig. 3(a) to illustrate this. It can be seen that when segregation is ignored the peak OH level observed in the mixing layer is too large and its position is too high. We again calculated Da values for each species using the same method as discussed previously. Again we found strong agreement between high Da and a significant micromixing effect on calculated species concentration. Those species for which large differences were seen between the two methods were the ones which had Da values greater than approximately 5. Fig. 3(b) shows the calculated Da for a selection of species, OH can be seen to have a high value. A more sophisticated method, namely Computational Singular Perturbation, is used to calculate chemical timescales for CBM-IV in [6]. The seven fastest species for their daytime, urban case are those seven species which have been found here to be affected by micromixing.



(a) (b)
Figure 3. Profiles taken along line 2.5m from windward (right) wall using CBM-IV mechanism. (a) shows mean and rms OH volume fraction from plain ADR model and FMC, (b) shows Damköhler number for four species

4. CONCLUSIONS

The Field Monte Carlo method has here been used to model the dispersion of reactive pollutants within a street canyon. This has been done with both a simple chemistry and with the more complex CBM-IV mechanism. It was found that the two mechanisms give very similar predictions for NO_2 and O_3 concentrations. The rms of concentration was found to be very high in the mixing layer at roof top level. It was found that neglecting segregation does not lead to significant errors in the calculation of major species concentrations. However a difference is seen for the photostationary state defect using the simple chemistry and in the concentration of NO_3 , OH, HO_2 , C_2O_3 , XO_2 , XO_2N and PHO using CBM-IV. These seven species have large Da compared to others in the mechanism

Acknowledgements This work has been funded by the EPSRC. AG acknowledges a Scholarship from The Leathersellers' Company.

5. REFERENCES

- [1] Baik, J-J., Kang, Y-S. and Kim, J-J. 2007. Modelling reactive pollutant dispersion in an urban street canyon. *Atmos. Environ.* 41, 934-949.
- [2] Baker, J., Walker, H. L. and Cai, X. 2004. A study of the dispersion and transport of reactive pollutants in and above street canyons—a large eddy simulation. *Atmos. Environ.* 38, 6883-6892.
- [3] Garmory, A., Britter, R. E. and Mastorakos, E. 2007. Simulation of the evolution of aircraft exhaust plumes including detailed chemistry and segregation. Submitted to *Journal of Geophysical Research*.
- [4] Garmory, A., Richardson, E. S. and Mastorakos, E. 2006. Micromixing effects in a reacting plume by the Stochastic Fields method. *Atmos. Environ.* 40, 1078-1091.
- [5] Gery et al. 1989. A photochemical kinetics mechanism for urban and regional scale computer modelling. *Journal of Geophysical Research.* 94 (D10), 12925-12956.
- [6] Neophytou, M. K., Goussis, D. A., van Loon, M. and Mastorakos, E. 2004. Reduced chemical mechanisms for atmospheric pollution using Computational Singular Perturbation analysis. *Atmos Environ.* 38, 3661-3673.
- [7] Valiño, L. 1998. A field Monte Carlo formulation for calculating the probability density function of a single scalar in a turbulent flow. *Flow Turbulence and Combustion.* 60, 157-172.

AN APPLICATION OF THE THERMO-RADIATIVE SOLENE MODEL FOR THE EVALUATION OF STREET CANYON ENERGY BALANCE

Marcin Idczak^(1,2), Dominique Groleau⁽³⁾, Patrice Mestayer⁽¹⁾, Jean-Michel Rosant⁽¹⁾, Jean-Francois Sini⁽¹⁾

¹Laboratoire de Mécanique des Fluides, UMR 6598 CNRS, Ecole Centrale de Nantes, Nantes, France

²Institute of Heating and Ventilation, Warsaw University of Technology, Warsaw, Poland

³CERMA, UMR 1563, Ecole Nationale Supérieure d'Architecture de Nantes, Nantes, France

ABSTRACT

This paper presents street canyon energy balance measurements compared to numerical simulations. Field measurements were conducted during the campaign JAPEX (Idczak et al 2006). Four lines of buildings composed of steel containers were installed to form three parallel street canyons at 1:5 scale. The aspect ratio was 0.40. Meteorological conditions were measured at ground level and on a 10 m mast. Also long-wave and short-wave radiation and surface temperatures were measured inside the street canyon at selected points. In addition, the net radiative balance was registered at the canyon top. Numerical simulations were carried out with SOLENE, a software developed for environmental assessment of urban structures. Using the meteorological measurements as model input, the simulated surface temperatures and radiation fluxes were correlated with the measurements for a day with clear sky conditions. The comparison showed a good agreement demonstrating SOLENE's applicability for energy balance analysis of a narrow street canyon with low thermal capacity of building walls.

1. INTRODUCTION

The investigation of how radiative energy is converted into heat within a street canyon is important for various reasons as, e.g., the impact of energy fluxes on in-canyon airflow and further on pollutant dispersion, urban buildings energy loads or thermal comfort within the street. However, works presenting a complete measurement-based analysis of all street canyon energy balance components are very rare. Often street canyon energy budget studies are supported with the results of numerical simulations. This paper presents street canyon energy budget measurements compared to numerical simulations with the thermo-radiative model SOLENE. The aim of the work was to validate the use of SOLENE for street canyon energy balance analysis.

2. METHODOLOGY

2.1. Measurements

The JAPEX campaign was conducted at the experimental site constructed within the framework of the PICADA project (Demilecamps and Andre, 2005), situated in the industrial area in Guerville (48°56'N, 1°44'W), France, about 40 km west from Paris. Four consecutive rows of buildings formed 3 similar and parallel street canyons at a 1:5 scale (Figure 1). Each building was composed of 4 superimposed, empty steel containers. The buildings dimensions were: length $L = 18.3$ m, height $H = 5.2$ m, and width $B = 2.4$ m. The street width was $W = 2.1$ m. The aspect ratio (W/H) was approximately 0.40. The street axis formed an angle of 54° with north. The steel containers walls were lined with cement panels. At $z = 2.5$ m, at containers junction, the panels were joined with a stripe of tin plate 0.32 m wide. The soil was covered with bright gravel. The measurement period lasted from July 7 to October 20, 2004.



Figure 1. Guerville experimental site: a) site overview, b) instrumentation in the investigated street.

The central street was instrumented with following sensors (Figure 2):

- two pyranometers (CG1 Kipp & Zonen) placed within the canyon at $y = 0.3$ m from the wall, facing the southern façade at two levels: KL at $z = 1$ m and KH at $z = 2.10$ m,
- two pyrgeometers (CM6B Kipp & Zonen) placed within the canyon at $y = 0.3$ m from the wall, facing the southern façade at two levels: LL at $z = 1$ m and LH at $z = 2.47$ m,
- one net radiometer Rn (NR-LITE Kipp & Zonen) placed in the street centre at the canyon top at $z = 5.2$ m,
- 16 thermocouples measuring surface temperatures inside the canyon at various levels (type T 36 AWG),
- one pyranometer measuring global solar radiation on a horizontal surface,
- other instruments not relevant for this study (see Idczak et al., 2006).

The acquisition rate was 10 values/minute. Averaged data were stored each 15 min.

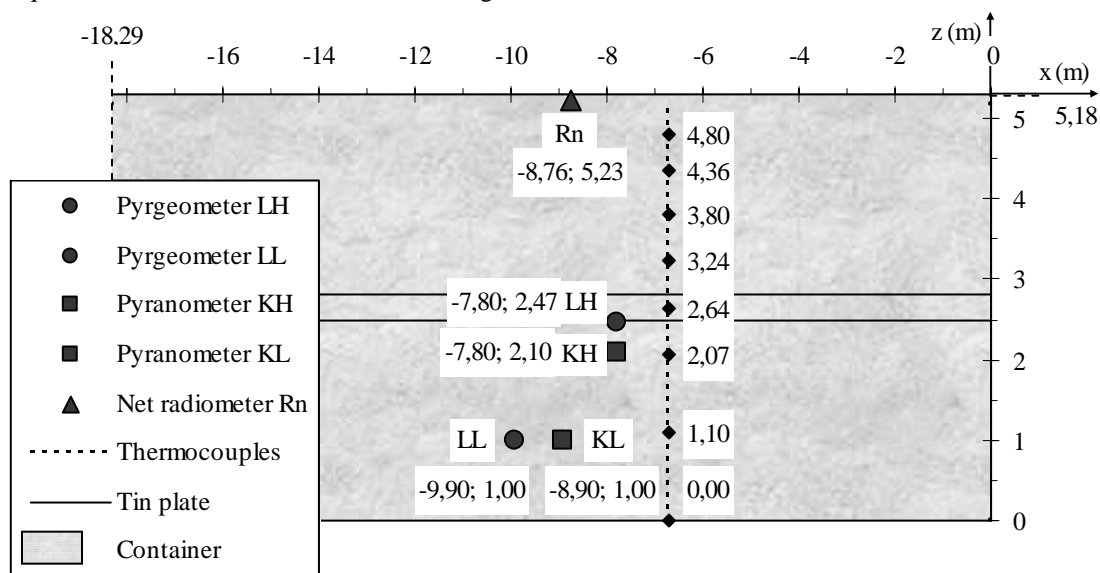


Figure 2. Positions (x,z coordinates) of the instruments in front of the southern façade.

2.2. Simulations

Using the reference meteorological measurements as model input the simulations were carried out using SOLENE, for a day with clear sky conditions (28 July 2004). SOLENE has been developed at Cerma Laboratory in order to study the environmental aspects of urban structures (Miguet et al. 1996). Based on the 3D model of finite elements it allows evaluation of direct and diffuse solar radiation components and determination of solar energy absorbed, taking into account multiple reflections between the buildings and the ground. SOLENE enables estimation of the resulting surface temperatures as well as the infrared radiative fluxes.

The computational domain has been limited to the central street canyon comprising two parallel walls and the street surface. A triangular grid of 14273 cells was applied. The resolution was chosen to allow accurate results with a reasonable running time. The physical properties of canyon materials used for calculations (Table 1) were applied according to ASHRAE Fundamentals (2001). The simulations were carried out with 15 minutes time step for the period of 24 hours.

Table 1. Physical properties of street canyon materials

	d [m]	a [-]	ϵ [-]	λ [W/mK]	c_p [J/kgK]	ρ [kg/m ³]
	Thickness	Surface albedo	Emissivity	Thermal conductivity	Specific heat	Volumic mass
Canyon walls - upper and lower container						
Cement panel	0.013	0.6	0.95	0.900	800	2000
Air gap	0.030	-	-	0.026	1005	1.2
Steel	0.003	-	-	45.300	500	7830
Canyon walls - containers junction						
Tin plate	0.002	0.7	0.30	45.300	500	7830
Air gap	0.041	-	-	0.026	1005	1.2
Steel	0.003	-	-	45.300	500	7830
Bottom of the canyon						
Gravel	0.150	0.4	0.95	1.100	870	2100
Soil	2.000	-	-	1.300	920	1800

3. RESULTS AND DISCUSSION

Following figures compare the simulated canyon surface temperature profiles with the measurements at selected points. The first graph shows the soil temperature at the point where canyon wall meets the street surface (3a,d), next two of the surface of the lower (3b,e) and upper (3c,f) container wall. The simulated diurnal cycles show a good agreement with the measurements, however there are some temperature values differences especially relevant at extremes.

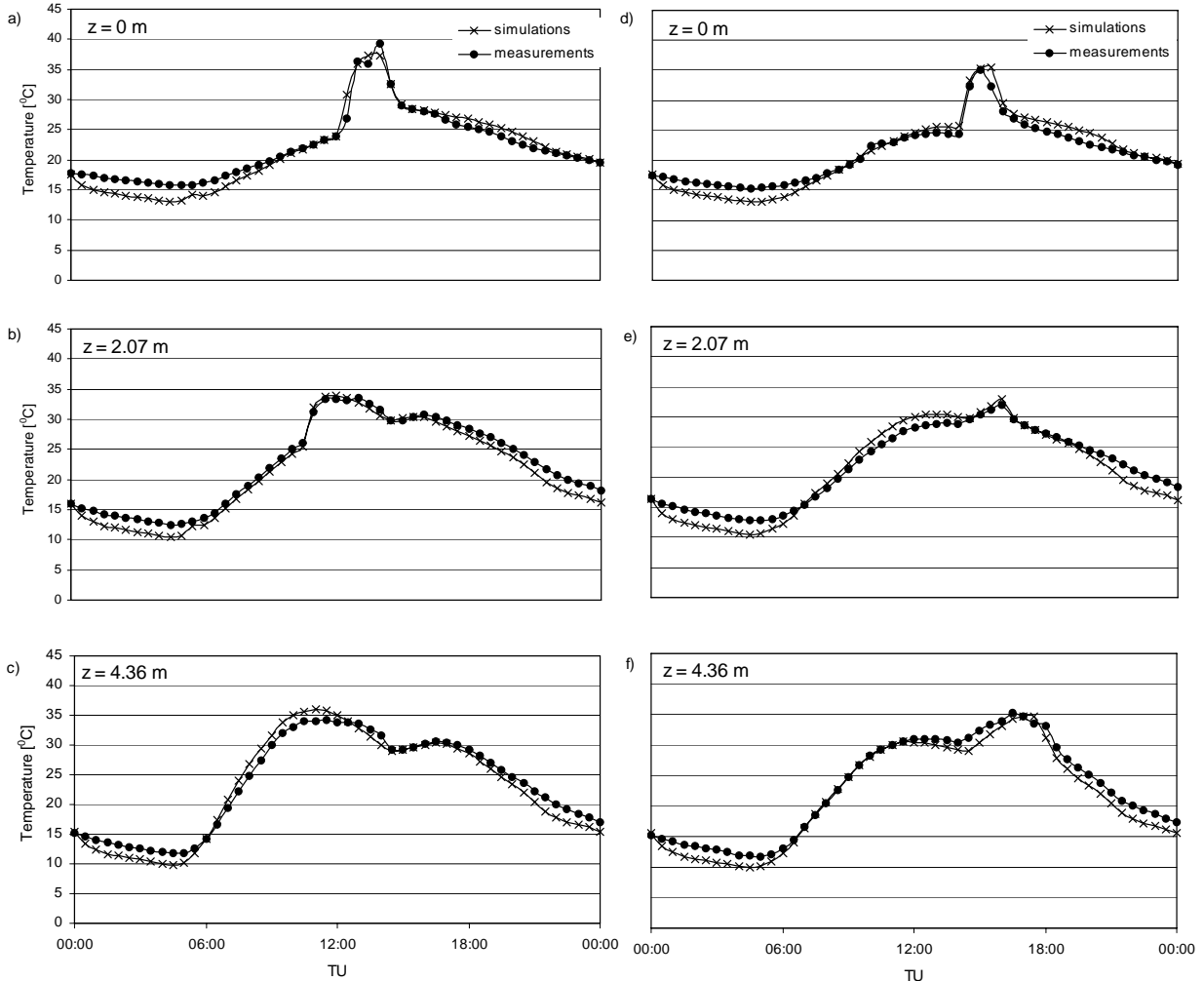


Figure 3. Street canyon surface temperature measurements versus simulations: left - southern façade, right – northern façade.

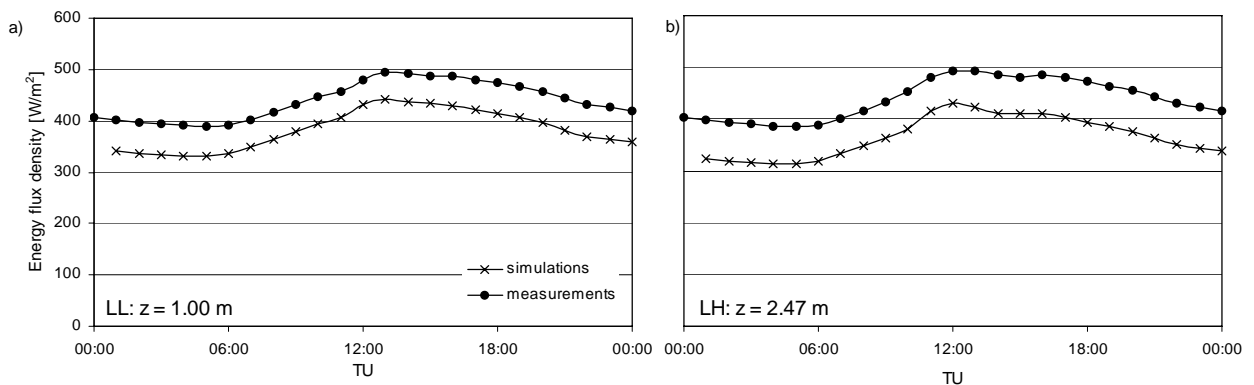


Figure 4. Pyrometers measurements versus simulations: a) LL, b) LH.

Figure 4 presents the comparison between the simulations and measurements of pyrometers LL and LH. The radiometers faced the southern façade measuring infrared radiation emitted and reflected by the wall. The simulated daily profiles are identical to the measured ones but with a nearly constant shift of about 50 W/m^2

lower. This underestimation is probably caused by a model deficiency since for the infrared radiation SOLENE computes the surface emissions without taking into account the multiple reflections within the canyon. A rough calculation shows, e.g., that the direct reflection of the atmospheric and opposite wall infrared fluxes has a magnitude of 30-40 W/m² at the least.

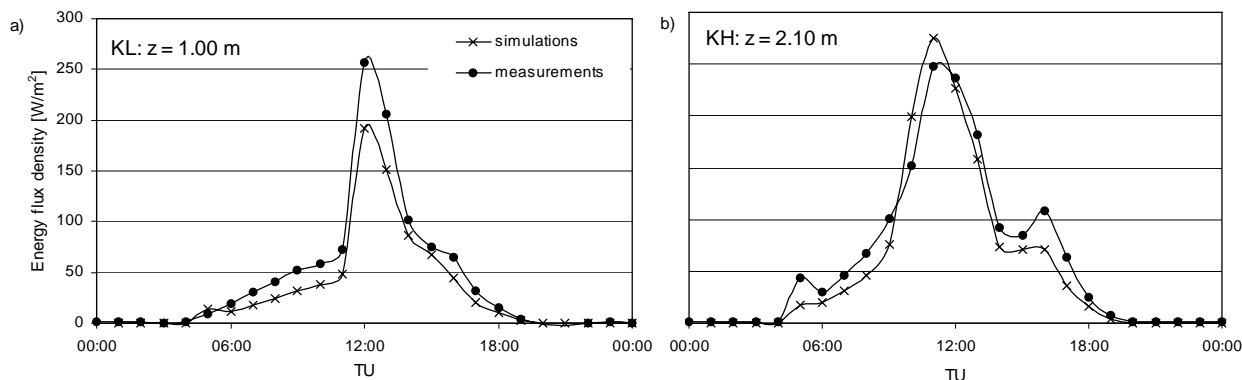


Figure 5. Pyranometers measurements versus simulations: a) KL, b) KH.

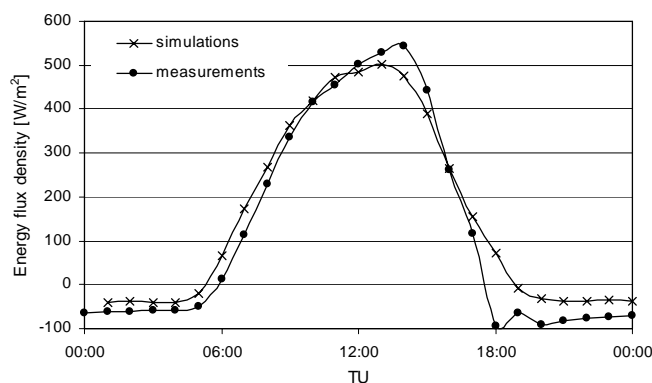


Figure 6. Net radiometer (Rn) measurements versus simulations.

Figure 5 presents the comparison between the simulations and measurements of pyranometers KH and KL. Radiometers faced the southern façade measuring the solar radiation reflected from the wall. The simulations show good agreement with the measurements, however the simulated radiative flux is underestimated in the lower part of the canyon. Figure 6 presents the comparison between the net radiation simulations at canyon top and the measurements of the net radiometer. The agreement is satisfactory.

4. CONCLUSIONS

The results of simulations show a good agreement with the measurements. The SOLENE model can be a useful tool allowing to conduct an analysis of energy balance of a narrow street canyon with low thermal capacity of building walls. Further studies need to follow to verify the SOLENE's general applicability for street canyon energy balance modelling. Some developments in the model are considered to improve the coherence of the simulation results with the measurements, especially to improve the simulation of infrared radiative fluxes within the canyon.

5. ACKNOWLEDGEMENTS

The presented work was carried out within ATREUS network, operating in the framework of European Commission Training and Mobility of Researchers Programme.

6. REFERENCES

- [1] ASHRAE Handbook, Fundamentals 2001, ASHRAE, Atlanta, Georgia, 2001.
- [2] Demilecamps L, André H (2005) Le projet PICADA (Photocatalytic Innovative Coverings Applications for Depollution Assessment). Travaux 821:69-73.
- [3] Idczak M., Mestayer P.G., Rosant J.-M., Sini J.-F., Violeau M., Micrometeorological measurements in a street canyon during the joint ATREUS-PICADA experiment, *Boundary-Layer Meteorology*, to appear (DOI 10.1007/s10546-006-9095-z), 2006.
- [4] Miguet F., Groleau D., Marenne C., 1996, A combined sunlight and skylight tool for microclimatic analysis in urban architectures, In: *Solar energy in architecture and urban planning*, Fourth European Conference, Berlin, 1996.

COMPUTATIONAL SIMULATION OF THE RESIDENCE OF AIRBORNE POLLUTANTS IN THE WAKE OF A 3-DIMENSIONAL CUBE

I. Mavroidis¹, S. Andronopoulos^{2,} and J.G. Bartzis^{2,3}*

¹*Hellenic Open University, Patras Greece*

²*Environmental Research Laboratory/INT-RP, NCSR Demokritos,
15310 Aghia Paraskevi Attikis, Greece*

³*University of Western Macedonia, Dept. of Engineering and Management of Energy Resources, Bakola &
Sialvera Str., 50100, Kozani, Greece*

ABSTRACT

This paper presents a computational investigation of the residence of atmospheric contaminants in the wake of an isolated cubical building using the computational fluid dynamics code ADREA-HF. Characteristic concentration decay times describing the detrainment behaviour of gas in the near-wake are assessed for different atmospheric stability conditions and the results are compared with experiments conducted in the field (Mavroidis et al., 1999). Two building orientations are examined, with the mean wind direction approximately normal to or at 45° to the leading face of the cubical building. The results showed that the non-dimensional residence time (τ) is independent of the atmospheric stability conditions, as also indicated by the experimental measurements. Both mean concentrations and characteristic decay times calculated by the model agree in general with the experimental values. The transient behaviour of the concentration fluctuations in the wake of the building is also studied through the model results.

1. INTRODUCTION

Information on flow and dispersion around an isolated obstacle is very useful in identifying the effect of a building or any other construction on the behaviour of plumes released in their vicinity. Although the effect of atmospheric stability on the dispersion of a plume in the atmosphere has been the subject of numerous investigations, there is limited work on the effects of atmospheric stability on dispersion in the wakes of buildings (e.g. Zhang et al., 1996). One of the aspects of building influenced dispersion that requires special attention is the residence of contaminants in the near wake of an obstacle. This is because when entrainment of a contaminant into the wake of an obstacle ceases, a transient, secondary wake-source is generated. This source decays gradually as contaminant is detrained from the wake. Characterisation of this behaviour is of particular interest when contaminants are released for a finite length of time or when there is a temporary shift in the wind direction. The residence behaviour of contaminants has been mainly investigated in the wind tunnel for different shapes and orientations of obstacles, while limited research has also been undertaken in the field. A more detailed review of such investigations is provided by Mavroidis et al. (1999).

The present work aims to calculate, using the computational fluid dynamics (CFD) code ADREA-HF, characteristic concentration decay times in the near wake of an isolated cubical building and to compare them with detailed results from field experiments. The main purpose is to evaluate the performance of the ADREA-HF model in the prediction of the transient feature of concentration decay in an obstacle-obstructed flow, when the gas source is cut-off. An important feature of the work described in this paper is that it examines, using a CFD code, the detrainment behaviour of a gas plume in the near wake of the obstacle under different stability conditions, including under very low wind speeds.

2. METHODOLOGY

2.1 Field Experiments

The field experiments, conducted southwest of Salt Lake City in the USA, are described in detail by Mavroidis et al. (1999). The roughness length of the site, calculated from velocity profile measurements, was approximately 16 mm. A 2 m plywood cube was used for the experiments, which could be readily rotated to the required orientation. Two orientations of the cube were investigated, such that the mean wind direction was approximately normal to or at 45° to the leading face of the cube. Propylene was used as a tracer gas. The gas source was located 2.5H upwind of the cube and at the building height (H). The tracer gas was released at a steady rate for a minimum period of 30 s to fill the wake region with contaminant. The release conditions were such that the gas behaved essentially as a passive tracer. Then the gas source was cut-off and the decay of concentration was monitored by fast-response point monitors (UVIC detectors) located within the near-wake region. Five detectors were located across the width of the wake, with a separation of 0.375H (0.75 m) between them, at a height of 0.5H and at a distance of 0.75H downwind of the rear face of the cube. Two additional detectors were deployed, one located at the centre of the upwind face of the cube and the other 3.0H downwind of the rear face of the cube, on the centreline and at height of 0.5H. Experiments were performed at different times of the day to cover a variety of stability conditions, ranging from unstable to

* **Corresponding Author.** Tel. +30 210 6503426, e-mail: sandron@ipta.demokritos.gr

stable. The tracer concentration measurements were supported by meteorological data collected by an ultrasonic anemometer located at the same height and upwind distance as the gas source. In the present paper CFD calculations are presented and compared for six experimental cases. The main experimental and meteorological details are presented in Table 1.

Table 1. Experimental and meteorological details for the six simulated experiments (the desired wind direction is 180°)

Experimental case	Orientation of cube (°)	C ₃ H ₆ flowrate (m ³ /s)	Mean wind speed (m/s)	Mean wind direction (°)	T (°C)	Monin-Obukhov length (m)
UTE02/2	0	1.38x10 ⁻⁵	1.12	165.0	9.9	0.6
UTF04/2	0	7.07x10 ⁻⁵	0.38	170.6	15.2	14.8
UTE05/5	0	2.77x10 ⁻⁵	1.20	172.8	24.4	-2.2
UTK01/2	45	4.15x10 ⁻⁵	0.53	165.2	19.5	1.2
UTK06/8	45	7.07x10 ⁻⁵	1.60	164.2	18.5	1.4
UTK09/3	45	1.14x10 ⁻⁴	2.02	178.8	27.0	-0.9

2.2 Modelling Approach

The CFD code ADREA-HF, developed by the Environmental Research Laboratory, has been used for the simulations presented in this article. The purpose of ADREA-HF is to simulate the dispersion of buoyant or passive pollutants over complex geometries (Andronopoulos et al. 1994, Statharas et al. 2000, Venetsanos et al. 2003). ADREA-HF is a finite volumes code that solves the Reynolds-averaged equations for the mixture mass, momentum, energy, pollutant mass fraction and the variance of the pollutant mass fraction. Turbulence closure is obtained through the eddy viscosity concept, which is calculated by a 1-equation *k-l* model. The turbulent kinetic energy *k* is calculated by a transport equation. The effective length scale *l* depends on the flow stability and on the distance from solid boundaries, so in the general case it is three-dimensional. For the simulations presented in this article, a uniform length scale approach has been adopted, taking into account the shortest distance from the solid boundary. Details of the modelling approach regarding the concentration variance are included in Andronopoulos et al. (2002).

In this paper the results of the computational simulations for the six experimental cases listed in Table 1 are presented. In the simulations all the experimental and atmospheric conditions have been taken into account: gas source dimensions, release rate, physical properties of the gas, atmospheric stability, wind velocity and temperature. The CFD code was run with the gas source switched on, until a steady state situation was achieved. At this time the source was switched off and the run continued until the concentration dropped to values close to zero. The calculated concentration-time history at the locations of the five experimental sensors inside the building wake was used to estimate the residence time. Two characteristic cases of the calculated concentration decay are shown in Figure 1 in semi-log plots. It can be seen that it is reasonable to assume that the concentration decreases exponentially. Therefore, the residence time (*T_d*) has been defined as the time it takes for concentration to decay to 1/e of its original value after the source was switched off. The non-dimensional residence time (*τ*) was derived by the equation $\tau = UT_d/H$, where *U* is the wind speed (m/s) at obstacle height and *H* is the obstacle height (m), according to Mavroidis et al. (1999). The same approach was applied to estimate the transient behaviour of the concentration fluctuation (which was defined as the square root of the concentration variance calculated by the CFD code).

In addition to the above, seven additional computational simulations have been performed to investigate the effect of the atmospheric stability conditions on the residence times. In these simulations all the parameters were kept constant (gas release rate, wind velocity, temperature) except for the atmospheric stability which was varied, in order to cover the range between Pasquill classes A to G. These simulations were performed for wind direction perpendicular to the cube's front face (i.e. orientation of cube 0°).

3. RESULTS AND DISCUSSION

The concentration-time histories presented in Figure 1 show the exponential concentration decay and also that concentrations are more uniformly distributed in the building wake when the building is oriented at 45° to the wind. This is due to the wider wake and increased mixing present in this case. Furthermore the concentration decays much faster in the case with unstable atmospheric conditions, due to the increased buoyancy-generated mixing, but also due to the mechanically-generated mixing caused by the higher wind speed.

In Table 2, the experimental and calculated values of the non-dimensional residence time *τ* and of the residence time *T_d* are presented for the concentration in the simulated real cases. The cube orientations relative to the wind direction and the gas source, as well as the atmospheric stability conditions are also

reported. It can be observed that the calculated values are on the average 43% higher than the experimental ones for the 0° cube orientation, while they are on the average 10% lower than the experimental for the 45° cube orientation. It is noted that higher values of τ and T_d indicate lower dilution rates of the contaminant in the building wake. The second observation is that although the T_d is smaller in the unstable atmospheric conditions (both experimental and calculated), the non-dimensional τ remains almost constant. The experimental τ values are distinctively larger when the cube is orientated at 45° to the direction of the wind and the gas source. The calculated τ values are also larger for this cube orientation but to a smaller extent.

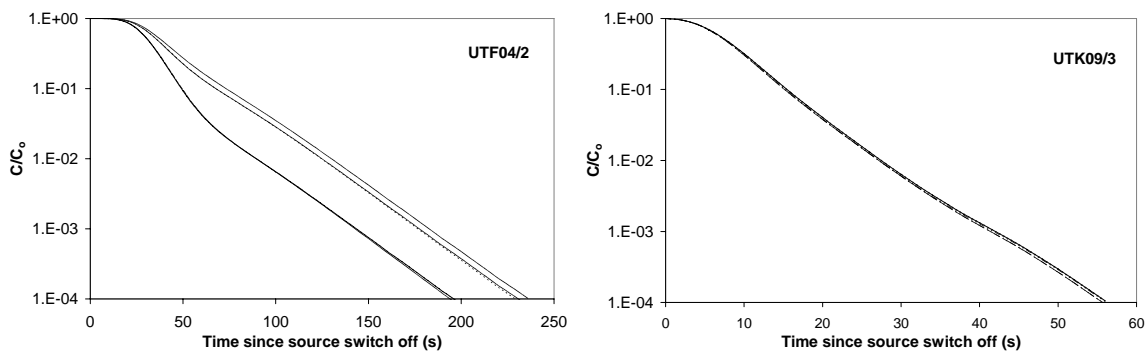


Figure 1. Calculated concentration decay at the sensors located in the building wake; case UTF04/2: cube orientation 0°, stable atmospheric conditions; case UTK09/3: cube orientation 45°, unstable atmospheric conditions

Table 2. Comparison between experimental and calculated values of the non-dimensional residence time (τ) and of the residence time (T_d) for concentration for the simulated real cases

Experimental case	Orientation of cube (°)	Atmospheric stability	Experimental τ	Experimental T_d (s)	Calculated τ	Calculated T_d (s)
UTE02/2	0	Stable	5.72	10.22	8.09	14.45
UTF04/2	0	Stable	5.54	29.17	7.48	39.36
UTE05/5	0	Unstable	5.30	8.84	8.10	13.50
UTK01/2	45	Stable	9.10	34.34	7.51	28.34
UTK06/8	45	Stable	9.38	11.72	8.97	11.22
UTK09/3	45	Unstable	10.28	10.18	9.36	9.27

The transient behaviour of the concentration fluctuations in the building wake have been studied through the computational simulations by calculating the respective τ and T_d in the same way as for the concentrations. The results are reported in Table 3. No experimental data are available for the decay of the concentration fluctuations; therefore Table 3 includes only calculated values. It is noted that the concentration fluctuations have slightly higher residence times than the concentrations. Regarding the dependence on the stability conditions the conclusions are similar to those for concentrations.

Table 3. Calculated values of the non-dimensional residence time (τ) and of the residence time (T_d) for concentration fluctuations for the simulated real cases

Experimental case	Orientation of cube (°)	Atmospheric stability	Calculated τ	Calculated T_d (s)
UTE02/2	0	Stable	8.43	15.06
UTF04/2	0	Stable	7.30	38.41
UTE05/5	0	Unstable	8.60	14.33
UTK01/2	45	Stable	7.38	27.84
UTK06/8	45	Stable	9.49	11.86
UTK09/3	45	Unstable	10.15	10.05

The isolated influence of the atmospheric stability on the pollutant residence time in the building wake is seen in Table 4. In these simulations all the parameters are kept constant except for the stability. It is noted that, as expected, the residence times increase as we pass from unstable to stable conditions. This increase is slow in the unstable classes (A, B, C), while it is steeper in the stable conditions (from E to F and G).

Table 4. Calculated values of the residence time (T_d) for concentration and concentration fluctuations for different atmospheric stability conditions (cube orientation 0°)

Simulated Atmospheric Stability	Concentration T_d (s)	Conc. fluctuation T_d (s)
A	12.62	13.45
B	12.77	13.57
C	12.91	13.69
D	13.26	14.02
E	13.86	14.53
F	15.01	15.57
G	17.17	17.60

4. CONCLUSIONS

The concentration decay in the wake of an isolated cubical obstacle after an upwind gas source has been switched off is examined in this paper using a CFD code and the results are compared with field experimental data. The simulations show that the concentration decays exponentially, in agreement with the experimental observations and this decay is faster for unstable atmospheric conditions. Two orientations of the cubical obstacle relative to the direction of the wind have been examined. When the orientation is at 45° , the concentrations in the obstacle wake are more uniformly distributed, as it appears from the results of the calculations at the locations of the sensors in the downwind building wake.

In the simulation of the field experimental cases, the CFD code underestimated the dilution rate of the contaminant in the building wake, in comparison to the experimental data, when the wind direction was perpendicular to the cube's front face. When the cube was oriented at 45° to the wind direction, the dilution rate in the building wake was overestimated, but to a smaller extent.

The residence time T_d (both experimental and calculated) is smaller in the case of unstable atmospheric conditions, because then the gas is diluted faster than when the conditions are stable. In contrary, the non-dimensional time τ does not exhibit any dependence on atmospheric stability both in the model and the experiments. However, the experimental time τ is substantially larger when the cube is orientated at 45° relative to the wind direction, a characteristic that the model predicts to a smaller degree. The transient response of concentration fluctuations when the gas is switched off is slightly slower than that for concentrations, but exhibit the same behaviour regarding their dependence on stability conditions.

Computational simulations of "theoretical" cases with the wind direction normal to the cube's front face, in which only the stability conditions varied, have demonstrated a gradual increase of the contaminant residence time in the building wake, as stability conditions move from unstable to stable. The increase becomes steeper as the very stable conditions are reached.

5. ACKNOWLEDGEMENTS

The field experiments were performed with the support of the Atmospheric Dispersion Modelling Group at DSTL Porton Down for under agreement 2044/15/CBDE.

6. REFERENCES

- Andronopoulos, S., Bartzis, J.G., Würtz, J., Asimakopoulos, D. (1994) Modelling the effects of obstacles on the dispersion of denser-than-air gases, *Journal of Hazardous Materials* 37, 327-352.
- Andronopoulos, S., Grigoriadis, D., Robins, A., Venetsanos, A., Rafailidis, S. and Bartzis, J.G. (2002) Three-dimensional modelling of concentration fluctuations in complicated geometry, *Environmental Fluid Mechanics* 1, 415 – 440.
- Mavroidis, I., Griffiths, R.F., Jones, C.D. and Bilotft, C. (1999) Experimental investigation of the residence of contaminants in the wake of an obstacle under different stability conditions, *Atmospheric Environment* 33, 939-949.
- Statharas, J.C., Venetsanos, A.G., Bartzis, J.G., Würtz, J., Schmitchen, U., (2000) Analysis of data from spilling experiments performed with liquid hydrogen, *Journal of Hazardous Materials* 77, 57-75
- Venetsanos, A.G., Huld, T., Adams, P., Bartzis, J.G., (2003) Source, dispersion and combustion modelling of an accidental release of hydrogen in an urban environment, *Journal of Hazardous Materials* 105, 1-25.
- Zhang, Y.Q., Arya, S.P. and Snyder, W.H. (1996) A comparison of numerical and physical modeling of stable atmospheric flow and dispersion around a cubical building, *Atmospheric Environment* 30(8), 1327-1345.

A POTENTIAL RISKS IN INDUSTRIAL SITES – WIND TUNNEL STUDY

Z. Janour¹, K. Bezpalcova¹, M. Yassin¹, K. Brych², F. Dittrř², F. Dittrich³

¹Institute of Thermomechanics AS CR, Prague +420266053273, janour@it.cas.cz, ²Institute of Hydrodynamics, ³Regional Authority of the Pardubice Region

ABSTRACT

Gaseous dispersion over complicated urban area after an accident with an escape of chlorine in chemical factory is investigated experimentally in a wind tunnel experiments under neutral conditions by using a Laser Doppler Anemometer and Analyser IREX. Diffusion fields in a turbulent boundary layer are simulated using a model of landscape surrounds the factory at a scale of 1:1000. The obtained results indicate that the morphology is one of the important parameters in studying atmospheric diffusion. The strong turbulent mixing inside the urban surface layer is created rapid decreasing of the surface concentrations. Moreover, the diffusion measured in these experiments may be used to develop and evaluate operational models to predict the dispersion chlorine in chemical factory.

Keywords: *Atmospheric turbulence, Flow visualization, Gas dispersion, Wind tunnel modeling.*

1. INTRODUCTION

One of the most significant cases of environment pollution is an accident with an escape of harmful substances. The possible source of such an escape is a device that contains a bigger amount of a harmful gas or contains a substance, which can release gas in appropriate conditions, e.g. a cooling system full of ammonia, containers with a liquid gas (chlorine, propane-butane...) and gases developed in fire of plastic. Another activity that can participate in an atmospheric pollution is an intentional fault. More and more frequent attacks of radical groups are aiming to cause as large impact as possible. Sarin leakage in the subway of Tokyo, events of September 11th, and attack on Spanish trains have unfortunately proved this hypothesis. Such attacks can have a character of accident with a release of bigger amount of a dangerous substance into the ABL.

Numerous studies have investigated gases dispersion through wind tunnel experiments in industrial areas e.g. Hatcher and Maroney, (1999); Singh, (1990); Quaranta at el. (2000) and others. However, some of these studies are not suitable for predicting concentrations because the number of data is insufficient to determine the ground level concentration. Despite of, several prediction models (Hyun Sun Oh and Young Sung Ghim, (2001) and others) have been developed for the diffusion process in the internal boundary layer, it is difficult to apply them directly to air pollution under complicated geometry, meteorology, and source conditions. The aim of the present work is to present and discuss the results of the wind tunnel study of the gases dispersion over urban area after an accident with an escape of chlorine in chemical factory to compare these results with the corresponding operational model data.

2. EXPERIMENTAL SET-UP

2.1 THE WIND TUNNEL MODEL

Diffusion experiments were carried out in the stratified boundary layer wind tunnel in the Institute of Thermomechanics, Czech. It is open-circuit tunnel. The width and height of the test section were 1.5 and 1.5m. The upwind fetch was 25.5m. A free stream velocity of $U_{ref} = 4\text{m/s}$ was employed and spires and roughness blocks were set on the wind tunnel floor at the entrance.

The power law $U \propto Z^n$ was applied to the vertical wind profile. The typical value of $1/4$ for the power number n in an urban area was employed. However there is a range of other possible values for n . For details of such typical values of the power law exponent for different terrain types, refer to Snyder(1985).

2.2 INSTRUMENTATION

The reference velocity U_{ref} and the temperature were measured by a complete anemometer with velocity sensor and temperature sensor - Steel Clad Transducer 54T28 (DANTEC – uncertainty $\pm 0.02\text{ m/s}$, $\pm 0.2\text{ }^\circ\text{C}$) on the axis of the inlet to the working section.

The turbulence characteristics of the flow field were measured by a 2D fibre-optic Laser Doppler Anemometer. Concentrations measurements were carry out with the ten probe infrared CO₂ analyser IREX. The LDA probe head and IREX sampling needle has been mounted on the computer-controlled 3D traversing system that enables displacements all over the test section with precision of order 0.1 mm for each directions.



Figure 1 Spires and roughness elements inside the Environmental wind tunnel of the IT

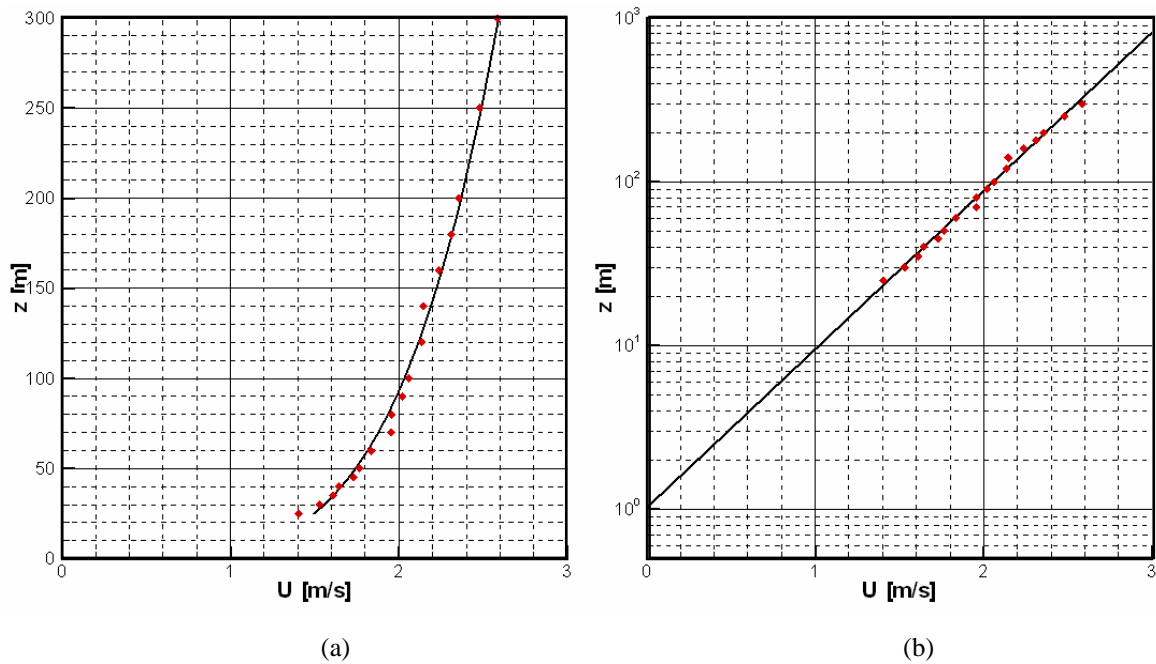


Figure 2 Mean velocity profile across the surface layer (a) and across the urban boundary layer (b)

2.3 SIMILARITY CONDITIONS

The similarity requirements for wind tunnel experiments on atmospheric diffusion problems mainly include the following: a) the geometry of the topography; b) the ratio of the pollutant releasing speed to that of the air flow, and atmospheric conditions and c) the ground boundary layer characteristics (roughness, wind profile, etc.). Further, the three parameters representing the ratio of inertial properties to the molecular properties are (1) Reynolds number Re ; (2) Peclet number and (3) Schmidt number. The similarity of geometry, flow field, and emission conditions were considered. A neutrally stratified boundary layer over agricultural landscape was modelled at the inlet using a modified spires and roughness configuration which is shown in Fig. 1. Mean velocity profile across the surface layer and across the urban boundary layer are shown in Fig.2. The following values of parameters of the atmospheric boundary layer in full scale were determined from the profiles: roughness length $z_0 = 0,6$ m, (for agricultural area $z_0 \approx 0,5$ according to ASCE (1995)), power law exponent $n=0,2$ (for agricultural area is $n \approx 0,29$ according to ASCE (1995)) and zero ground displacement $d_0 = 6$ m.

In addition, a model of a landscape on scale 1:1000 is shown in Fig. 3 which was manufactured and mounted into working section of the wind tunnel to model the boundary conditions on the surface.



Fig. 3 Model of the landscape on scale 1:1000

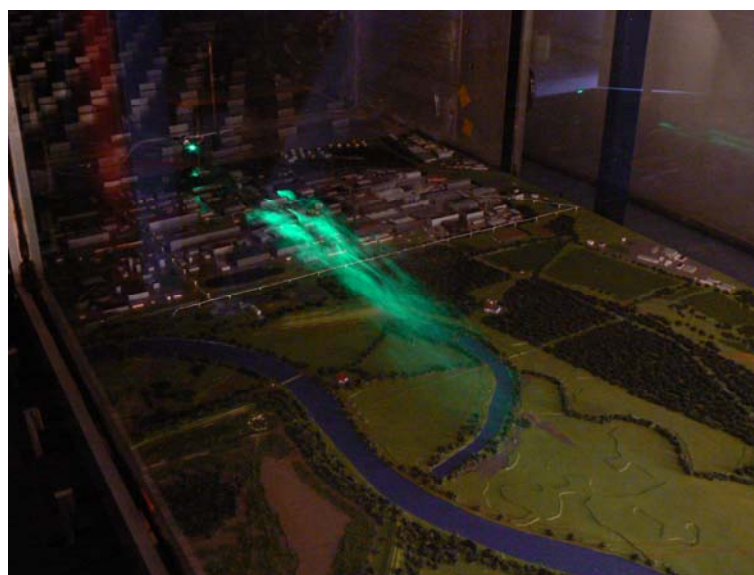


Fig. 4 Plume spread visualisation

3. RESULTS AND DISCUSSIONS

To clarify the change in the dispersion characteristics with changes in wind direction, smoke visualization was done in the wind tunnel to see what kind of dispersion characteristics appear in the landscape model. The diffusion field measurements were performed for three different wind velocity directions. Fig. 4 illustrates a qualitative analysis of the plume spreading started using the visualisation method. The surface concentrations that are pasted on landscape photograph for MW and SW wind direction as an example of them are shown in Figs. 5a and 5b. The 30 ppm contour is pointed up in the figure as the upper limit for human disablement. An influence of buildings configuration is evident from the figure. System of rows of five stories long buildings surrounds the surface point source. The strong turbulent mixing inside the urban surface layer causes rapid decreasing of the surface concentrations for NW approaching wind, which is shown in Fig. 5a and increasing the area with the high level of the surface concentrations can be described by channelling effect for SW approaching wind direction, which is fig. 5b as the consequence of the buildings configuration.

The results were compared with results received from numerical simulation by commercial operational Gaussian type model. This model did not take into account the complicated terrain and therefore the contours are symmetric one.

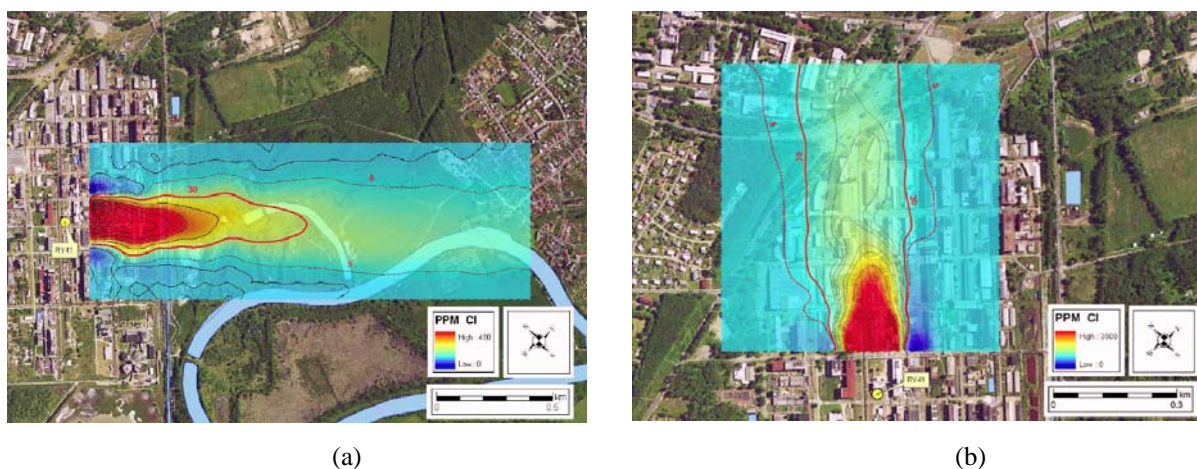


Fig. 5 Concentration contours at height 1.7 m in ppm scale (a) NW wind direction, (b) SW wind direction.

4. CONCLUSIONS

The gaseous diffusion over complicated urban area using wind tunnel experiments under neutral atmospheric conditions with different wind directions may be summarized as the follows: (a) The wind direction is one of the important parameters in studying atmospheric diffusion over complicated terrain, (b) The strong turbulent mixing inside the urban surface layer is created rapid decreasing of the surface concentrations, (c) An influence of buildings configuration is observed in the surface gaseous concentrations .

5. ACKNOWLEDGEMENTS

This work was supported by the Ministry of Education, Youth and Sports of the Czech Republic within the framework of the COST 732 project and Research project Z20760514.

6. REFERENCES

- ASCE 1995. Manual of Practice for Wind Tunnel Studies of Buildings and Structures, American Society of Civil Engineers, Aerospace Division.
- Bezpalcova et.al.2007. Modelling of Release and dispersion of Harmful Gas - Case of the Prague Downtown, 6th International Conference on Urban Air Quality, Cyprus.
- Hatcher and R. N. Maroney 1977. Dispersion in the wake of a model industrial complex, Joint Conference on Application on air pollution meteorology, Utah, USA, November.
- Hyun Sun Oh and Young Sung Ghim 2001. Numerical study of atmospheric dispersion of a substance released from an industrial complex in the southern coast of Korea , Atmospheric Environment 35, pp.3103-3111.
- Quaranta N., De Martini A., Bellasio R., Bianconi R., Marioni M.2000. A modeling system for the simulation of Industrial accidents, 7th Int. Conf. on Harmonisation within Atmospheric Dispersion Modelling for Regulatory Purposes.
- Singh M. P.1990. Air Pollution dispersion modeling: Case studies of some recent industrial accidents, Lecture, SMR/463-19, 4-15 June, USA..
- Snyder W.H 1985. Fluid modeling of pollutant transport and diffusion in stably stratified flows over complex terrain. Ann. Rev. Fluid Mech. 17, pp. 239- 266.

AIR QUALITY AT THE AIRPORT BUDAPEST AND INVERSE DISPERSION MODELLING TO DETERMINE THE STRENGTH OF DIFFERENT EMISSION SOURCES

Klaus Schäfer, Gregor Schürmann, Carsten Jahn, Herbert Hoffmann, Stefan Emeis
Forschungszentrum Karlsruhe GmbH
Institut für Meteorologie und Klimaforschung, Atmosphärische Umweltforschung
Kreuzeckbahnstr. 19, D-82467 Garmisch-Partenkirchen
Phone: +49 8821 183 192, Fax: +49 8821 73573, e-mail: klaus.schaefer@imk.fzk.de

ABSTRACT

A measurement campaign on the airport Budapest was performed to investigate airport air quality and to identify major sources of air pollutants. At four different locations, concentrations of CO, NO and NO₂ as well as meteorological parameters were measured simultaneously by in-situ and open-path techniques (DOAS and FTIR). To quantify emissions on the airport, inverse dispersion modelling with a Bayesian approach was used on the basis of hourly averaged concentration measurements.

Single short-term emissions rates were highest for a car park. During the whole campaign, aircraft emissions on the taxiway were most important at the terminal area. In general similar levels of emissions are reached for the car park and the freight area. Even though the most important source for NO_x on an airport, the emission of starting aircraft, were not considered, the results reveal, that dealing with air quality, all sources of NO_x are important, and not only aircrafts.

1. INTRODUCTION

Emission sources on an airport can be subdivided into 5 parts: aircrafts, point sources, cars, ground support emissions and others (e.g.: painting, maintenance of aircrafts). The strengths of these emissions usually are calculated from emission indices which were measured in test beds. With this procedure the open question remains, whether the results correspond to real in use emissions. The most specific airport-related part of these sources are obviously aircrafts. For NO_x and CO, aircraft emission data exist, which were measured in a test bed for each engine for four different thrust levels (7 % Idle, 30 % Approach, 85 % Climb out, 100 % Take off) during new engine certification procedures, which are recommended by the International Civil Aviation Organization (ICAO, 1993). Following these data, CO emissions are low for take-off due to the complete combustion of the kerosene and high during taxiing. A converse behaviour can be found for NO_x emissions. During take-off, emissions are highest due to the high temperature in the engine, while during taxiing, lowest emissions are found. The impact of air traffic on the atmosphere was subject to several works in the last years: an overview can be found in Rogers et al. (2002), while the specific influence of airports was investigated only in a few studies as Moussiopoulos et al. (1997), Yu et al. (2004) or Unal et al. (2005).

The investigation of the air quality at the airport Budapest Ferihegy was subject to a detailed measurement campaign in April 2005 (12 - 27 April), whose results are presented here. The measurement devices were situated at different locations around Terminal 2. With that measurement set up, the influence of Terminal 2 upon air quality can be investigated, because some measurements were upwind of the airport and representative for background concentrations and others were located in the polluted plume of Terminal 2. Goals during the investigation were the determination of concentration levels by the mean of measurements of air pollutants (CO, NO, NO₂) at different locations and an apportionment of emission rates for different sources by the mean of a combination of measurements and dispersion models with inverse modelling.

The objective of the campaign was to give a long-term strategic framework to reduce specific emissions from air traffic in the context of airport expansion plans required to meet future demands of air traffic.

2. METHODOLOGY

Concentrations of NO_x and CO were measured at four different locations (Figure 1) with in-situ and open-path devices. Inverse dispersion modelling then was used to quantify emissions of NO_x of 13 source regions, (including taxiways, aircraft stands, car park and freight area) around Terminal 2. The setup was chosen to account for the predominant north-westerly wind direction in Budapest. In case of such wind directions, the measurement devices at the fire brigade depot (firestation) were assumed to serve as measurement station for background concentrations. Although upwind of this station the city of Budapest is located, parts of polluted air from Budapest will be brought towards Terminal 2. But having in mind, that the investigated area is separated from other big sources and the city border is approx. 3 km away, it can be assumed, that the air from Budapest is already homogeneously mixed and therefore background concentrations are measured at the fire station.

During the measurement campaign, open-path and in-situ devices were operated to continuously measure concentrations. In-situ devices measure the concentration at one point and such devices were operated to measure concentrations of NO_x and CO among others. Open-path devices are capable to measure the mean concentration along an absorption path (Fourier Transform Infrared Spectrometry – FTIR: CO, see Haus et

al., 1994: freight area and museum, Differential Optical Absorption Spectroscopy – DOAS: NO, NO₂, see OPSIS, 1997: freight area).

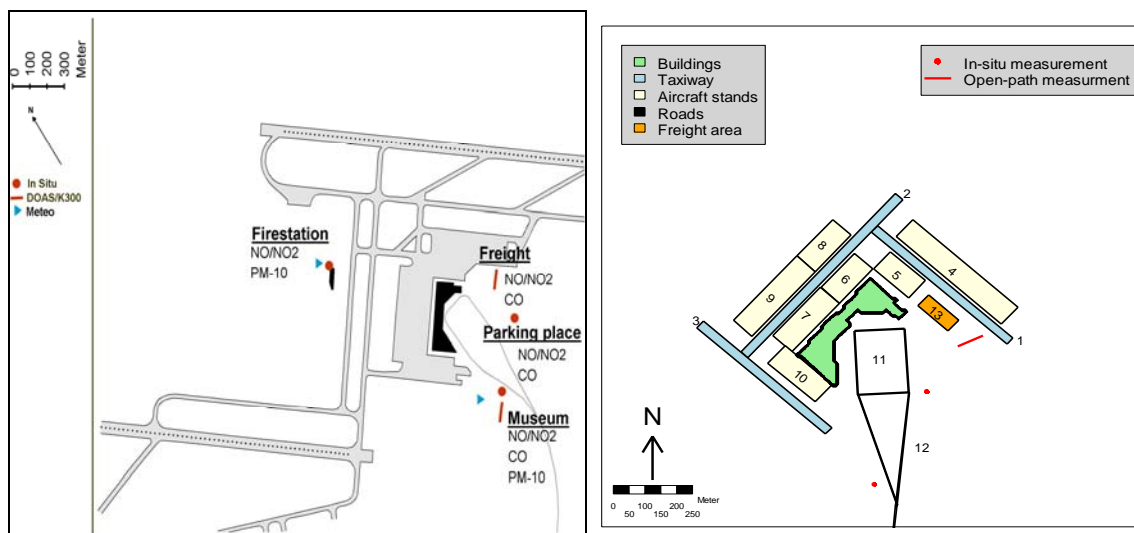


Figure 1 (left): Setup of the measurement campaign and devices to measure concentration of CO, NO/NO₂ and PM10 at Terminal 2 of the airport Budapest Ferihegy.

Figure 2 (right): Defined source regions for inverse application. The numbering of the sources corresponds to the numbering used in the presentation of inverse results.

Different measurement devices to record meteorological conditions were operated on the airport. These data are needed as basic input data for the dispersion model. A weather station was operated near the fire brigade depot and an ultrasonic anemometer (USA) was installed at the museum place which measured also turbulence parameters.

Emission source strengths and concentration measurements in the atmosphere are related through the process of air transport and dispersion, chemical reactions and removal from the air (deposition, wash out). If only transport and dispersion are considered, the problem is mathematically linear:

$$\bar{c} = F * \bar{q} + \bar{b} \quad (1)$$

The problem consists of a vector of measured concentrations \bar{c} , of a dispersion matrix F that is computed with a dispersion model, of a vector of source strengths \bar{q} that is the outcome of the method and of a vector of background concentrations \bar{b} that has to be evaluated. Inverse methods to solve equation (1) for all kind of problems on a scale between 10 to 1000 m have been recently used and led to the development of an inverse dispersion model (Schürmann et al., 2006). Applying this model to the situation at Budapest Ferihegy and considering the four measurement locations (1 upwind, 3 downwind of terminal 2), problem (1) is underdetermined, because the number of unknown sources exceeds the number of available measurements. Due to this problem, further information has to be used to find a solution to problem (1). The chosen method to overcome these problems is the use of a-priori knowledge about the source strengths, meaning that best knowledge about emission rate is assigned to each source region. Then Bayesian statistic is used to solve equation (1). Tarantola (1987) describes various methods to find a solution with Bayesian methods. Here the Newton method for the linear case is computed. The starting point is the formulation of a cost-function that has to be minimized:

$$J = (F\bar{q} - (\bar{c} - \bar{b}))^T C_M^{-1} (F\bar{q} - (\bar{c} - \bar{b})) + (\bar{q} - \bar{q}_{\text{prior}})^T C_{\text{prior}}^{-1} (\bar{q} - \bar{q}_{\text{prior}}) = \min \quad (2)$$

with J the cost function, C_M the covariance matrix of the model and measurement, \bar{q}_{prior} an a-priori estimation of the source strength and C_{prior} the corresponding covariance matrix. In the linear case, the minimization of equation (2) leads to the solution:

$$\bar{q} = \bar{q}_{\text{prior}} - (F^T C_M^{-1} F + C_{\text{prior}}^{-1})^{-1} F^T C_M^{-1} (F\bar{q}_{\text{prior}} - (\bar{c} - \bar{b})) \quad (3)$$

This approach has the advantage that in case of too few or insufficient measurements, the estimation of \bar{q} is possible, but partly or fully dominated by the a-priori estimation \bar{q}_{prior} . The main drawback of the method is

the high influence of the a-priori estimations on the solution. Therefore a careful evaluation of prior information needs to be done.

As defined in equation (1), the matrix F describes the relationship between emissions and concentrations. The determination of this matrix was done by modeling with the dispersion model AUSTAL2000 (Janicke, 2004), which is a Lagrangian particle dispersion model (a description of the underlying theory can be found in Rodean, 1996). This type of models is known to deliver best results in complex situations. Using the model for each source separately with defined source strength, the influence of each source upon the concentration at a specific measurement location can be evaluated. Assuming no chemical transformation, this leads directly to the model matrix F :

$$F_{ij} = c_i / q_j \quad (4)$$

The applied setup of the model consists of 13 source regions of which 3 represent taxiways, 7 represent aircraft stands, 2 represent roads and 1 represents the freight area north-west of the terminal building (see Figure 2). The inversion was only performed for westerly wind directions, when the measurements at the fire brigade depot were located in background air.

Table 1: Results of inverse methods with two different sets of a-priori NO_x emission rates. The given correlations and standard deviations are taken from the covariance matrix of the a-posteriori results according to case A. High correlations between two sources are indicating, that these two sources can't be estimated independently and as a consequence only the sum of the sources is given.

Source	A-prio A [mg/s]	A-posterio A [mg/s]	A-prio B [mg/s]	A-posterio B [mg/s]	Remarks	Time
Taxiway (3) (per aircraft)	58 ± 58 58 ± 58 58 ± 58 58 ± 58 58 ± 58	6 ± 13 41 ± 51 32 ± 30 27 ± 25 37 ± 24	35 ± 35 35 ± 35 35 ± 35 35 ± 35 35 ± 35	8 ± 12 38 ± 35 30 ± 26 27 ± 22 35 ± 22	Changing Winds	April 18; 22:00 CET April 18; 23:00 CET April 26; 17:00 CET April 26; 18:00 CET April 26; 19:00 CET
Aircraft Stand 6/8	100 ± 100	14 ± 74	20 ± 50	21 ± 39	Correlation: - 0.82	April 21; 23:00 CET
Aircraft Stand 10	100 ± 100	31 ± 76	20 ± 50	18 ± 45		April 18; 23:00 CET
Aircraft Stand 9/10	100 ± 100	13 ± 49	20 ± 50	6 ± 28	Correlation: - 0.84	April 18.; 21: 00 CET
Car park 11	300 ± 300 300 ± 300	455 ± 187 656 ± 159	500 ± 300 500 ± 300	982 ± 153 923 ± 142		April 18; 19: 00 CET April 18; 20: 00 CET
Car park (11) and road (12)	400 ± 316 400 ± 316 400 ± 316	-25 ± 212 -96 ± 182 -54 ± 184	650 ± 335 650 ± 335 650 ± 335	201 ± 202 166 ± 179 54 ± 176	Correlation: - 0.72 Correlation: - 0.87 Correlation: - 0.86	April 21; 18:00 CET April 21; 19:00 CET April 21; 22:00 CET
Road 12	100 ± 100	180 ± 81	150 ± 150	209 ± 81		April 21; 16:00 CET
Freight (13) and aircraft stand (4) (Total emissions)	100 ± 400 / 600 ± 245 100 ± 400 / 200 ± 141	-108 ± 49 / 585 ± 243 (477 ± 248) -55 ± 50 / 195 ± 141 (140 ± 149)	300 ± 300 / 120 ± 122 300 ± 300 / 40 ± 71	-10 ± 28 / 110 ± 122 (100 ± 125) -4 ± 38 / 35 ± 71 (31 ± 80)	Correlation: - 0.93 Correlation: - 0.74	April 21; 18:00 CET April 21; 19:00 CET
	100 ± 400 / 400 ± 200	-109 ± 54 / 386 ± 198 (277 ± 206)	300 ± 300 / 80 ± 100	-20 ± 30 / 70 ± 100 (50 ± 104)	Correlation: - 0.96	April 21; 22:00 CET
Freight 13	100 ± 400 100 ± 400 100 ± 400 100 ± 400 100 ± 400 100 ± 400	814 ± 325 344 ± 118 586 ± 350 304 ± 122 378 ± 97 129 ± 81	300 ± 300 300 ± 300 300 ± 300 300 ± 300 300 ± 300 300 ± 300	796 ± 263 420 ± 112 582 ± 276 394 ± 115 469 ± 87 236 ± 67		April 26; 12:00 CET April 26; 13:00 CET April 26; 14:00 CET April 26; 16:00 CET April 26; 17:00 CET April 26; 18:00 CET

3. RESULTS AND DISCUSSION

The applied inverse procedure starts with the estimation of prior knowledge (a-priori) about the emission rates of the considered sources. The results of the inverse methods sometimes are called a-posteriori emission

rates. To determine a-priori emission rates of taxiway and aircraft stands, results from an earlier investigation on the airport Zurich (Schürmann et al., 2007) were used. Two sets of a-priori emission rates were applied. With such a procedure, the importance of the chosen a-priori can be observed. The chosen a-priori and the results are given in Table 1.

NO_x emission rates for single sources were calculated only for a few cases (Table 1). Main reason for this is the high amount of sources compared with the relative few measurements. Hence an independent estimation of single sources was only possible in a few cases. A first set of a-priori information revealed a systematic overestimation of taxiway and aircraft stand emissions. Hence a lower a-priori emission rate was used for a second calculation with the inverse method. This second set of a-priori information provided better results and especially a smaller bias between modelled and measured concentrations. Assuming, that the chosen second a-priori emission rates are also valid for those cases, when only a little signal of the single source can be found in the measurements due to bad wind directions, the integration of the emissions for the whole period reveals, that aircraft emissions seem to be the most important around Terminal 2, but that freight and car park emissions reach similar emission levels. Further investigation should focus on the latter two kind of emissions, because the calculation of aircraft emissions can be done more precisely than the quantification of car park and freight emissions.

4. CONCLUSIONS

Inverse dispersion modelling with a Bayesian approach turns out to be a suitable tool to investigate source strengths on an airport. Open-path measurement systems are suitable for this task because these measurements can catch the entire exhaust plume and provide path-averaged data for numerical simulations which use certain grids. Overall, emissions of taxiing aircrafts were the most important sources for NO_x around Terminal 2 during the measurement campaign. But emissions on runways were not considered, because they were not located in the measurement area. It is well known, that NO_x emissions of an aircraft are highest during take-off. Other important sources of NO_x are the freight and car park area, whose emissions reached similar levels as aircraft emissions on the taxiway.

5. ACKNOWLEDGEMENTS

The authors like to thank Alföldi Balint, Veronika Groma and János Osán from KFKI AEKI and Edgar Flores from IMK-IFU as well as Magdolna Kalocsai and her team of the environmental department of the Budapest Ferihegy airport authorities for fruitful collaboration.

6. REFERENCES

- Schürmann, G., Schäfer, K., Jahn, C., Hoffmann, H., Bauerfeind, M., Fleuti, E., Rappenglück, B. 2007. The impact of NO_x, CO and VOC emissions on the air quality of the airport Zurich. *Atmospheric Environment* 41, 103-118, doi:10.1016/j.atmosenv.2006.07.030.
- ICAO 1993. Environmental Protection, Annex 16, Vol. II, Aircraft Engine Emissions, 2nd edition. International Civil Aviation Organization (ICAO) Document Sales Unit, 1000 Sherbrooke Street West, Suite 400, Montreal, Quebec H3A 2R2, Canada.
- Rogers, H.L., Lee, D.S., Raper, D.W., Foster, P.M.D.F., Wilson, C.W., Newton, P.J. 2002. The impact of aviation on the atmosphere. *The Aeronautical Journal* 106, 521 – 546.
- Moussiopoulos, N., Sahm, P., Karatzas, K., Papalexiou, S., Karagiannidis, A. 1997. Assessing the impact of the new Athens airport to urban air quality with contemporary air pollution models. *Atmos. Environ.* 31, 1497 – 1511.
- Yu, K.N., Cheung, Y.P., Cheung, T., Henry, R.C. 2004. Identifying the impact of large urban airports on local air quality by nonparametric regression. *Atmos. Environ.* 38, 4501 – 4507.
- Unal, A., Yongtao, H., Chang, M.E., Odman, M.T., Russell, A.G. 2005. Airport related emissions and impacts on air quality: Application to the Atlanta International Airport. *Atmos. Environ.* 39, 5787 – 5798.
- Haus, R., Schäfer, K., Bautzer, W., Heland, J. Mosebach, H., Bittner, H., Eisenmann, T. 1994. Mobile FTIS-Monitoring of Air Pollution. *Applied Optics* 33, 24, 5682-5689.
- OPSIS 1997. DOAS User Guide, OPSIS AB, Furulund, Sweden.
- Schürmann, G., Schäfer, K., Emeis, S., Jahn, C., Hoffmann, H. 2006. Several remote sensing methods for direct determination of aircraft emission at the airports Zurich and Budapest. In: 2nd conference Environment and Transport, including 15th conference Transport and Air Pollution, Robert Joumard (ed.), Actes INRETS, Institut National de Recherche Sur les Transports et leur Securite, Bron cedex, France, Vol. 1, 351-358.
- Tarantola, A. 1987. Inverse Problem Theory: Methods for Data Fitting and Model Parameter Estimation. Elsevier, Amsterdam, Netherlands.
- Janicke, B. 2004. Austal2000, Programmbeschreibung zu Version 2.1, Stand 2004-12-23, Ingenieurbüro Janicke, Dunum, Germany.
- Rodean, H.C. 1996. Stochastic Lagrangian models of turbulent diffusion. *Meteorological Monographs (Volume 26, Number 48)*, American Meteorological Society, Boston, USA.

RELEASE AND DISPERSION OF HARMFUL GAS MODELLING INSIDE THE UABL

Klára Bezpalcová¹, Karel Klouda², Zbyněk Jaňour¹

¹*Institute of Thermomechanics, Academy of Sciences of the Czech Republic, Prague*

²*Czech State Office for Nuclear Safety, Prague*

ABSTRACT

Presented research deals with very dangerous gas dispersion in the complex urban geometry of downtown of Prague, Czech Republic, as a precaution of possible chemical or biological terrorist attack. It is concerned with the study of the pollutant dispersion emitted from a point source with changes of wind direction within urban boundary layer. This was experimentally investigated in a wind tunnel and also examined using a theoretical dispersion models (mostly based on parametric model, e.g. Gaussian type), used by decision-making bodies, e.g. Integrated Safety System of the Czech Republic and strengthened by the SODAR field measurement.

1. INTRODUCTION

The dispersion of pollutants in urban areas is still one of the most challenging tasks in environmental sciences. Complex processes like the dispersion of car exhaust in street canyons or the dispersion of accidental releases of harmful substances in built-up areas are not yet fully understood.

The wind tunnel modelling of atmospheric boundary layer is based on the similarity theory used in fluid mechanics and described e.g. in Triton, 1988. The practical use of the similarity theory at the field of physical modelling can be found e.g. in Plate, 1981.

Presented research dealt with dangerous gas dispersion in the complex urban geometry of downtown of Prague (Old Town Square) as a precaution of possible chemical or biological terrorist attack. It is concerned with the study of the pollutant dispersion emitted from a point source with changes of wind direction within urban area. This was experimentally investigated in a wind tunnel. The wind tunnel modelling allowed studying the effect of physical and chemical properties of pollutant on flow and pollutant diffusion within urban canopy. Pentyl acetate with very similar physical and chemical properties as sarine gas (i.e. it is an active gas, which tends to be absorbed or caught by ground and building surfaces) and propane (passive tracer, which does not interact with the model) were used as a tracer gas.

2. EXPERIMENTAL METHODS

Measurements have been carried out in the Environmental wind tunnel of the Institute of Thermomechanics located in the Aerodynamics Laboratory in Nový Knín. The tunnel is designed as an open-circuit facility that is operated as a fan driven one (see Fig. 1, left picture). It has the cross section 1.5 m x 1.5 m and the length to the development section 25.5 m. The long development section with variable roughness elements on the floor and turbulence generators is shown in the right picture in Fig. 1. An appropriate configuration of roughness elements and spires has been set up inside the wind tunnel to model an urban boundary layer according to guidelines (VDI guidelines 3783, 1999, Snyder, 1981) corresponds with the neutrally stratified urban ABL in the corresponding scale of the model.

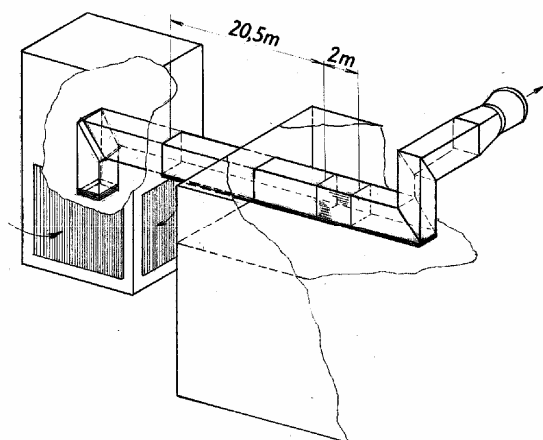


Figure 1: Sketch of the environmental wind tunnel of the Institute of Thermomechanics (left picture); the development section of the wind tunnel with spires and roughness elements (right picture).

Figure 2 shows a model of the Old Town Square and its surroundings in the scale 1:270 built in the laboratory workshop and the bird-eye photograph of this area with depicted source positions and examined wind directions.

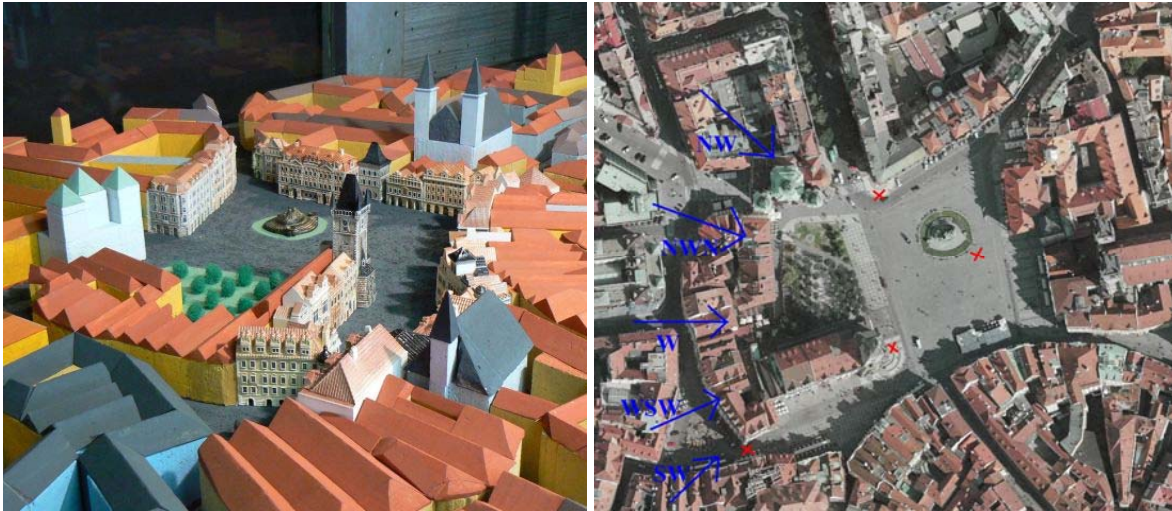


Figure 2: The model of the Old Town Square in the tunnel (left picture); bird-eye photograph of the model area with depicted source positions (red crosses) and examined wind directions (right picture).

3. FLOW VISUALISATION

The first experimental campaign in the wind tunnel was flow visualisation by a smoke and laser light sheet. Some examples of the results are shown in Fig. 3. This method showed that the dispersion is highly intermittent, a tracer tend to stay on the ground or on the building walls. Since the flow is highly intermittent, tracer could even travel against the mean wind direction.

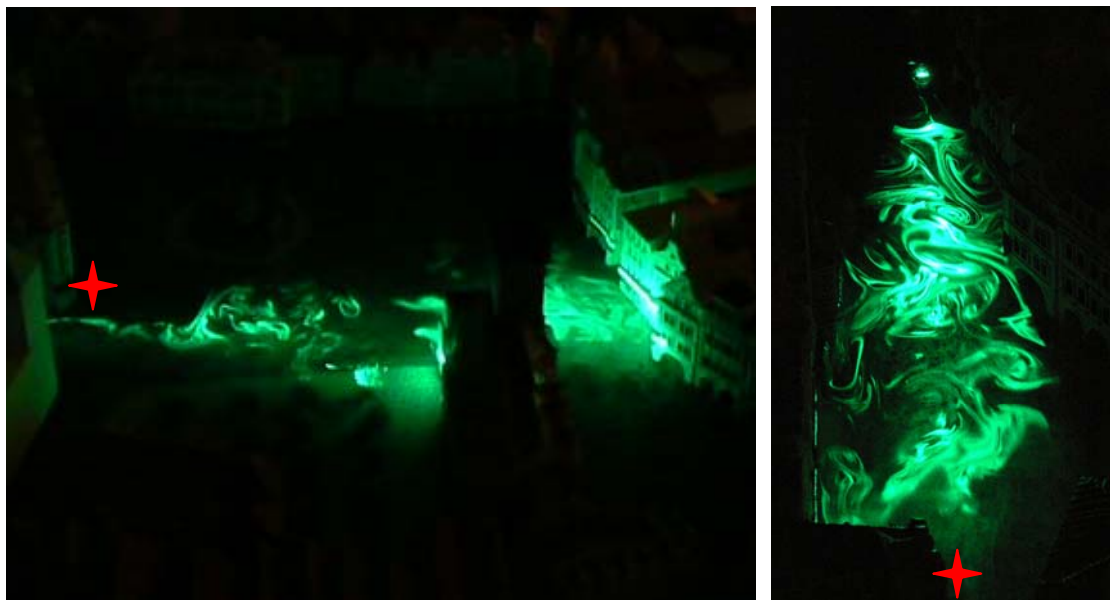


Figure 3: The flow visualisation, the source is depicted by the red cross, wind is blowing from left to right, and the light sheet is in the 2 m height in full scale.

4. CONCENTRATION MEASUREMENT

Dimensionless concentration c^* , which allows us to use model results at the reality when fulfill physical modelling criteria is defined as:

$$c^* = \frac{c U_{ref} H^2}{Q} \quad (1)$$

where c is concentration measured on model (in reality), U_{ref} is the reference wind speed (e.g. measured at 10 m at the meteorological station), H is average building height (0.1 m at the model scale, 27 m in full scale in our case), and Q is source strength. In case of propane this formula is valid without any other corrections.

In the case of the pentyl acetate we did not know the source strength because the release of this gas was based on an evaporation of the liquid. Q was estimated on the base of calculation showed in Klouda et al. (2006) as a linear function of the wind speed U_{ref} and an area of the source A and as an exponential function q of the temperature T

$$Q_{pentyl\ acetat} = U_{ref} A q(T) \quad (2)$$

Combination of equations (1) and (2) results in:

$$c^* = \frac{c H^2}{A q(T)} \quad (3)$$

where the dimensionless concentration is independent on the wind speed by definition (U_{ref} do not appear in the equation (3)). This is a consequence of two contradictory processes: the faster wind speed causes the greater evaporation of pentyl acetate, however, the pentyl acetate is also more diluted by bigger amount of oncoming air. These two contradictory processes have the same influence on the measured concentration and therefore it is independent on the wind speed, which was experimentally verified several times. The measurement on the model in the wind tunnel was conducted at different temperatures since the tunnel was sucking the air from outside (diurnal temperature variation took place, etc.). However, the resultant dimensionless concentration was normalised to 20°C due to knowledge of the temperature function $q(T)$.

The results obtained from measurement conducted with the propane and pentyl acetate differ by factor of approximately 20 – see Fig. 4. There are two reasons for this disagreement: (i) the evaporation is dependent on the wind speed next to the surface, but we used for calculation the reference wind speed above the roof level, (ii) the pentyl acetate is not passive pollutant, e.g. the sorption can take place. The magnitude of the first reason was estimated to be in order of 10, the active behaviour is much weaker, the factor of 2.

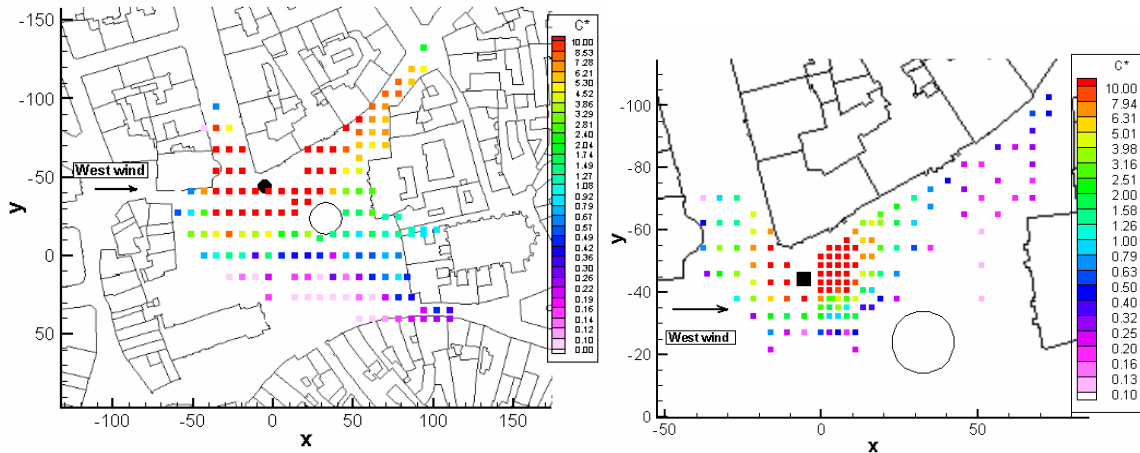


Figure 4: Concentration field from the source located near mouth of the Parizska street for the west wind in the case of propane (left picture) and pentyl acetate (right picture) was used as a tracer gas.

5. OPERATIONAL MODELS

Operational models usually work with very rough parameterisation and do not taken into account influence of the building set-up on the flow. Very typical outputs of these models are circle (e.g. model ATP-4B), or a sector of the circle oriented with the wind speed (e.g. model POISON), or an ellipse (e.g. model ALOHA), where all occupants should be vacated. The major difference between dispersion in urban canopies and above flat terrain is considerable spread against the mean wind direction caused by influence of an urban layout, where blocks of buildings and street canyon cause enhanced vertical and horizontal mixing and guide the flow. These aspects are not taken into account in the operational models and therefore they are complete misleading in the urban areas, in the sense of the spread area and also magnitude of measured concentration. Another aspect during the field campaigns is accessibility of the on-site meteorological data, e.g. wind direction and wind speed. Therefore the SODAR measurement on site was conducted and the comparison of these data with the nearest meteorological station showed significant shift in the wind direction (up to 20°) and also in the wind speed. Since the station is above the valley in which is situated the modelled area the measured wind speed on this station was higher than in the same elevation on the Old Town Square.

6. CONCLUSION

An interesting behaviour of an intentionally released dangerous gas inside an urban canopy has been found: the flow visualisation showed the high intermittent character of the dispersion processes within the urban canopy, the very toxic sarine gas (modelled by pentyl acetate gas) tends to stay near the ground and on the building walls due to a sorption processes, and a comparison between passive (propane) and active (pentyl acetate) tracers were conducted.

The comparison of the wind tunnel results with the operational model completely failed and the SODAR measurement shows another problem of the operational model usage: the input of these models is at least wind direction and wind speed, which can be on the site significantly different from the nearest regular meteorological measurement.

ACKNOWLEDGEMENT

Authors acknowledge financial support of projects OC 113 and AV0Z20760514 of the Ministry of Education, Youth and Sports of the Czech Republic. Author also would like to thanks to Faculty of Safety Engineering, Technical University Ostrava and the LIDAR company for conducting the SODAR measurement.

REFERENCES

Klouda, K., Dudáček, A., Bezpalcová K. (2006) A deliberation about a misuse of "home-made" prepared sarine gas (in Czech), Conference Požární ochrana 2006, FBI VŠB-TU Ostrava, pp. 169-186.

VDI Guidelines 3783, part 12 (1999) Environmental Meteorology, Physical modelling of flow and dispersion processes in the atmospheric boundary layer, application of wind tunnels, Issue German/English, VDI Handbuch Reinhaltung Luft, Band 1b, Vorentwurf August 1999.

Plate, E. J.: Engineering Meteorology, Elsevie, 1981

Snyder, W. H. (1981) Guideline for Fluid Modeling of Atmospheric Diffusion, Report No. 600/8-81-009, Enviromental Sciences Research Laboratory, Office of Research and Development, U.S. Environmental Protection Agency, Research Triangle Park, NC 27711.

Tritton, D. J.: Physical Fluid Dynamics, Oxford University Press, 1988

TREES IN URBAN STREET CANYONS AND THEIR IMPACT ON THE DISPERSION OF AUTOMOBILE EXHAUSTS

Christof Gromke*, Bodo Ruck

Laboratory of Building- and Environmental Aerodynamics
Institute for Hydromechanics, University of Karlsruhe, Germany

*corresponding author, Tel.: + 49-721-608-7307, fax: + 49-721-608-3191, gromke@ifh.uka.de

ABSTRACT

The aim of the present study is to clarify the influence of trees on the dispersion of automobile exhausts in urban street canyons. For this purpose, measurements have been performed with a small scale wind tunnel model of an idealized, isolated street canyon with model trees placed along the canyon center axis. Sulfur hexafluoride (SF_6) was released from a line source embedded in the street surface, simulating vehicle exhaust emissions. The influence of various tree planting arrangements on the concentrations at the canyon walls was investigated with an approaching boundary layer flow perpendicular to the canyon axis. Increasing pollutant concentrations at the leeward wall and decreasing pollutant concentrations at the windward wall were found for increasing plant density. At the ends of the street canyon, i.e. towards the intersections, a remarkable relative increase of concentrations at both canyon walls was observed. The results indicate that due to tree planting, typical vortex structures observed in empty street canyons were either significantly weakened or no longer present.

1. INTRODUCTION

Due to increasing traffic, air pollution in urban street canyons induced by cars is becoming a more and more serious problem in regard to the healthiness of people living or working in city centers. Beside gaseous exhaust emissions, particulate matter released by vehicles, such as motor combustion residues, abrasion of tires and brake disks, or entrained by vehicles such as roadside deposited dust, have to be diluted and removed efficiently from the street canyon. In the last three decades, a large number of investigations concerning flow and concentration fields inside empty urban street canyons have been performed and the pollutant dispersion processes are well understood (Chang and Meroney 2003, Gerdes and Olivari 1999, Baik and Kim 1999, Ahmad et al. 2005, Vardoulakis et al. 2003, Li et al. 2006). However, pollutant dispersion processes in the presence of obstacles, such as trees inside the street canyon have not been investigated systematically, except in Gromke and Ruck 2007.

2. METHODOLOGY

An isolated street canyon model at scale 1:150 (Figure 1) with aspect ratio $H/W = 1$ and length to width ratio $L/W = 10$ was exposed to a perpendicular approaching boundary layer flow. The wind profile was characterized by a profile exponent $\alpha = 0.30$ according to the exponential wind law, see also Gromke and Ruck 2005. The flow field inside the empty street canyon and its dominating vortex structures like canyon vortex and corner eddies are sketched in Figure 1 (right). Model trees with either impermeable or permeable spherical crowns of diameter 15 m and a brunch free trunk of 4.5 m height were aligned equidistantly along the canyon center axis. The spacing between the trees was varied with 15, 20, 25 and 30 m. Sulfur hexafluoride was emitted from a line source at street level and tracer gas concentrations were measured by means of an electron capture detector (ECD) at both canyon walls A and B. The measured concentrations have been normalized according to the formula

$$c^+ = \frac{c_{\text{meas}} L_{\text{ref}} u_{\text{ref}}}{Q_T/l}$$

with c_{meas} : measured concentration, L_{ref} : reference length characterizing a building dimension ($L_{\text{ref}} = H$), u_{ref} : reference velocity characterizing the atmospheric flow ($u_{\text{ref}} = u_H$) and Q_T/l : tracer gas source strength per unit length of the line source. Additionally, all lengths in the subsequent concentration plots have been normalized by the reference length $L_{\text{ref}} = H$. These normalizations allow a transfer of measured concentration data to situations with different boundary conditions, e.g. differing reference velocity or building height.

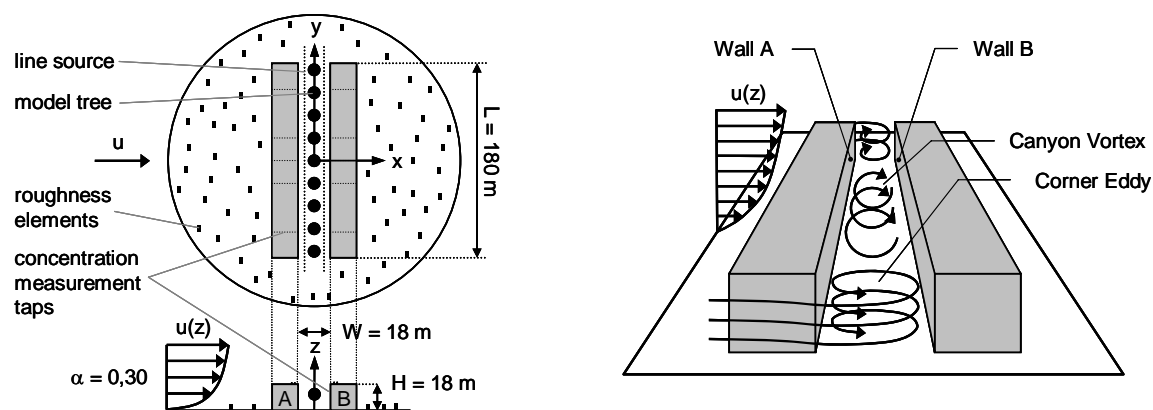


Figure 1. Model setup and flow field inside empty street canyon of aspect ratio $H/W = 1$.

3. RESULTS AND DISCUSSION

3.1 Empty street canyon without tree planting (reference case)

Figure 2 shows normalized concentrations at the canyon walls for the reference case without trees. The average pollutant concentration at wall A is 3.6 times higher than at wall B, which can be easily explained by means of the prevailing flow field in the canyon middle part. At roof level, an exchange of polluted canyon air with unpolluted air of the atmospheric flow takes place. Air of the atmospheric flow is entrained into the canyon vortex and transported downward into the street canyon in front of wall B. When recirculating from wall B towards wall A, traffic exhaust emissions are accumulated at the street level. Thus, the upward streaming part of the canyon vortex in front of wall A contains higher exhaust concentrations. The lower concentrations at the street ends are due to the superposition of the canyon vortex and sidewise entering corner eddies, leading to an enhanced exchange of air.

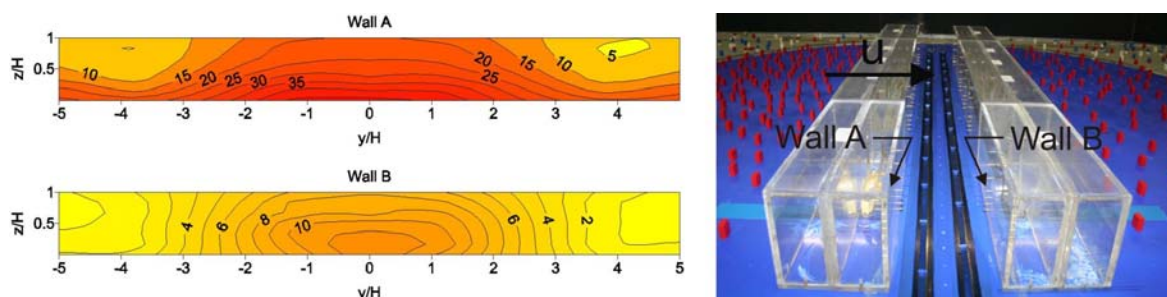


Figure 2. Normalized wall concentrations for empty street canyon without trees (reference case).

3.2 Tree planting with impermeable crowns and spacing 30 m

In the case of an equidistant tree planting spaced by 30 m, the gap between neighbouring trees amounts to 15 m at the crown waists and 20 % of the total canyon volume is occupied by crowns. In Figure 3 (left), the relative changes in concentration are shown for wall A and wall B when compared to the reference case of the empty street canyon (Figure 2).

At wall A, moderate concentration increases in the range of 0 to 20 % were measured in the canyon middle part ($-1.5 < y/H < +1.5$). In contrast, concentration decreases up to 40 % were measured in the middle part of wall B. These observations indicate modifications of the flow field inside the canyon due to the tree planting, which was supported by laser Doppler velocimetry (LDV) measurements showing changed entrainment conditions at the roof top level. Since the interspaces between crown waists and canyon walls amounts to only 1.5 m, it is obvious that the development of a canyon vortex is significantly restrained or even totally inhibited. In order to understand the decrease in concentration at wall B, one has to remember that exhaust concentrations found at this wall in the empty street canyon originate from traffic emissions released at street level, which have been transported by the canyon vortex itself towards wall B. Consequently, a weakened or missing canyon vortex leads to lower concentrations at wall B. At the canyon's outer parts, pronounced relative increases in concentration at both walls were observed. The outermost tree crowns represent obstacles, which hinder corner eddies to enter the street canyon and, thus, limit the natural ventilation. Flow

field investigations with laser Doppler velocimetry revealed a considerable reduction of the lateral inflow volume rate caused by the blocking effect of the outermost tree crowns. In comparison to the reference case, an increase of wall average concentration at wall A of 14 % and a decrease at wall B of 26 % was measured.

3.3 Tree planting with impermeable crowns and spacing 15 m

Within this configuration, the closest possible tree spacing is realized. Neighbouring trees touching each other at the crown waists and 39 % of the canyon volume is occupied by tree crowns. The relative change in concentration at the canyon walls is shown in Figure 3 (right).

Again, two distinct regions of concentration changes can be found at both walls. An enhanced concentration level was observed when compared to the planting with tree spacing of 30 m (Figure 3, left). Since there is no free gap remaining between the waists of the crowns, the canyon vortex strength is additionally weakened. The wall average concentrations increase to 45 % at wall A and decrease to 44 % at wall B in comparison to the reference case without trees.

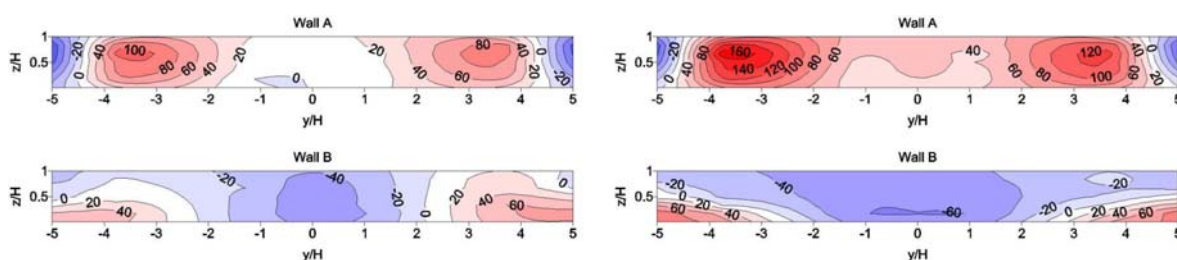


Figure 3. Relative changes in concentration for tree planting with spacing 30 m (left) and spacing 15 m (right) when compared to the reference case (Figure 2).

3.4 Tree plantings with impermeable crowns and spacings of 20 and 25 m

Further measurements of planting configurations with tree spacings of 20 and 25 m have been performed. The results fit well into the trend set by the planting configurations with spacings of 15 and 30 m (Figure 3). The wall average concentrations and relative changes when compared to the empty reference canyon are summarized in Table 1.

Table 1. Wall average concentrations and relative changes when compared to the reference case

Tree spacing [m]	empty		30		25		20		15	
	A	B	A	B	A	B	A	B	A	B
norm. concentration [-]	19,5	5,4	22,3	4,0	23,6	3,9	24,7	3,6	28,3	3,0
rel. change [%]	0	0	+14	-26	+21	-28	+27	-33	+45	-44

3.5 Tree planting with permeable crowns and spacing 15 m

In order to take the influence of real crown permeability into account, spherical crowns have been made out of an open-pored foam material 10 ppi (10 pores per inch). This material is characterized by a relative pore volume of 97 % and a pressure loss coefficient $\lambda = 210 - 275 \text{ Pa}/(\text{Pa}/\text{m})$ for flow velocities in the range of 0 to 7 m/s.

In Figure 4, the relative change in concentration for a tree planting with spacing 15 m and permeable crowns of 15 m diameter when compared to the configuration with impermeable crowns (chapter 3.3) is shown. At wall A, marked changes in concentration are not registered. At wall B, the relative change in concentration is more distinct. The mean relative change in comparison to impermeable crowns amounts to +4 % for wall A and to -15 % for wall B. The decrease in concentration at the outer parts of wall B can be ascribed to the crown permeability, which is blocking the corner eddies less effectively. It was found, that with the typical low wind conditions in street canyons, the crown permeability does not strongly influence the measured wall concentrations.

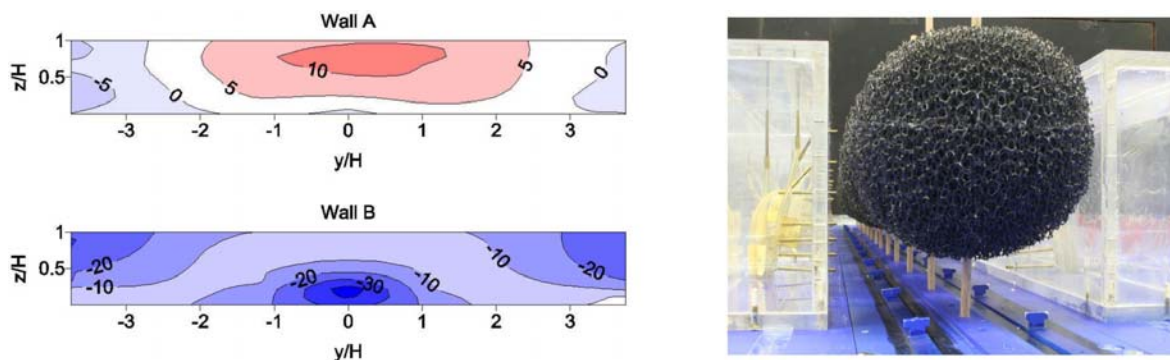


Figure 4. Relative changes in concentration for tree planting with spacing 15 m and permeable crowns when compared to tree planting with impermeable crowns.

4. CONCLUSION

In the present study, the influence of tree planting in street canyons have been investigated with respect to dispersion and removal of traffic-induced pollutants. The investigations have been performed in an atmospheric boundary layer wind tunnel with a simulated urban street canyon in perpendicular cross flow. Inside the street canyon, an avenue-like tree planting was realized and the exhaust emissions were simulated by a line source positioned at the center line of the street canyon. The tree spacing was varied systematically and wall concentration measurements have been performed. In comparison to the empty, tree-free street canyon, concentration increases at the leeward wall (wall A) and decreases at the windward wall (wall B) were found in the canyon middle part. With tree planting, high relative increases in concentration at both walls were measured towards the street ends at the canyon's outer parts. In general, the concentration level rises with higher tree density, i.e. with smaller tree spacings. Tree crowns represent flow obstacles which damp the natural ventilation and, thus, the dispersion and removal of pollutants. The entrainment conditions at the roof top level and at the lateral inlet cross sections of the canyon are altered significantly with trees leading to weakened or even suppressed canyon vortex and corner eddies. The influence of crown permeability on the concentration level was found to be not of primary significance. The investigations have shown that by providing sufficient tree spacing, the atmospheric wind is able to intrude into the street canyon avoiding relevant concentration increases. Thus, for a planting configuration with tree crowns of 15 m diameter and a tree spacing of 30 m, the average concentration at the leeward wall A was only moderately increased by 14 % when compared to the reference case without trees. In contrast, when doubling the tree plant density to a spacing of 15 m, a large increase in concentration of 45 % was observed.

5. ACKNOWLEDGEMENTS

The authors would like to thank the Deutsche Forschungsgemeinschaft DFG for financial support (Grant No. Ru 345/28). Thanks are also due to Lars Venema from TU Delft for his helpful support in this research project.

6. REFERENCES

- Ahmad, K., Khare, M., Chaudhry, K. K. 2005: Wind tunnel simulation studies on dispersion at urban street canyons and intersections - a review, *J. Wind Eng. Ind. Aerod.* 93, 697-717.
- Baik, J.-J., Kim J.-J. 1999: A numerical study of flow and pollutant dispersion characteristics in urban street canyons, *J. Appl. Meteorol.* 38, 1576-1589.
- Chang, C.-H., Meroney, R. N. 2003: Concentration and flow distribution in urban street canyons: wind tunnel and computational data, *J. Wind Eng. Ind. Aerod.* 91, 1141-1154.
- Gerdes, F., Olivari, D. 1999: Analysis of pollutant dispersion in an urban street canyon, *J. Wind Eng. Ind. Aerod.* 82, 105-124.
- Gromke, C. Ruck, B. 2005: Die Simulation atmosphärischer Grenzschichten in Windkanälen, *Proceedings 13th GALA Fachtagung Lasermethoden in der Strömungsmechanik, Cottbus, Germany* 51.1-51.8.
- Gromke, C., Ruck, B. 2007: Influence of trees on the dispersion of pollutants in an urban street canyon - experimental investigation of the flow and concentration field, *Atmos. Environ.*, doi:10.1016/j.atmosenv.2006.12.043.
- Li, X.-X., Liu, C.-H., Leung, D. Y. C., Lam, K. M. 2006: Recent progress in CFD modelling of wind field and pollutant transport in street canyons, *Atmos. Environ.* 40, 5640-5658.
- Vardoulakis, S., Fisher, B. E. A., Pericleous, K., Gonzalez-Flesca, N. 2003: Modelling air quality in street canyons: a review, *Atmos. Environ.* 37, 155-182.

SIMULATION OF GRAVITY WAVES AND MODEL VALIDATION TO LABORATORY EXPERIMENTS

Norbert Rácz¹, Gergely Kristóf¹, Tamás Weidinger², Miklós Balogh¹

¹Department of Fluid Mechanics, Budapest University of Technology and Economics

²Department of Meteorology, Eötvös Loránd University

ABSTRACT

A correction method to general purpose CFD (Computational Fluid Dynamics) solvers for simulating flows in stratified atmosphere has been developed. This new approach has many potential fields of application in air quality assessment including UHI (urban heat island) induced urban ventilation, plumes of large cooling towers, and forest fire simulation. Validation to laboratory experiments and also to full-scale atmospheric flow is a very important step toward the practical application of the method. In the case of full-scale flow internal gravity waves seem to be a more solid basis for validation than thermal convection flow can be. In this study the simulation results of quasi-two-dimensional lee-wave evolution in linearly stratified fluid has been compared to the corresponding experiments. Flow structures and characteristic measures of wave patterns obtained by simulation are in line with experimental observations.

1. INTRODUCTION

Extension of the scope of general purpose CFD solvers to atmospheric flow problems involving extensive vertical convection can deliver the advantages of highly developed engineering tools such as accurate description of problem geometry or high flexibility in meshing to new application areas. Combining micro- and meso-scale models is often demanded by climatology and environmental technology. For these purposes nested models are most commonly used involving interpolation of variables between grid interfaces between different resolution models which is the source of numerical errors and model uncertainties (Sarma et al., 1999) eg. gravity waves are partially reflected from model interfaces. Our purpose is to reformulate the mathematical model in a commonly used CFD solver in order for micro- and meso-scale flows in one common system to be analyzed, in such a way, that the micro structures could be studied by a simple local grid refinement process. A novel system of transformations and a set of necessary source terms have been developed to achieve the best agreement between governing equations of atmospheric flow and mathematical model available in CFD solvers.

Before practical application it is necessary to validate this method to measured data. Reproducible measurement data are available mostly from laboratory experiments. Since laboratory scale experiments on atmospheric flow are based on approximate mathematical description, only partial validation of the complete mathematical model is possible on the basis of these data. Effect of variable density and atmospheric turbulence are not modeled correctly in water tank experiments, and not used in comparative calculations either, therefore only the most important part of the mathematical model describing the effect of atmospheric stratification is introduced in this paper. The complete mathematical model is aimed to be published in another paper submitted to the same conference.

Simulation of a quasi-two-dimensional lee-wave evolution in a linearly stratified fluid has been compared to the corresponding experiment. Amplitudes and wavelengths were extracted from flow patterns obtained for different obstacle shapes at several flow velocities. Flow patterns were also compared as in the experiments flow visualization was done by dyeing the different layers of the stratified fluid. These comparisons indicate that the observed gravity current was well simulated in terms of depth, propagation speed, pattern and reflection. Further work is needed for the comparison to full-scale measurements.

2. METHODOLOGY

In those cases when density depends only on temperature, the ideal gas law with constant pressure (incompressible ideal gas), or Boussinesq approximation with constant β thermal expansion coefficient can be used. Potential temperature formulation allows the application of incompressible models. As the potential temperature in standard atmosphere is a linear function of vertical coordinate, it leads to a parabolic vertical pressure profile and thus causes several order of magnitude differences between horizontal and vertical components of the pressure gradient vector, which can give rise to numerical instabilities in pressure based solvers. In order to solve this problem we transform the physical temperature T into the temperature field \tilde{T} used in the simulation system with a simple linear expression (Eq.1). Definition of mean temperature (Eq.2) is based on standard ICAO temperature profile. At the beginning of the simulation the temperature field can be initialized to T_0 constant. Density perturbation $\tilde{\rho}$ defined by Eq.3 is used for evaluating buoyancy force in the momentum equation. Constant ρ_0 density is used at every other places in the model equations.

$$T = \tilde{T} - T_0 + \bar{T} \quad (1)$$

$$\bar{T} = T_0 - \gamma z \quad (2)$$

$$\tilde{\rho} = \rho_0 - \rho_0 \beta (\tilde{T} - T_0) \quad (3)$$

Since the temperature perturbation is not invariant in the presence of vertical flows the energy equation have to be corrected by an additional volume source proportional to the product of vertical velocity gradient and the difference between dry adiabatic and standard temperature gradients.

$$S_T = -c_p \rho w (\Gamma - \gamma) \quad (4)$$

$$N = \sqrt{-g / \rho \cdot \partial_z \rho} \quad (5)$$

$$N = \sqrt{g \cdot \beta \cdot (\Gamma - \gamma)} \quad (6)$$

Brunt-Väisälä frequency N can be evaluated on the basis of Eq.5, in which g is the gravity constant and $\partial_z \rho$ is the density gradient in the experiment. Stable stratification was achieved by layering variable concentration of salt solution in a water tank. Value of parameter $\Gamma - \gamma$ of the simulation has been obtained from the condition of identical Brunt-Väisälä frequency.

3. RESULTS AND DISCUSSION

As a validation of our transformation tool internal gravity waves were examined generated by symmetric and asymmetric obstacles. The shape is characterized by a Gaussian function:

$$z(x) = a \exp(-b|x|^{2\gamma}) \quad (7)$$

where a , b , γ are parameters what represent the different shapes and x is the horizontal coordinate of the obstacle. The measurements were performed in a narrow plexi glass tank with a size of 2.4 m * 0.4 m * 0.0087 m filled with linearly stratified salt water (Gyüre and János, 2003) towing the obstacles in the bottom of the tank. The range of parameters, obstacle height $h = 2-4$ cm, towing velocity $U = 1-15$ cm/s and Brunt-Väisälä frequency $N = 1.09-1.55$ s⁻¹ corresponds to an atmospheric flow up to a level of 5-10 km for an obstacle height of 600 m and wind speed of 10-70 m/s.

The Reynolds number however cannot be kept in the experiment because of the working fluid, it varies between 10² and 10³ (in full scale flow around 10⁸-10⁹).

The flow was considered two dimensional unsteady, incompressible in the simulation. Due to the low Reynolds number range turbulence models cannot be applied laminar approach was used instead. Terrain following grid was used with an approximate number of 65 * 320 elements. In the case setups constant inlet flow speed and moving bottom wall (in the experiment stationary wall and towed obstacle) and rigid upper wall was used as boundary conditions.

Because of the larger number of simulation setups we restrict the discussion of results to a representative case (**Figure 1.**) where an obstacle with steep upstream edge and a gentle leeward slope was investigated.

Avoiding the interaction of propagating wave fronts toward the top surface and reflected waves data extraction was made after a short transient period and before interference would occur. According to measurements 10-15 buoyancy period was enough to build up a quasi-steady state pattern.

At the upper surface we did not apply any damping layer as in the measurements free top surface was applied and it was experienced totally reflective, no visual disturbances found.

During the averaging of amplitudes and wavelengths only a few wave fronts were used in order to avoid interference. In those cases where steepening and wave breaking occurred samples was excluded from the averaging.

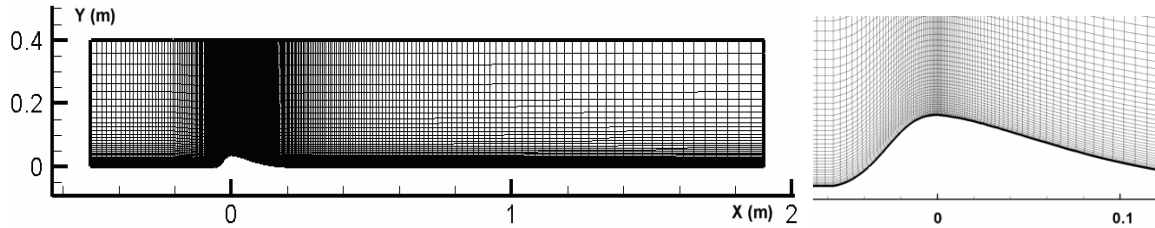


Figure 1: Computational domain and numerical grid in case of gentle leeward side obstacle

Both qualitative and quantitative agreement can be found concerning the normalized amplitudes and wavelength as well (Figure 2). In case of low inlet velocities (Figure 2.) wave breaking and rotors also can be found as a sign of higher non-linearity.

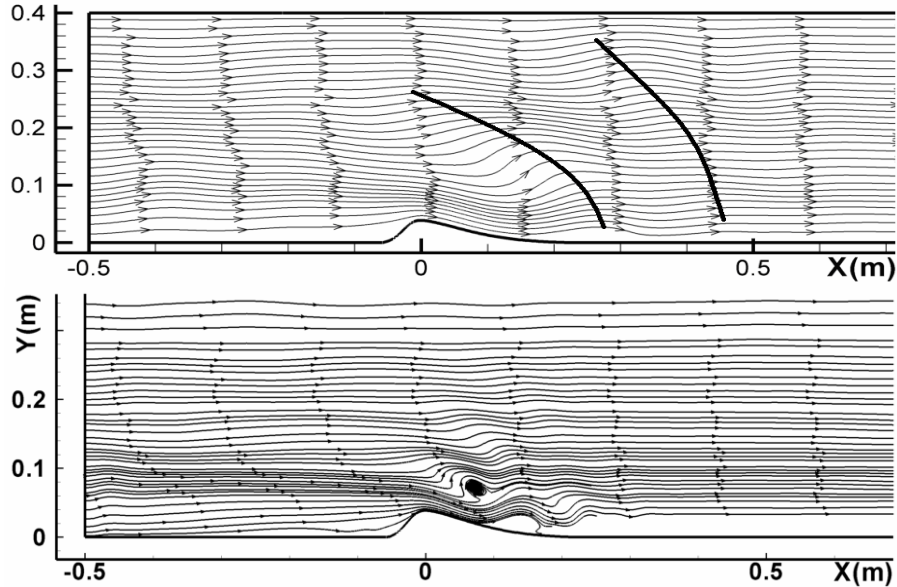


Figure 2: Contours of computed streamlines and solid lines indicate propagating wave fronts at $U/Nh = 1.4$ (top) and $U/Nh = 0.3$ (bottom) non-dimensional flow velocity

The results are however visible follows the linear theory based on Eq.8 (Scorer, 1949) and this tendency is stronger in case of steeper leeward side obstacles.

$$\lambda = \frac{2\pi U}{N} \quad (8)$$

In our experience in those cases where large pressure gradient i.e. steep leeward cases are examined, flow separation occurred. Behind the obstacles depending on the velocity of the undisturbed flow separation bubbles can be found which is obviously modifies both the shape and the size of the leeward side.

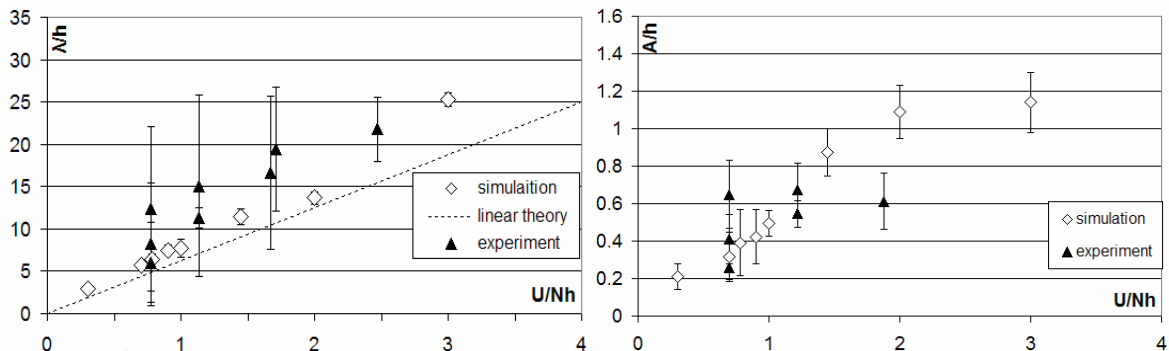


Figure 3.: Normalized averaged wave length (left) and amplitude (right) as a function of non-dimensional horizontal flow velocity in case of gentle leeward slope

This modified leeward causes longer waves with smaller amplitudes (**Figure 3.**) in the simulation especially for those cases where steep leeward side was examined. In the presented first case this effect is weak due to the gentle slope where no separation occurred. (**Figure 2**)

4. CONCLUSIONS

General purpose CFD software has been adapted to simulate atmospheric flow including stratification and compressibility effects. Non-hydrostatic formulation of the governing equations has been employed with realizable k- ϵ turbulence model. Compressibility and thermal stratification effects were taken into account by utilizing a novel system of transformations to the field variables and addition consequential source terms to the standard set of transport equations. A simplified version of the model has been validated for such cases where the flow strongly depends on the state of stratification, earlier for small scale measurements of heat island convection and now for internal gravity wave phenomena. These studies show good agreement concerning the main features of the flow and furthermore good quantitative match as well. In the aforementioned cases only the stratification module could be validated due to the applied working fluid in the experiment therefore validation to full-scale atmospheric flows is a further very important step toward the practical application. Here the effect of stratification to turbulence and compressibility effects need to be checked against full scale experiments. Preliminary tests have been made for simulating heat island phenomena at Szeged, Hungary (Kristóf et al, 2006).

This new approximation has many potential fields of application in air quality assessment including UHI induced urban ventilation, plumes of large cooling towers, and forest fire simulation or calculation of pollutant transport. Taking the advantage of the integrated simulation system with simple local grid refinement any details of the flow structure could be explored beside that the flow in meso-scale is modelled correctly as well.

5. ACKNOWLEDGEMENTS

This work has been supported by the Hungarian Research Fund under contract number OTKA T049573 and National Research and Development Program under contract number NKFP 3A/088/2004.

REFERENCES

- Gyüre, B. and Jánosi, I.M., 2003. Stratified flow over asymmetric and double bell-shaped obstacles. *Dynamics of Atmospheres and Oceans* 37, 155-170.
- Kristóf, G., Bányai, T. and Rác, N. 2006. Development of computational model for urban heat island convection using general purpose CFD solver. In *Preprints of the 6th International Conference on Urban Climate*, Göteborg, Sweden, 822-825.
- Sarma, A., Ahmad, N., Bacon, D., Boybeyi, Z., Dunn, T., Hall, M. and Lee, P. 1999. Application of Adaptive Grid Refinement to Plume Modeling, *Air Pollution VII*, WIT Press, Southampton, 59-68.
- Scorer, R.S. 1949. Theory of waves in the lee of mountains. *Q.J.R. Meteorol. Soc.* 75, 41-56.

**NUMERICAL OF STUDY OF THE WIND FLOW AND THE DISPERSION OF TRAFFIC
EMITTED POLLUTION WITH RANS CFD IN THE SIR JOHN CASS PRIMARY SCHOOL AREA
IN CENTRAL LONDON**

F. Barmpas¹, N. Moussiopoulos¹, I. Ossanlis¹ and R. Colvile²

¹ Aristotle University of Thessaloniki, Laboratory of Heat transfer and Environmental Engineering, Box 483,
Aristotle University, Gr-54124, Thessaloniki, Greece

²Imperial London College Consultants 47 Prince's Gate, Exhibition Road
London SW7 2QA, UK

ABSTRACT

A project whose aim was to quantify the potential achievable reduction in nitrogen oxides concentrations, achieved by treating a façade of the Sir John Cass Primary School located within the Central London area with photocatalytic paint, and to identify the resulting air quality improvement in measurements of nitrogen dioxide in roadside and urban background air nearby was undertaken by the Imperial London College Consultants. Towards this aim, a numerical study was conducted by the Aristotle University using the CFD code ANSYS™ CFX 5.7.1 in an effort to assess the air quality near the Sir John Cass primary School and elucidate the variance of traffic emitted NO_x in an area close to the school and across the wall which was going to be treated with photocatalytic materials.

1. INTRODUCTION

The use of TiO₂ based materials known to exhibit photocatalytic properties, like the ones developed within the frame of the PICADA project (www.picada-project.com) is gradually becoming accepted as a viable means of improving the air quality in urban environments. In view of this development, a project was completed by the Corporation of London and the Imperial College London Consultants Ltd with the support of Millennium Chemicals UK Ltd. The aim was to (a) quantify the potential achievable reduction in nitrogen oxides concentrations via the treatment of a façade of the Sir John Cass Primary School located within the Central London area with photocatalytic paint, and (b) identify the resulting air quality improvement in measurements of nitrogen dioxide.

Within the frame of this project, the Laboratory of Heat Transfer and Environmental Engineering undertook an extensive numerical modeling campaign in order to assess the air quality within the greater area surrounding the school and to elucidate how the concentration of traffic emitted NO_x varies across the building façade. Previous research has shown that the dispersion mechanism depended heavily on the complex interaction of different street canyons (Leitl et al., 2000, Scarpedas et al. 1999, Moussiopoulos et al. 2005). In view of those findings it was decided to conduct the study using the advanced Computational Fluid Dynamics (CFD) ANSYS™ CFX 5.7.1 code, rather than the less accurate but simpler to use, street canyon plume dispersion models .

2. METHODOLOGY

2.1 Computational domain and mesh

The computational domain under consideration was constructed using Geographical Information System input regarding the complex building geometries of the greater Sir John Cass Primary School area, provided by the Corporation of London. In particular, a 3D CAD model of the area around the school was constructed using the commercial ANSYS™ ICEM 5.1 grid generating code, which included apart from the school building, ten other block shaped buildings within the immediate vicinity of the school (Figure 1). The finite-volume approach using a high-resolution unstructured, tetrahedral mesh with sufficient local grid refinement near the building walls, to accurately resolve the important features of the flow in areas of most interest, was used in order to describe the aforementioned computational domain. The mesh comprised of a total of 2500000 grid cells, with a minimum grid cell size of 0.3 m close to the building walls and an expansion ratio of 1.2. However, the grid was further refined close to the walls of the school building, where the minimum cell size was set to 0.1 m. At the top face boundary of the domain a symmetry condition was applied, while the lateral face boundaries of the domain, depending on the direction of the approaching flow were declared as inlet and outlet boundaries.

2.2 Turbulence Modelling

Numerical modeling of turbulence plays a crucial role in providing accurate predictions for wind fields, necessary to reliably predict transport and dispersion of pollutants in the vicinity of buildings. In ANSYS™ CFX 5.7.1, the Reynolds stresses and turbulent fluxes of scalar quantities can be calculated by several linear and nonlinear turbulence models. In all cases considered, the 3D Reynolds Averaged Navier Stokes (RANS) equations were solved coupled with the standard κ - ϵ two-equation turbulence model by Jones and Launder. The specific turbulence model was chosen because it is widely used and has been tested for various similar cases with very satisfactory results, as it has proved to provide stable solutions. The standard values for the wall functions were also used to allow the description of the airflow inside the viscous sub-layer near the walls.

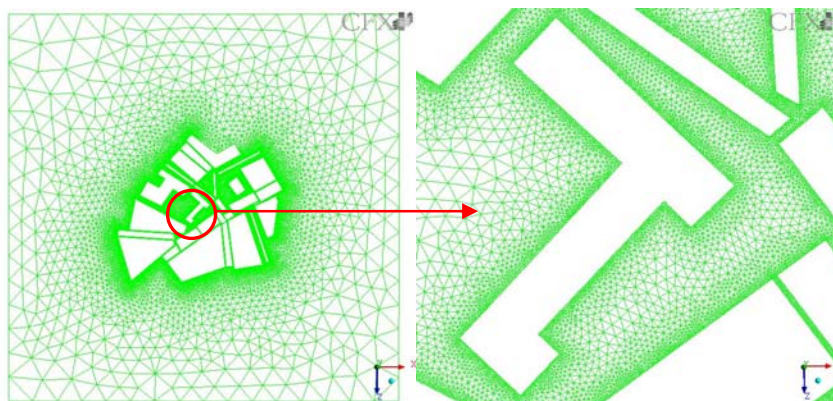


Figure 1: Computational domain and mesh with local grid refinement at the areas of interest

2.3 Boundary conditions

An inlet logarithmic wind profile with a reference speed $U_{ref} = 5 \text{ m s}^{-1}$ was assumed at the surface layer height $\delta=200 \text{ m}$, for all wind directions considered. In all cases the approaching atmospheric boundary layer (ABL) characteristics were assumed in accordance with VDI 3783/Part 12. In particular, a neutrally stratified approaching boundary layer with a roughness height of the ground $z_0 = 0.5 \text{ m}$, a power law exponent $\alpha = 0.25$ and turbulence intensity of 25 % was assumed. All building walls were treated as rough with a set roughness height of $z_0 = 0.1 \text{ m}$. Furthermore, in all cases considered, no heat transfer effects were taken into account. Finally, the main roads contributing to the traffic emitted pollution were treated as area sources, coinciding with the locations of traffic queues and regions of free-flowing traffic. Measured source strengths and their locations were provided by the Imperial College London Consultants Ltd (Figure 2). It should be noted that at neutrally stratified atmospheres concentration at a specific point varies linearly with the velocity.

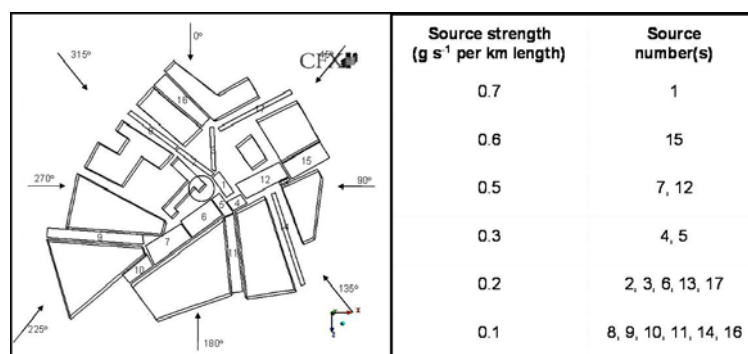


Figure 2: Source locations and modeled approaching wind directions. The circle denotes our area of interest.

3. RESULTS AND DISCUSSIONS

A series of 3D numerical simulations for eight different approaching wind directions were performed. Numerical results for the flow and concentration fields were extracted at horizontal and vertical levels around the side of the school building where the courtyards lies. In addition, concentration results were extracted at a specific location where a monitoring station exists. Results clearly indicate that depending on the approaching wind direction large variations on the effectiveness of the ventilation near the school area should be expected. From the analysis of the numerical concentration results near the monitoring station it is evident

that the highest concentrations near the school should be expected in the case when the wind is approaching from the South, South – East and East directions. On the other hand when the wind is approaching from the South – West, West and North – West minimum concentrations should be expected (Figure 3).

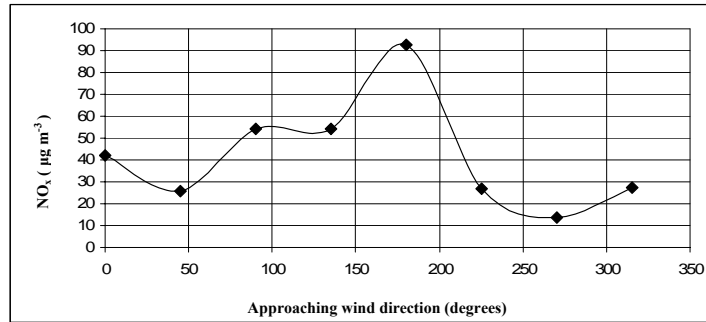


Figure 3: NO_x concentrations at the monitoring location for eight different approaching wind directions

Furthermore, when the flow approaches from the North East, East, or South East traffic emitted pollution from the main contributing nearby roads causes strong variability in NO_x concentrations across the treated wall. The effect of traffic emitted pollution from nearby roads has a much weaker influence on the NO_x concentrations when the wind is approaching from the South West and West. In the case when the wind is approaching from the North West and the North, the numerical results indicate that a significant amount of NO_x is transported from Aldgate back towards the treated wall due to the formation of an intense horizontal recirculation zone, giving rise to spatial variability in concentration across the wall surface (Figure 4).

Close examination of the vector plots extracted at vertical levels close to the area of interest, indicates the formation of relatively large re-circulation zones in front of the school where the courtyard lies, which leads to the entrapment of the traffic emitted pollutants. Furthermore, depending on the approaching wind direction the intensity and direction of rotation of those vortices varies. Comparison of the results for the cases of an approaching wind direction of 180° and 270°, which pose the cases with maximum and minimum predicted concentrations respectively, clearly indicate that in the former case the vortex which forms near the treated wall acts in driving pollutants towards the school building area while in the latter case in flushing pollution away from the school building area (Figure 5).

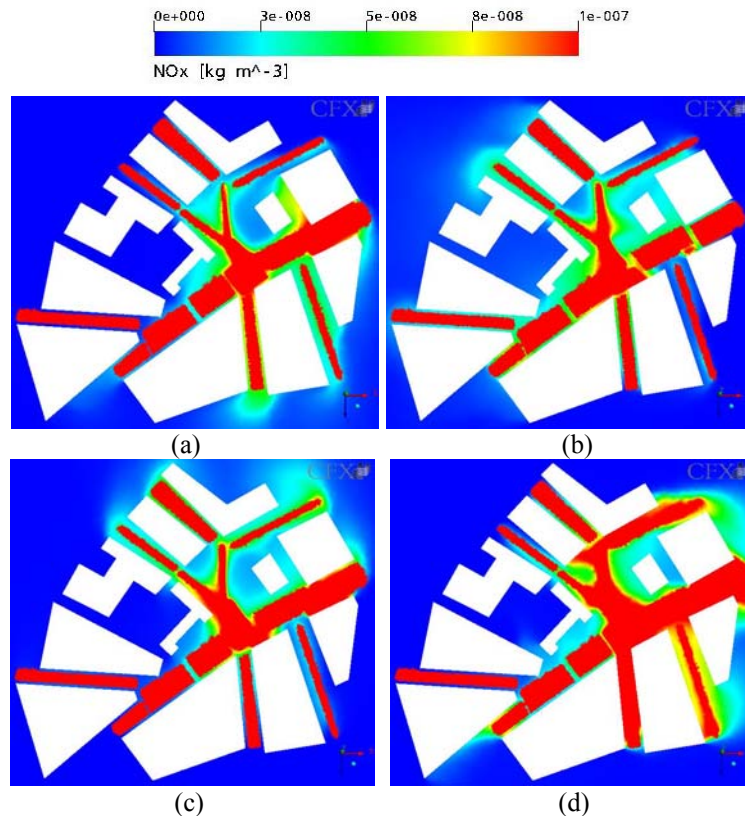


Figure 4: Concentration field of traffic emitted NO_x for approaching wind directions of (a) 0° , (b) 90° , (c) 180° and (d) 270° .

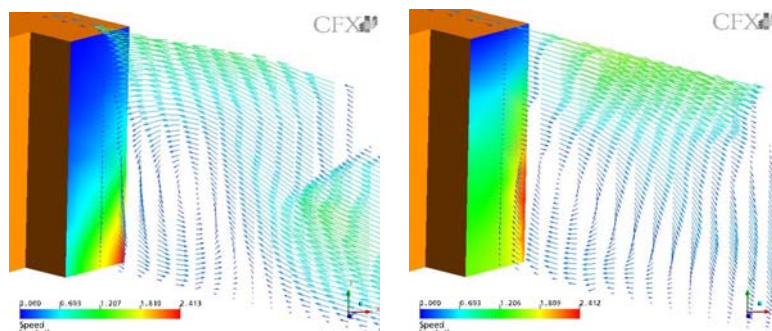


Figure 5: Vector plots at vertical levels perpendicular to the treated façade for approaching wind directions of (a) 180° and (b) 270° .

CONCLUSIONS

Overall in conclusion, the numerical results indicate high variations in the concentrations traffic emitted NO_x from the main contributing roads nearby, near the vicinity of the school and even more on the treated wall, depending on the direction of the approaching atmospheric boundary layer. What is more, the area in front of the Sir John Cass Primary School is relatively open and normally one would expect very low traffic emitted pollutant concentrations at the vicinity of the school. However the results have shown that the complex 3D effects of the shape of the school building itself as well as of the building geometries surrounding the school can lead to the entrapment of pollution near the school. What is more, the interaction between the wall and the courtyard in front of it seems to result into the accumulation of pollution on that wall which further increases the average concentration of NO_x near the school area. It is therefore evident, that in assessing the air quality and the exposure of vulnerable population groups, to potentially hazardous traffic emitted pollution the effects of the complex urban geometry needs to be accurately resolved via advanced Computational Fluid Dynamics techniques.

5. ACKNOWLEDGEMENTS

The authors gratefully acknowledge support from the Corporation of London, the Imperial College London Consultants and Millennium Chemicals UK Ltd.

6. REFERENCES

Leitl, B., Chauvet, C. and Schatzmann, M. 2001. Effects of geometrical simplifications and idealization on the accuracy of micro scale dispersion modeling. Extended abstract for the 3rd International Conference on Urban Air Quality, March 19-23, 2001, Loutraki, Greece

Moussiopoulos, N., Ossanlis, I., and Barmpas, P. 2005. A study of heat transfer effects on air pollution dispersion in street canyons by numerical simulations. *Int. J. Environment and Pollution* **25**, Nos. 1/2/3/4

Official PICADA web site: www.picada-project.com

Scarpadas, A. 2000. Modelling Air Flow and Pollutant Dispersion at Urban Canyon Intersections. Ph.D. Dissertation, University of London, UK.

VDI 3738, Part 12 2000. Environmental meteorology, Physical modeling of flow and dispersion processes in the atmospheric boundary layer, Application of wind tunnels. VDI, Germany.

EVALUATION AND INTER-COMPARISON OF OPEN ROAD LINE SOURCE MODELS CURRENTLY BEING USED IN THE NORDIC COUNTRIES: A NORPAC PROJECT

Janne Berger^a, Sam-Erik Walker^a, Bruce Denby^a, Per Løfstrøm^b, Matthias Ketzel^b, Ruwim Berkowicz^b

^aNorwegian Institute for Air Research (NILU) P.O. BOX 100, 2027 Kjeller, Norway; jbe@nilu.no

^bNational Environmental Research Institute (NERI)

ABSTRACT

The aim of this study was to inter-compare operational open road line source models that are currently in use in Denmark and Norway. Calculations using the OML and WORM models have been carried out using Danish and Norwegian datasets in order to inter-compare and evaluate the models. The inter-comparison focused on NO_x as the compound of interest, since its emissions are better defined than, for example, particulate matter. Preliminary results show that traffic produced turbulence has a significant effect for lower wind speeds. Both models perform well on the Danish dataset, however, WORM tends to overestimate concentrations on this dataset. Both models underestimate the Norwegian dataset.

1. INTRODUCTION

In order to evaluate and develop dispersion models, comparisons between different models and between different datasets is crucial. This paper describes model results from two open road line source models applied to two different datasets from measurement campaigns at open roads near Copenhagen and Oslo. The study is a part of NORPAC, which is a Nordic project on PM measurements and modelling. The preliminary results presented here represent the first stage, covering Norwegian and Danish models and datasets, in a Nordic inter-comparison project that will eventually involve Swedish and Finnish models and datasets. A description of the two models involved so far follows in section 2, and the results are described in section 3.

2. METHODOLOGY

Each of the countries involved in the inter-comparison provided their own monitoring datasets and performed the model calculations with their own models. A selection of the data was carried out to test the performance of the models under different conditions. The 3 selections presented here included all downwind data, all downwind data with wind speeds > 2 m/s and all downwind data with wind speeds >2 m/s and with wind directions within 30° of the perpendicular. The inter-comparison was conducted using two different models applied to two different datasets from measurement campaigns in Denmark and Norway.

Datasets

Both the datasets used were made during intensive campaigns near highways where 3 air quality stations were positioned at different distances from the road in the dominant downwind direction. 1 extra station was placed on the opposite side of the road to provide background concentrations. Meteorological measurements were also made at nearby masts. The datasets provided including air quality data, original and pre-processed meteorological data, traffic flow data, fleet composition data and emission data.

NO_x is used in this inter-comparison as its emissions are better defined than for other compounds. The inter-comparison was aimed at assessing the quality and variability of the transport and dispersion models, rather than the emissions. In this paper results from the inter-comparison are shown for just one station from each of the datasets. Both these stations were positioned approximately 50 m from the highway.

The OML model

The OML model is an atmospheric dispersion model developed by the National Environmental Research Institute (NERI) in Denmark. It assumes that the dispersion of a plume develops in a steady state Gaussian manner, according to the slender plume approximation. As input, the model uses emission data, meteorology (wind speed, wind direction, radiation, stability, turbulence parameters), traffic data, and information about the surrounding terrain. There are two versions of the model; OML-Point and OML-Multi. The latter, which is applied in this study, treats the highway as an area source.

The model is modified towards highway traffic, as traffic produced turbulence (TPT) is now integrated in the model. Close to a source there is an initial dispersion, which in the case of a highway source, is dominated by TPT. The movement of the vehicles creates turbulence which dominates close to the source. TPT is estimated using the same procedure as in the street pollution model OSPM (Berkowicz, 2000), where TPT is a function of the number of vehicles, vehicle size, and vehicle speed. However, at longer distances from the highway,

the atmospheric turbulence dominates, as the TPT is assumed to decrease exponentially with the distance from the road.

The WORM model

The WORM model (Weak Wind Open Road Model) is a recently developed integrated Gaussian line source model at NILU, similar to the CAR-FMI model (Härkönen et al., 1996). The model calculates hourly average concentrations based on emission data and meteorology. The model uses Gaussian quadrature to integrate the line source, which is highly accurate, also in situations when the wind blows parallel to the road. The model incorporates a meteorological pre-processor used to calculate turbulence parameters based on standard boundary layer (M-O) similarity theory. For the current version of the WORM model, a minimum value of horizontal plume diffusivity (σ_v) equal to 0.5 m/s is used. Traffic turbulence in WORM is modelled using the same semi-empirical formulation for traffic-originated turbulence as used in the CAR-FMI model (Härkönen et al., 1996, Eq. 9), defining initial size of the plume σ_{z0} and $\sigma_{y0} = 2\sigma_{z0}$. The model has been applied for data assimilation studies in Oslo (Walker, 2006).

3. RESULTS AND DISCUSSION

Modelling results for OML and WORM – all data

Figure 3.1 shows scatter plots of modelled and observed concentrations of NO_x for OML and WORM applied to both the Danish and Norwegian data. The background is excluded in order to capture the emission contribution from the road only. For the WORM model wind speeds below 0.5 ms^{-1} are excluded, otherwise all wind directions and wind speeds are included. Both models perform well on the Danish data, except for a slight overestimation for WORM. Both models underestimate the Norwegian data significantly.

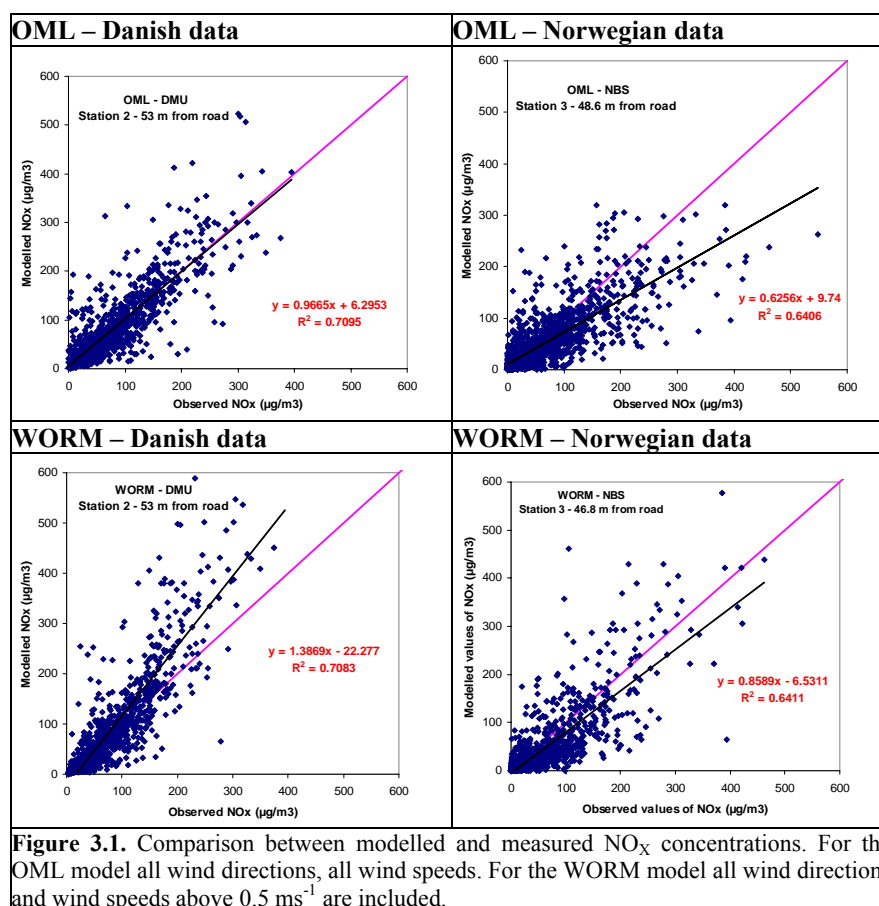
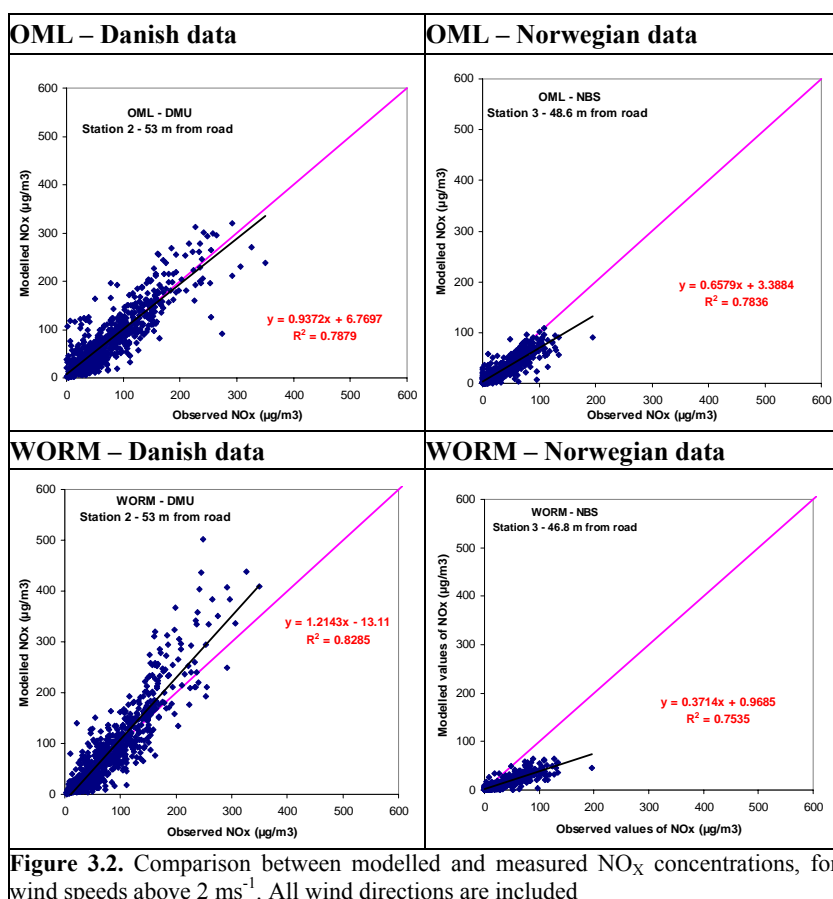


Figure 3.1. Comparison between modelled and measured NO_x concentrations. For the OML model all wind directions, all wind speeds. For the WORM model all wind directions and wind speeds above 0.5 ms^{-1} are included.

Modelling results for OML and WORM $u > 2 \text{ ms}^{-1}$

Based on the knowledge that the model performance for low wind speeds is poorer than for higher wind speeds we excluded data for which the wind speeds were below 2 ms^{-1} . These results are shown in figure 3.2, where the conditions are the same as in figure 3.1, except with the exclusion of low wind speeds. The effect of this filtering is not as visible for OML as it is for WORM where there is a significant under-prediction for these higher wind speed cases, especially for the Norwegian data.



Modelling results for OML and WORM $u > 2 \text{ ms}^{-1}$ and $\theta \perp \text{road} \pm 30^\circ$

Line source models are often inaccurate for winds that are directed parallel to the road, due to both numerical and physical considerations. This aspect has been tested by filtering the data presented in figure 3.2 above so as to only allow data where the wind blows perpendicular to the road $\pm 30^\circ$. Data for which the wind speeds are below 2 ms⁻¹ are also excluded, as in figure 3.2. These are highly idealised conditions for slender plume Gaussian models and the expectation is that the models should perform best under these circumstances. Making this selection significantly reduces the number of data points from the Norwegian site but the results are similar to those obtained for all wind directions, figure 3.2, and are not shown here see table 1 for a summary). There seems to be no significant improvement resulting from the exclusion of wind directions outside of this 30° sector, indicating that both models perform well for all wind directions.

The results are further summarised below in table 1 where the fractional bias and regression coefficients are shown for the 3 selection criteria and the four combinations of model and datasets.

Table 1. Fractional bias (top) and correlation (bottom) for OML and WORM applied to the Danish and Norwegian datasets for all the three alternatives.

Fractional bias (FB)				
Model	OML	OML	WORM	WORM
Dataset	DMU	NBS	DMU	NBS
All data	0.04	-0.24	0.12	-0.30
$u > 2 \text{ ms}^{-1}$	0.03	-0.28	0.05	-0.86
$u > 2 \text{ ms}^{-1}, \theta \perp \text{road} \pm 30^\circ$	0.01	-0.11	0.09	-0.70
Correlation coefficient R ²				
Model	OML	OML	WORM	WORM
Dataset	DMU	NBS	DMU	NBS
All data	0.71	0.64	0.71	0.64
$u > 2 \text{ ms}^{-1}$	0.79	0.78	0.83	0.75
$u > 2 \text{ ms}^{-1}, \theta \perp \text{road} \pm 30^\circ$	0.87	0.77	0.85	0.84

4. CONCLUSION AND DISCUSSION

The two open road line source models, OML and WORM, have been compared and evaluated based on their application to two datasets from measurement campaigns in Denmark and Norway. In general it can be seen that both models perform quite well on the Danish data set with the WORM model overestimating the concentrations the most by an average of around 12%. Both models, on the other hand underestimate concentrations for the Norwegian dataset. This underestimation is most pronounced for the WORM model. The same tendencies occur for both the filtered and unfiltered datasets. There does not seem to be a significant degradation in the results when all wind directions are included in the analysis indicating that both models perform well for all wind directions. Correlation of the models are quite similar on similar datasets. Correlation for both models generally improves when wind speeds < 2m/s are excluded.

Both models are based on the same theoretical basis, i.e. Gaussian slender plume approximation, and use similar turbulence parameterizations. The major difference that should separate the models is the inclusion of traffic produced turbulence. It is interesting to note that the relative bias of WORM, in regard to OML, is positive for the Danish data set and negative for the Norwegian dataset, table 1. The conclusion is that there must be a difference between the two sites that is not accounted for in the WORM model and this difference is expected to be the TPT. The Danish measurements were carried out on a much more highly trafficked road than the Norwegian measurements, 14 000 VEH/day compared to 5 978 VEH/day, and the average traffic speed at the Danish site was also higher, 109 km/hr compared to 83 km/hr at the Norwegian site. As a result the TPT should be significantly higher at the Danish site. Since the WORM model does not take into account the TPT, as OML does, we would expect the WORM model to produce higher concentrations at the Danish site relative to those at the Norwegian site, since dilution by TPT is largest at that site. Independent runs carried out using the OML model without TPT indicate a significant increase in model concentrations, by a factor of 2 or more, when TPT is not included. This demonstrates the significance of this process. This however does not explain the significant negative bias of the WORM model and more attention will be given to this in the future.

The inter-comparison demonstrates the usefulness of comparing models on differing datasets and will lead to improved and more robust models in the future. Further work will be carried out in this study to include the Finnish and Swedish models and datasets.

REFERENCES

- Berkowicz, R., 2000 OSPM – a parameterised street pollution model. *Environmental Monitoring & Assessment* 65, 323-331.
- Jensen, S. S., Løfstrøm, P., Berkowicz, R., Olesen, H. R., Frydendal, J., Fuglsang, K., Hummelshøj, P., 2004 Air quality along motorways – Measurement campaign and model calculations. National Environmental Research Institute, Denmark, 67 p. – NERI report No. 522. <http://fagligerapporter.dmu.dk> (In Danish).
- Härkönen, J., Valkonen, E., Kukkonen, J., Rantakrans, E., Lahtinen, K., Karppinen, A., Jalkanen, L. 1996. A model for the dispersion of pollution from a road network. Finnish Meteorological Institute, Publ. on Air Quality 23, Helsinki.
- Walker, S.E. 2006. Air4EU case study D 7.1.4. Data assimilation in open road line source modelling. www.air4eu.nl/reports_products.html

CFD ANALYSIS OF WIND FLOW FIELD FOR EVALUATING NO₂, NO, AND OZONE VERTICAL DISTRIBUTION INSIDE A STREET-CANYON

Costabile, F., Sinesi, M. and Allegrini, I.

*Institute for atmospheric pollution, National Research Council, Via Salaria km 29,300 C.P.
10, 00016 Monterotondo Stazione, Rome, Italy (costabile@iia.cnr.it).*

ABSTRACT

The major objective of this paper is to provide insights into the factors influencing vertical distribution of reactive pollutants in urban canyon-like spaces. With this aim CFD simulations of wind flow field were combined to field intensive measurements taken in a Chinese urban street-canyon. Similar to the wind flow field, pollutant concentrations were found to be significantly different from roof to yard and had no obvious correlation with the distances from local traffic emission sources. Fine-scale CFD simulations gave insights into these findings showing as the modelled inside-canyon, inside-yard, and tree-generated recirculation vortices can efficiently support the understanding of the measured NO, NO₂, and O₃ patterns.

1. INTRODUCTION

Traffic-related pollution is currently one of the major topics of urban air quality, particularly in street-canyons where high pollutant concentrations can be hence induced (e.g.: Kukkonen et al., 2001; Pavageau et al., 1999; Zhou and Sperling, 2001). Computational Fluid Dynamics (CFD) models have been shown to be accurate tools for predicting urban airflow patterns and air pollutants dispersion on local scale (e.g.: Borrego et al., 2003). Fine-scale CFD simulations are able to account rigorously for urban topography, local aerodynamics and turbulence, and thermal heat fluxes (e.g.: Kondo et al., 2006).

This paper reports some results of a current study (Costabile et al., 2006a,b) aiming at understanding the fine scale motion of air pollutants within urban building environments. To this purpose measurements of NO, NO₂ and O₃ concentrations and CFD simulation of wind flow field have been performed in a Chinese street-canyon (Suzhou). The major objective is to provide insights into the factors influencing vertical distribution (yard-roof) of reactive pollutants such as Nitrogen Oxides and Ozone in urban canyon-like spaces.

2. METHODOLOGY

Continuous field measurements were carried out in Suzhou (China) for seven days (Jun29-Jul5, 2005) in a 30-meter wide street-canyon (width/height=1.8~3.5). Ambient concentrations of NO_x, NO₂, NO, O₃, wind speed and direction were measured at two sites: on the roof of a 20 meters high building and in the yard of the same building. The measurement protocol was already described by Costabile et al. (2006a,b).

Star-CCM+ software package (CD-Adapco®) was used as CFD code to calculate the fluid flow over a 3D grid. A box was constructed wrapping the study area and including all the objects (buildings, trees, etc.) affecting local wind field and pollutant dispersion. The initial dimensions (vertical and horizontal axis >3 and 2.5 times the taller building height, respectively) were optimised catching the significant pollutant dispersion phenomena (building cavities, local vortices, canyon effects), performing a solution sensitivity analysis (modelled/measured wind flow), and minimizing calculation time. The solid geometry was then subtracted to the box so the subtracted was just fluid. Boundary conditions were then assigned; flow inlet and outlet boundaries were selected according to the measurement data focussing on the two prevailing wind directions, perpendicular (180°) and parallel (270°) winds. Turbulence intensity and viscosity were set in the range of 0.01÷0.1 and 10÷100, respectively. Building boundaries were set as slip wall (flow slide parallel to the wall) and the ground boundary as non slip wall to take into account the roughness effect. A polyedrical volume mesh was used.

3. RESULTS AND DISCUSSION

Measurements show the wind flow field to be different from roof to yard (fig.1). These variations likely influenced considerably the concentrations of NO, NO₂ and O₃ that varied significantly inside the canyon relative to the height of the measurement points.

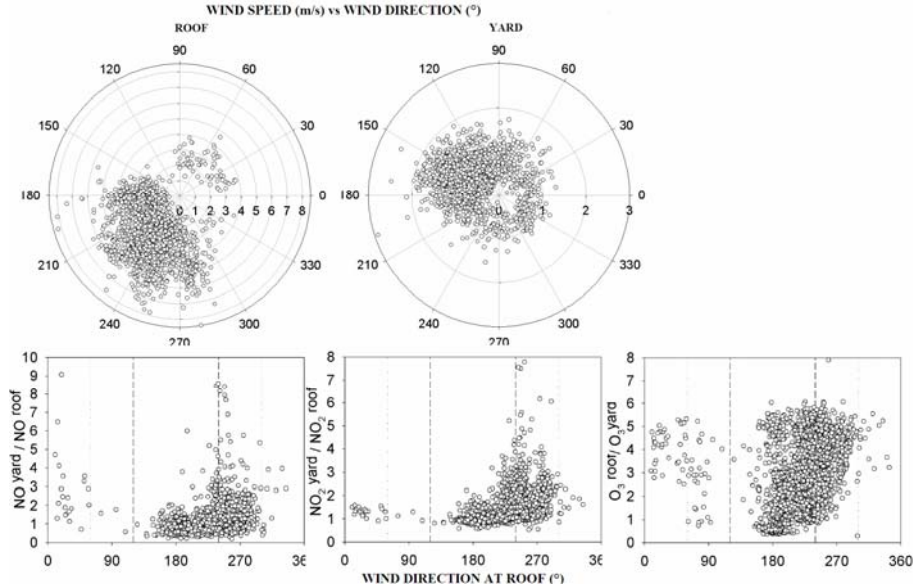


Figure 1. Wind roses (top), and yard/roof NO, NO₂, O₃ ratios vs roof wind direction (bottom).

Fine-scale CFD simulations can likely give insights into the measurement findings. Several inter-comparisons have been performed between the results obtained with CFD models and data from real sites, allowing to analyse models constraints and capabilities (e.g.: Borrego et al., 2003). The modelled horizontal wind velocities were compared with the measured inlet boundary conditions to study pollutant dispersion. Horizontal wind speeds were found to decrease from roof to yard mostly for parallel winds (270°, fig.2); in the yard hence pollutants were likely both less diluted and more entrapped than on the rooftop (that is, higher yard pollutant concentrations, fig.1). For perpendicular winds (~180°) the inside-canyon vortex (e.g.: Vardoulakis et al., 2003) induced in the windward yard weaker influences from local traffic emissions; on the contrary, the generated downward mass flow (fig.3) can probably explain the little pollutant vertical variation measured (pollutant ratios ~ 1, fig.1). Inside-yard and tree-generated vortices were found to be significant (fig.3, 4). This likely induced in the yard lower concentrations of local-traffic pollutants; as well, it can likely explain the strong horizontal wind direction differences measured from roof to yard (fig.1). Therefore, the extent of NO and NO₂ oxidation and the pollutant spatial variation appear to be more influenced by these vortex recirculation patterns in the canyon-like yard than by the distances from the local emission sources. The impact of polluted air masses from other streets (channelled by lateral narrow roads) was also found to be significant (fig.5) providing probable explanation to the high concentrations of primary pollutants often measured on the rooftop.

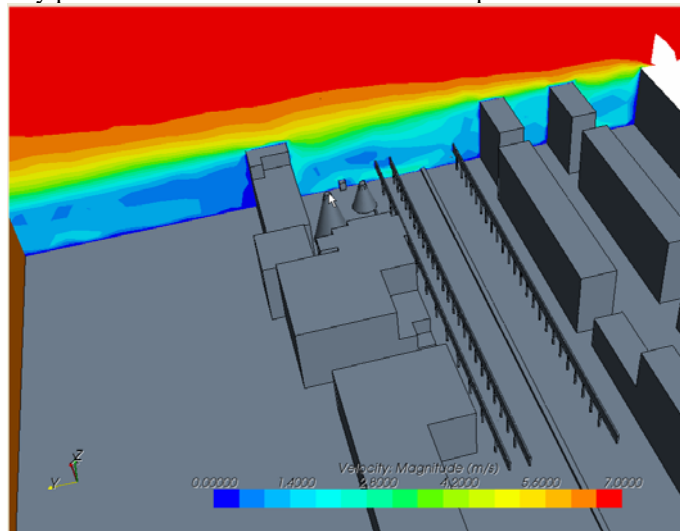


Figure 2. Vertical cross section slice of the modelled wind magnitude including the yard measurement site.

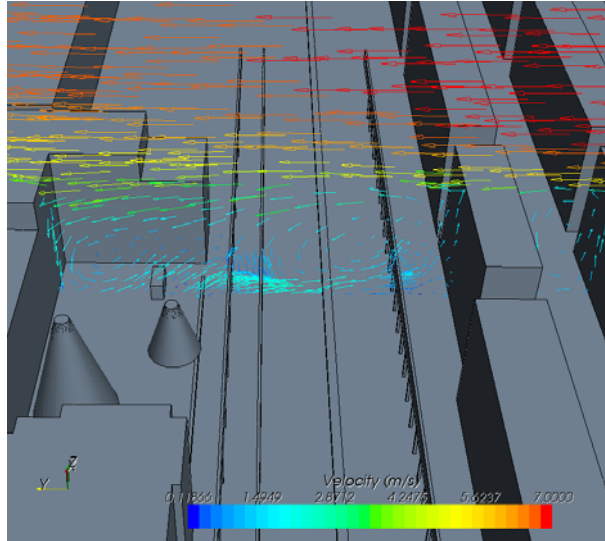


Figure 3. Vertical cross section slice of the modelled wind vector including the yard measurement site.

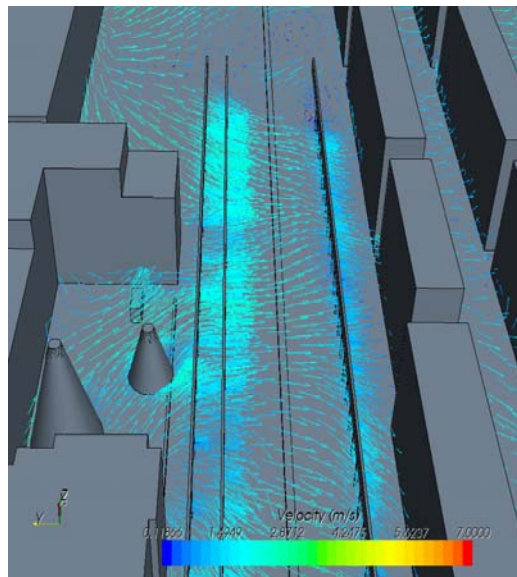


Figure 4. Horizontal cross section slice (5-meters high) of the modelled wind vectors.

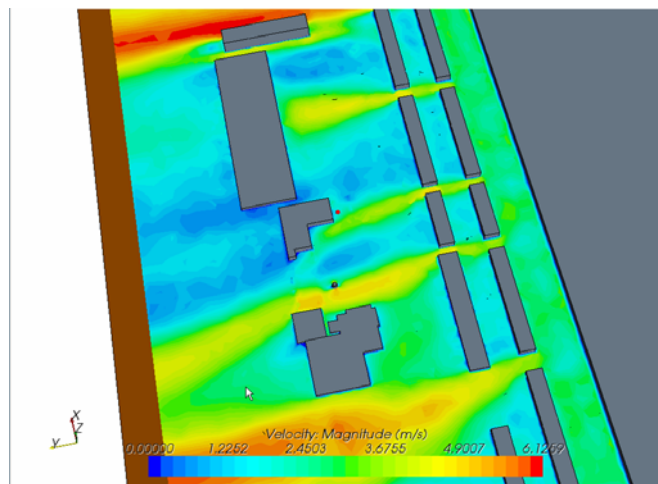


Figure 5. Horizontal cross section slice (15-meters high) of the modelled wind magnitude.

4. CONCLUSIONS

This paper presented the combined use of CFD modelling and field intensive measurements to give insights into the factors influencing vertical distribution of pollutants such as Nitrogen Oxides and Ozone in street-canyon.

Measurements showed wind flow fields to be different from roof to yard. As well, NO, NO₂ and O₃ concentrations varied significantly inside the canyon and had no obvious correlation with the distances from local traffic emission sources. Fine-scale CFD simulations gave insights into these findings showing as the modelled inside-canyon, inside-yard, and tree-generated recirculation vortexes can efficiently support the understanding of the measured NO, NO₂, and O₃ patterns.

The methodology has proved to be suitable for application where constant wind direction conditions are predominant (as the Suzhou case). Emission models able to compute emission data on different spatial and temporal scale are widely used to provide the pollutants spatial distribution. However, the selection of an adequate model and the precise quantification of pollutant amount emitted by vehicles to the atmosphere are difficult and final uncertainty on air quality prediction still remains. Therefore, the application of CFD combined to field measurements can well enhance the interpretation of field measurements, especially when looking at the spatial variations of reactive pollutants.

5. ACKNOWLEDGEMENTS

This study has been part of the Sino-Italian Cooperation Program for Environmental Protection held by the Italian Ministry of Environment, Land and Sea (IMELS) and the Chinese State Environmental Protection Agency. Funding from IMELS is gratefully acknowledged. The authors would also like to thank Suzhou EPB and EMC and particularly Hong Weimin and Liu Fenglei for the significant support. The help of Wang Fenjuan in taking measurements is also acknowledged.

6. REFERENCES

- Borrego,C., Tchepel,O., Costa, A.M., Amorim, J.H., Mirando, A.I., 2003. Emission and dispersion modelling of Lisbon air quality at local scale. *Atmospheric Environment* 37, 5197–5205
- Costabile, F. , Wang, F., Hong, W., Liu, F. and Allegrini, I., 2006a. Spatial Distribution of Traffic Air Pollution and Evaluation of Transport Vehicle Emission Dispersion in Ambient Air in Urban Areas. *JSME International journal-B* 49 (1) 27-34.
- Costabile,F., Wang, Hong, Liu, & Allegrini,I. 2006b. CFD modelling of traffic-related air pollutants around urban street-canyon in Suzhou. In: *Air Pollution*, pp.297-306. J. Longhurst & C.A. Brebbia (ed.), WIT press, UK.
- Kondo, H., K. Asahi, T. Tomizuka, M. Suzuki (2006). Numerical analysis of diffusion around a suspended expressway by a multi-scale CFD model. *Atmos. Environ.* 40: 2852-2859.
- Kukkonen, J., Valkonen, E., Walden, J., Koskentalo, T., Aarnio, P., Karppinen, A., Berkowicz, R., Kartastenpaa, R., 2001. A measurement campaign in a street canyon in Helsinki and comparison of results with predictions of the OSPM model. *Atmospheric Environment* 35, 231–243.
- Pavageau, M., Schatzmann, M., 1999. Wind tunnel measurements of concentration fluctuations in an urban street canyon. *Atmospheric Environment* 33, 3961–3971.
- Vardoulakis, S., Fisher, B., Pericleous, K., Gonzalez-Flesca, N, 2003. Modelling air quality in street canyons: a review. *Atmospheric Environment* 37, 155–182
- Zhou H, Sperling D,. Traffic emission pollution sampling and analysis on urban streets with high-rising buildings. *Transportation research part D6*, 2001: 269-181.

REFINEMENT AND STATISTICAL EVALUATION OF A MODELLING SYSTEM FOR PREDICTING FINE PARTICLE CONCENTRATIONS IN URBAN AREAS

Kauhaniemi M (1,*), Karppinen A (1), Härkönen J (1), Kousa A (2), Koskentalo T (2), Aarnio P (2), and
Kukkonen J (1)

1) Finnish Meteorological Institute (FMI), Helsinki, Finland
2) Helsinki Metropolitan Area Council (YTV), Helsinki, Finland

*) Mari.Kauhaniemi@fmi.fi, phone: +358-40-5171771, fax: +358-17-162301, Finnish Meteorological Institute,
Air Quality Research, P.O. Box 1627, 70211 Kuopio, Finland.

ABSTRACT

We present a modelling system that contains a treatment of particulate matter at an urban scale, combined with a statistical model for estimating the contribution of long-range transported aerosols (LRT) that utilises data from EMEP monitoring stations. The predicted results were compared against monitored data from two locations in Helsinki: urban roadside station at Vallila and urban background station at Kallio. The predicted daily average PM_{2.5} concentrations in 2002 agree fairly well with the measured values; the Index of Agreement IA values were 0.83 and 0.86 at Vallila and Kallio, respectively. Model slightly over predicts the measurements at Vallila (Fractional Bias FB=0.13) and under predicts at Kallio (FB=-0.09). The results show that the modelling system is a useful tool for the assessment of PM_{2.5} concentrations in urban areas.

1. INTRODUCTION

Ambient air pollution, especially fine particulate matter (PM_{2.5}), has been associated to excess mortality and morbidity at the current urban levels. The evidence on airborne particulate matter (PM) and its public health impact is consistent in showing adverse health effects at exposures that are currently experienced by urban populations in both developed and developing countries. According to the CAFÉ (Clean Air for Europe) programme, exposure to particulate matter was estimated to reduce average statistical life expectancy by approximately nine months in 25 member states of EU in the year 2000. This equates to approximately 3.6 million life years lost or 348 000 premature mortalities per year (European Commission, 2005).

The objective of this study is to present a combined modelling system that addresses particulate matter on an urban scale and long-range transported aerosols (LRT). We have evaluated the advantages and limitations of the statistical model (Karppinen et al., 2004) for computing the LRT'ed contribution to PM_{2.5} in U.K. and in Finland (Kukkonen et al., 2007). We also aim to evaluate the performance of the combined modelling system against measured PM_{2.5} data in Helsinki.

2. METHODOLOGY

Meteorological and Air Quality Measurements

The relevant meteorological parameters for the models are evaluated using data produced by a meteorological pre-processing model (Karppinen et al., 1997, 1998). The location of the study area, the meteorological stations and the background air quality measurement stations are presented in Figures 1a and b. We used a combination of the data from the stations at Helsinki-Vantaa airport and Helsinki-Isosaari. The mixing height of the atmospheric boundary layer was evaluated using the meteorological pre-processor, based on the sounding observations at Jokioinen (90 km northwest) and the routine meteorological observations.

The EMEP stations ('Co-operative programme for monitoring and evaluating of the long-range transmission of air pollutants in Europe') that are located nearest to Helsinki are shown in Figure 1a; these are Utö, Ähtäri and Virolahti. The following concentrations are measured daily at the EMEP stations: (i) SO₄²⁻ (sulphate), (ii) the sum of NO₃⁻ (nitrate) and HNO₃ (nitrogen acid), and (iii) the sum of NH₄⁺ (ammonium) and NH₃ (ammonia). The fine particle (PM_{2.5}) measurements of the Helsinki Metropolitan Area Council (YTV) monitoring stations at Vallila and Kallio were used. The location of the YTV monitoring stations in Helsinki metropolitan area is shown in Figure 1b. Monitoring station of Vallila represents urban roadside conditions. The Kallio station is an urban background monitoring station.

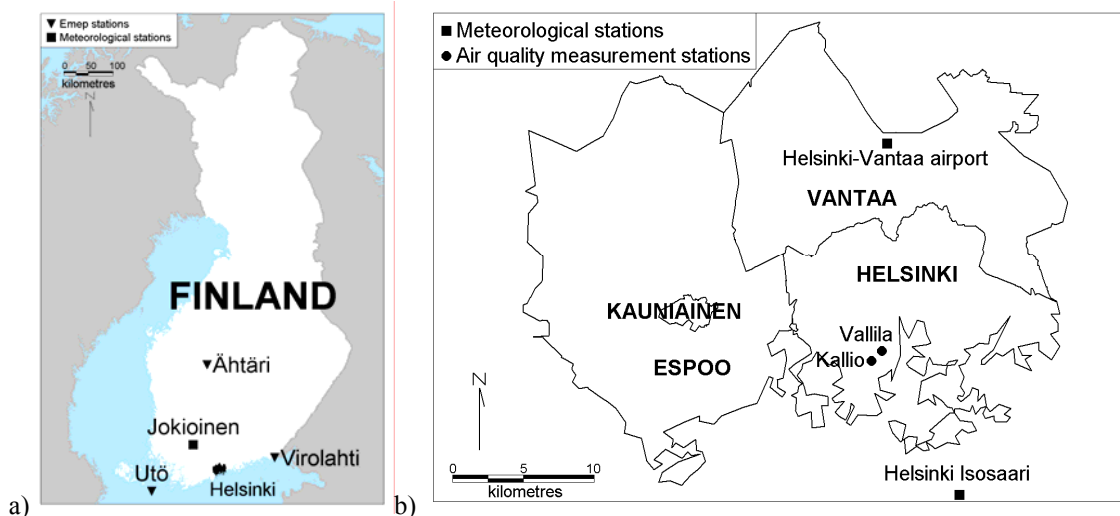


Figure 1. The meteorological and air quality monitoring stations in the Helsinki metropolitan area in 2002 (edited YTV, 2003).

Modelling System

The atmospheric dispersion of vehicular emissions is evaluated using a roadside dispersion model, CAR-FMI (Härkönen, 2002). The dispersion equation is based on an analytic solution of the Gaussian dilution equation for a finite line source. The dispersion parameters are modelled as function of the Monin-Obukhov length, the friction velocity and the mixing height. Traffic-originated turbulence is modelled with a semi-empirical treatment. The model includes the basic reactions of nitrogen oxides, oxygen and ozone, and the dry deposition of the fine particles. The model also takes into account the effect of the non-exhaust vehicular emissions and particulate matter suspended from the street surfaces, using empirical correlations.

The long-range transported contribution to urban particulate matter was evaluated with a statistical model (Kukkonen et al., 2007) that utilises, as input values, the daily sulphate, nitrate and ammonium ion concentrations measured at the EMEP stations. Currently, there is also an option to use representative regional background $PM_{2.5}$ concentration measurements in the Helsinki Metropolitan area. The regional background $PM_{2.5}$ concentrations can also be determined using the European-scale computations using the regional and continental-scale dispersion model SILAM (Sofiev et al, 2006).

3. RESULTS AND DISCUSSION

The mean, the maximum and the standard deviation, together with the statistical parameters for the predicted and observed daily average time series of $PM_{2.5}$ concentrations in 2002, for Vallila and Kallio monitoring stations are presented in Table 2.

Table 2. The statistical analysis of the predicted and observed daily average time series of $PM_{2.5}$ concentrations at the Vallila and Kallio monitoring stations for 2002 (the days 01.01.02 and 31.12.02 are omitted).

Statistical Parameter	Vallila		Kallio	
	Predicted	Observed	Predicted	Observed
Mean ($\mu\text{g}/\text{m}^3$)	11.2	9.90	7.92	8.64
Maximum ($\mu\text{g}/\text{m}^3$)	39.0	52.0	35.2	42.5
Standard deviation ($\mu\text{g}/\text{m}^3$)	5.31	6.75	4.80	5.89
Index of agreement (IA)		0.83		0.86
Pearson's correlation coefficient (COR)		0.74		0.77
Normalised mean square error (NMSE)		0.16		0.16
Fractional bias (FB)		0.13		-0.09
Number of data	360	360	358	358

At both stations the predicted $PM_{2.5}$ concentrations agree fairly well with the measured data. The model has slight over prediction for the station at Vallila and minor under prediction for the station at Kallio. The scatter plots of the predictions and observations at Vallila and Kallio in 2002 is presented in Figures 2a and b.

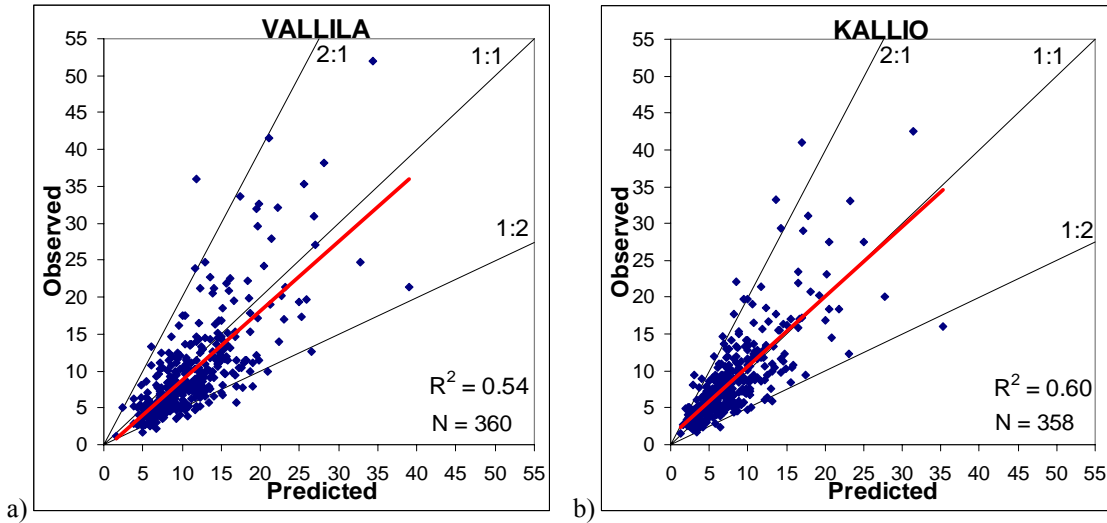


Figure 2. The scatter plots and the correlation coefficient squared (R^2) values of the predicted and observed daily average $PM_{2.5}$ concentrations in 2002, for the monitoring stations at Vallila (a) and Kallio (b).

Predicted total annual average concentration of $PM_{2.5}$ in the Helsinki metropolitan area and Helsinki city centre are presented in Figures 3a and b, respectively. On a yearly basis, the estimated contribution from regional and long-range transported origin to the observed $PM_{2.5}$ varies from 40 % at the most trafficked areas in Helsinki to nearly 100 % in the outskirts of the metropolitan area.

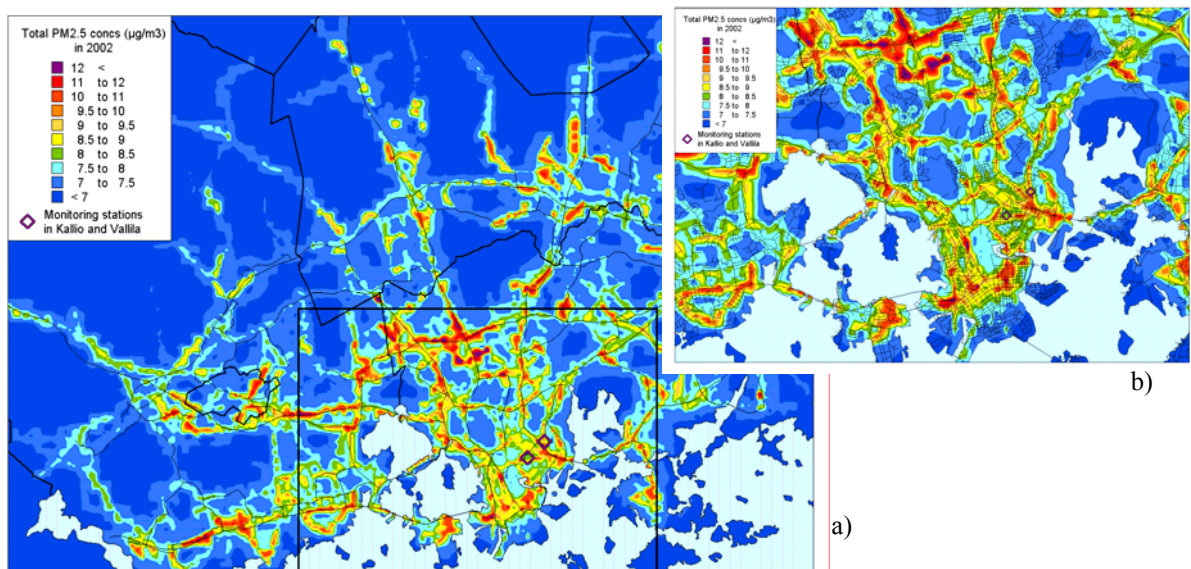


Figure 3. Predicted total annual average $PM_{2.5}$ concentrations [$\mu g/m^3$] in 2002, in the Helsinki metropolitan area (a) and in the centre of Helsinki (b). The main road and street network, and the monitoring stations of $PM_{2.5}$ are also presented in the figure.

4. CONCLUSIONS

The comparison of the modelled daily averaged values with the corresponding measurements showed a fairly good agreement. The results show that the statistical LRT model is a useful and simple tool for the assessment of LTR'ed PM_{2.5} that is applicable within a fairly good accuracy. Clearly, the model also has inherent limitations. The accuracy of the model presented depends on the chemical composition of PM_{2.5}, especially the content of carbonaceous species; however, measurements of these species at the EMEP stations have not been published. The ion sum parameter defined also contains in part the measurements of two gaseous substances (HNO₃, NH₃). If their concentrations were high, compared to the concentrations of the corresponding compounds in particulate form, there could be substantial inaccuracies in the model predictions.

5. ACKNOWLEDGEMENTS

This study is a part of the EC-funded FP5 projects SAPHIRE (Source Apportionment of Airborne Particulate Matter and Polycyclic Aromatic Hydrocarbons in Urban Regions of Europe; project number: EVK4-2002-00089) and OSCAR (EVK4-CT-2002-00083). Both these projects are part of the FP5 City of Tomorrow Cluster of European Air Quality Research (CLEAR). We also wish to thank for the contribution and funding of the national projects KOPRA and the Nordic cooperative project NORPAC.

6. REFERENCES

- European Commission, 2005. Proposal for a Directive of the European Parliament and of the Council on Ambient Air Quality and Cleaner Air for Europe, Brussels, 21.9.2005, COM(2005) 447 final, 2005/0183 (COD), the "CAFE" Directive, (<http://europa.eu.int/comm/environment/air/cafef/>).
- Härkönen, J., 2002. Regulatory dispersion modelling of traffic-originated pollution. Finnish Meteorological Institute, Contributions No. 38, FMI-CONT-38, ISSN 0782-6117, University Press, Helsinki, 103 p.
- Karppinen, A., Joffre, S. M., Vaajama, P., 1997. Boundary-layer parameterization for Finnish regulatory dispersion models, International Journal of Environment and Pollution, Vol. 8, Nos. 3-6, pp. 557-564.
- Karppinen, A., Kukkonen, J., Nordlund, G., Rantakrans, E., Valkama, I., 1998. A Dispersion Modelling System For Urban Air Pollution, Finnish Meteorological Institute Contributions 28, University Press, Helsinki, ISBN 951-697-480-5, 54 p.
- Karppinen, A., Härkönen, J., Kukkonen, J., Aarnio, P., and Koskentalo, T., 2004. Statistical model for assessing the portion of fine particulate matter transported regionally and long-range to urban air. Scandinavian Journal of Work, Environment & Health, 30 suppl 2, pp. 47-53.
- Kukkonen, J., Sokhi, R., Luhana, L., Härkönen, J., Salmi, T., and Karppinen, A., 2007. Evaluation and application of a statistical model for assessment of long-range transported proportion of PM_{2.5} in the United Kingdom and in Finland. Atmospheric Environment, in print.
- Sofiev, M., Siljamo, P., Valkama, I., Ilvonen, M., and Kukkonen, J., 2006. The evaluation of the Lagrangian dispersion modelling system SILAM using the ETEX data. Atmospheric Environment, 40:4, pp. 674-685.
- YTV, 2003. Ilmanlaatu pääkaupunkiseudulla vuonna 2002; Air Quality in Helsinki Metropolitan Area year 2002. Helsinki Metropolitan Area Series B 2003:11, YTV Helsinki Metropolitan Area Council, ISSN 0357-5454, ISBN 951-798-542-8, 53 p.

FLUID FLOW AND POLLUTANT DISPERSION WITHIN TWO-DIMENSIONAL STREET CANYONS – EVALUATION OF VARIOUS TURBULENCE MODELS AGAINST EXPERIMENTAL DATA

N. Koutsourakis^{1*}, J. G. Bartzis², N. C. Markatos³

¹ Environmental Research Laboratory, Institute of Nuclear Technology-Radiation Protection, National Centre for Scientific Research 'Demokritos', Aghia Paraskevi 15310, Greece

² Environmental Technology Laboratory, Department of Management and Engineering of Energy Resources, University of West Macedonia, Kastorias and Fleming Str., Kozani 50100, Greece

³ Computational Fluid Dynamics Unit, School of Chemical Engineering, National Technical University of Athens, 9 Iroon Polytechniou Str., Zografou Campus, Athens 15780, Greece

(* Author for correspondence; e-mail: nk@ipta.demokritos.gr)

ABSTRACT

The commercially available Computational Fluid Dynamics (CFD) code PHOENICS is used to assess the fluid flow and the pollutant dispersion in two-dimensional street canyons. The study is focused on the turbulence model, since that is the most questionable factor of the modelling. Three turbulence models, namely the $k-\varepsilon$, RNG $k-\varepsilon$ and Reynolds Stress Model (RSM) are examined and conclusions are reached about their applicability and ease of use. Results are compared with various datasets of experimental data, mainly taken from wind tunnels. Having validated the code for urban canyon flows, pollutant concentration results from a real street canyon at the suburb of Athens Aghia Varvara in Greece are presented. It is concluded that CFD is capable of dealing with urban flows and assisting the investigation of pollution trapping inside the canyons, with reasonable computer resources. However, more research should be performed on the turbulence model field.

1. INTRODUCTION

More than half of the world's population reside in cities. Vehicles are the main pollution source in urban areas and the vehicle fleet has decupled in the last 50 years (Fenger, 1999). Car exhausts release the pollutants in the constitutive elements of the cities, the street canyons, contributing in this way to the downgrading of the air quality. This is the main reason that the street canyon, the area between two buildings, has attracted the interest of many scientists. Early studies, almost four decades ago, revealed the characteristic recirculation vortex that dominates the whole canyon and results in the trapping of pollutants and in higher concentration levels at the upwind, or leeward, side. DePaul and Sheih (1986), who themselves performed a field experiment to investigate the flow characteristics inside a real street canyon, cite plenty of such early scientific works, both experimental and numerical.

Few years later, the use of Computational Fluid Dynamics (Hunter *et al.*, 1992, Sini *et al.*, 1996) was proved to be a very powerful tool for the urban canyon flow and dispersion investigation. Hassan and Crowther (1998) used the PHOENICS code with the standard $k-\varepsilon$ model of turbulence to solve the two-dimensional flow and dispersion for various aspect ratios of the canyon. Comparison of CFD with experimental data was encouraging. Jeong and Andrews (2002) also used the standard $k-\varepsilon$ for deep canyons and weighted their results with both reduced and full-scale experiments. Chan *et al.* (2002) compared the standard, the RNG and the realizable $k-\varepsilon$ turbulence models with wind tunnel concentration measurements and argued that the RNG $k-\varepsilon$ presented better performance. Large Eddy Simulation in street canyons is also reported in the literature (Walton and Cheng, 2002). At the same time, new field and wind tunnel experiments were conducted, partly through initiatives like the TRAPOS (<http://www2.dmu.dk/AtmosphericEnvironment/trapos>) project, providing new datasets for code evaluation. Such experimental datasets are also used in the current study, to assess the Reynolds Stress Model (RSM) performance in the street canyon flow compared to the standard and the RNG based $k-\varepsilon$ models, which are much more common than the RSM. For a complete review on street canyon flow and dispersion and relevant references, the reader is referred to Vardoulakis *et al.* (2003).

2. METHODOLOGY

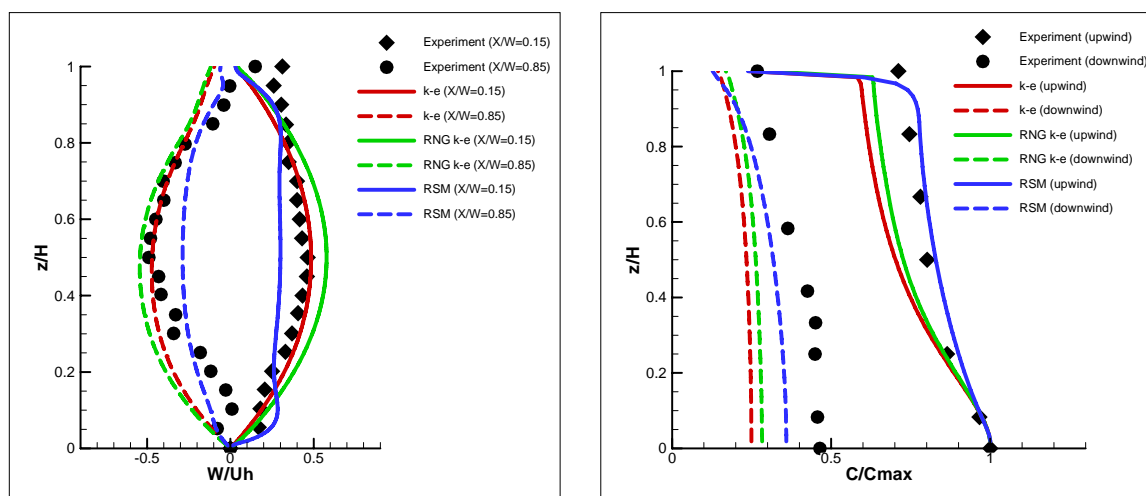
The CFD code PHOENICS, solving the Reynolds Averaged Navier Stokes (RANS) equations for the mean flow coupled with a turbulence closure model, is used for the flow calculations. Concentration is computed from its own transport equation. The code uses the finite volume and staggered grid techniques, the hybrid numerical scheme and the SIMPLEST algorithm to solve the resulting equations. A variety of turbulence models is offered, among which the standard $k-\varepsilon$, the RNG $k-\varepsilon$ and the Reynolds Stress Model (RSM) are tested. RSM was, in theory, expected to provide more accurate results, since it does not have the limitation of assuming isotropic turbulence. For more information on the solved equations and the turbulence models, the reader is referred to the online PHOENICS documentation (<http://www.cham.co.uk/website/new/top.htm>).

The reference case examined here is two-dimensional in the $x-z$ plane, where x is the free flow axis normal to the street and z the vertical one. The width W and the height H of the canyon is 20 m, hence the aspect ratio is 1. The flow is allowed another 20 m before and after the canyon to balance with the boundary conditions and the flow field expands until the top of the boundary layer, 100 m above the roofs, having a free stream velocity of $U_{ref} = 5$ m/s. The resulting 60×120 m² domain is discretized as a non-uniform structured grid, refined near the smooth solid surfaces. Starting with a 36×36 cells mesh and refining up to the very dense 288×288 cells, full grid independency is achieved with the 216×216 cells mesh, resulting in a typical non-dimensional distance from the wall $y^+ = 150$ above the roofs, small enough to apply the wall functions correctly. Inlet boundary conditions above the roof level consist of a typical urban boundary layer velocity profile, while for the turbulent kinetic energy k experimental values of real urban boundary layer are used (Huber, 1989). In the case of RSM, the main Reynolds stresses are provided as a percentage of k , while the shear Reynolds stress as analogous to the local velocity gradient. Sensitivity analysis was carried out for all inlet conditions. Relaxation factors were chosen to attain the lower errors possible and computation was stopped after achieving machine accuracy in all cases. To cope with different experiments examined, modifications of the above-mentioned parameters were applied.

The concentration field is directly related to the flow, since the pollutant is considered to be passive, thus making our interest on the flow field more direct. The pollutant is released from a specific cell close to the street at the centre of the canyon. Sensitivity analysis revealed that the horizontal position of the pollutant source does not play a significant role, while the vertical one does. Concentration results are non-dimensionalised as $C^* = C\rho U_{ref}HL/Q$, where C (kg/kg) is the pollutant mass fraction, ρ (kg/m³) the density, L the length of the canyon (1m for our two-dimensional calculation) and Q the source strength (kg/s).

3. RESULTS AND DISCUSSION

The reference case results are compared (Figure 1) with water-channel mean-flow measurements, obtained from Baik and Kim (2002). In Figure 2, comparison with wind tunnel concentration measurements from Hoydysh and Dabberdt (1988) is presented. New simulations were performed for this case, with aspect ratio $H/W = 1.25$ and free stream velocity 2 m/s, to reproduce the experimental data. In both cases the simulations were executed in full scale and grid independent results are presented.



Figures 1,2. Figure 1 (left) shows the normalized vertical velocity profiles upwind (at $X/W = 0.15$, where X is the horizontal distance from the upwind building) and downwind ($X/W = 0.85$) of the canyon. The vertical velocity W is normalized by the horizontal velocity U_h at the top of the canyon, in the middle of the buildings. The height z is normalized with the building height H . Experimental data are extracted from Baik and Kim (2002). Figure 2 (right) shows the concentration profiles at the upwind and downwind building walls. Concentration for each data set is normalized with the maximum concentration at the upwind side.

The RSM proved to be very sensitive to the relaxation factors and in some cases acceptable convergence was impossible to reach, especially with very dense meshes. Also, the computational time is much more (of the order of 10 times), mainly because of the lower relaxation factors required compared to the $k-\epsilon$ models. It should be noted that the non-dimensionalization with U_h in Figure 1, incorporates the uncertainty of determining U_h in a region where its gradients are very high. In spite of this, the $k-\epsilon$ model (red line) performs very well in the specific case, whereas the RNG $k-\epsilon$ slightly overpredicts the circulation strength. RSM has better performance only near the street canyon boundaries.

Similarly, the non-dimensionalization with C_{max} at Figure 2 might cover differences in absolute values. Despite this, the RSM seems to have better performance here, but we must take into account that three dimensional effects of the wind tunnel experiments are believed to have resulted in higher experimental values, as is commented by Walton and Cheng (2002). Three-dimensional effects are probably the reason that all three models appear to underpredict the concentration at the downwind building.

Hoydysh and Dabberdt (1988) also gave a rough estimate of the full-scale average ascending/descending velocity of the flow, which was about 0.25 m/s in each case with an error of the order of 40%, while the CFD results yield about 0.19 m/s for the RNG $k-\epsilon$ and the RSM models and about 0.16 m/s for the $k-\epsilon$.

An attempt was also made to assess the performance of the three turbulence models against the field data from DePaul and Sheih (1986). The real case geometry was reproduced ($H_{upwind} = 33.5$ m, $H_{downwind} = 40$ m, $W = 24.5$ m, rough walls) and the RSM had the worst behaviour, predicting two counter-rotating vortices inside the canyon, while the experiment had only one. All the models underpredicted the strength of the vortex, with the RNG $k-\epsilon$ performing slightly better than the standard $k-\epsilon$.

In Figure 3, CFD results are compared with experimental values from another wind tunnel study. Non-dimensional mean horizontal velocity U is plotted at the upwind and downwind sides of a canyon with $H/W = 1$ and rough walls. Experimental data are extracted from Kovar-Panskus et al. (2002). For this case, new CFD computations were performed, with $U_{ref} = 8$ m/s and sand-grain roughness $\epsilon_s = 1$ m, according to the scaling of the wall roughness elements described by Kovar-Panskus et al. (2002). Sensitivity analysis on this parameter showed no alteration of the conclusions reached. CFD was performed in full scale and while grid-independency could be achieved with the $k-\epsilon$ models, that was not the case with the RSM; hence RSM results presented here are those of the mesh that achieved the best agreement with the experimental data.

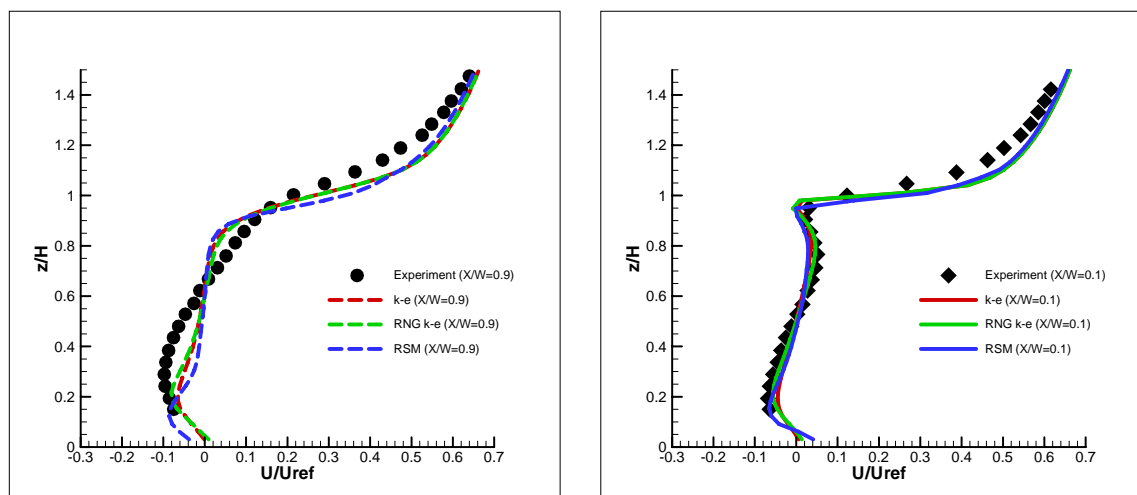


Figure 3. Non-dimensional horizontal velocity profile, at downwind (left) and upwind (right) side of a canyon with rough walls. X is the distance from the upwind building and z/H the non-dimensional height.

From Figure 3, the RNG $k-\epsilon$ model seems to have the best performance, with the $k-\epsilon$ being very close. All models appear to underpredict the strength of the vortex though and this needs further investigation.

The same experiment was conducted with an aspect ratio of $H/W = 0.5$ and results were presented from Sahn *et al.* (2002), along with predictions from various CFD codes using the $k-\epsilon$ model. New simulations were performed to compare with this case and conclusions were similar to those of Figure 3, namely a better performance of the RNG $k-\epsilon$ model, while the strength of the main vortex was still underpredicted by all three models. The RSM had convergence problems in this case.

From Figures 1, 2 and 3 it is deduced that the main mean flow characteristics and the concentration values inside the street canyon are reproduced with adequate precision from the CFD code for general purpose studies. Having established this, a real street canyon simulation was performed.

El. Venizelou avenue, the heaviest traffic street of Aghia Varvara city, was modelled due to the interest of the local authorities. Aghia Varvara is a small pretty suburb of Athens, with low buildings, having an average height of about 12 m at each side of the 24 m wide El. Venizelou avenue. Traffic counting at rush hour yielded about 1200 cars (from which about 12% of non-catalytic ones), 20 heavy vehicles, and 70 motorcycles per hour. Based on emission factors for various categories of vehicles from UK NAEI emissions inventory (<http://www.naei.org.uk/emissions/index.php>), each pollutant's source strength can be calculated. Simulation results (Figure 4) are obtained with the use of the RNG $k-\epsilon$ model. The two sources height is 20 cm. Based on the CFD results and the above mentioned calculations, maximum concentration C_{max} for CO is 2,7 mgr/m³, well below the 20 mgr/m³ limit and C_{max} for NO_x is very close to the limit of 0.4 mgr/m³, but we must take into account that this is the worst scenario for the heaviest traffic street of the city.

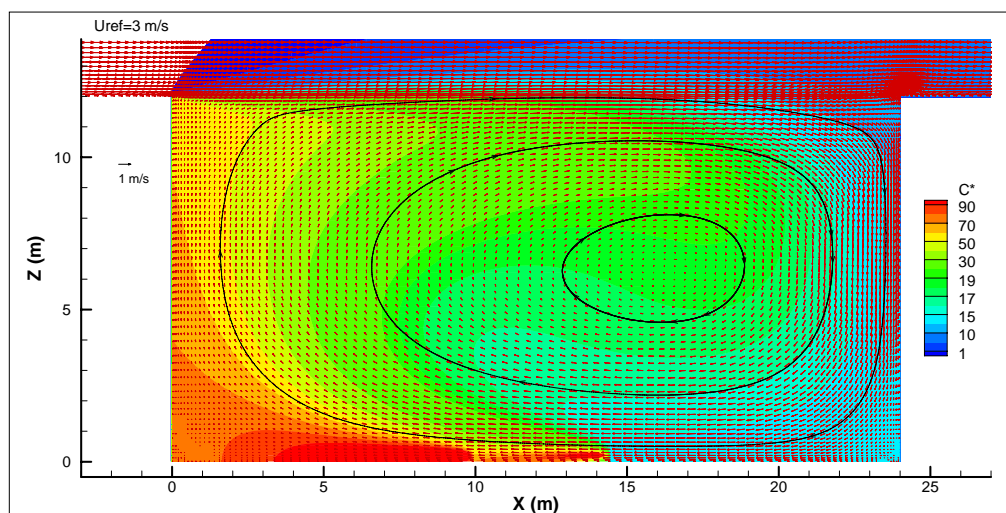


Figure 4. Fluid flow and pollutant dispersion in a real street canyon of Aghia Varvara city with $H/W = 0.5$. Non-dimensional pollutant concentration contours are plotted, along with the velocity vectors and chosen streamtraces. For this simulation, a 216×158 cells mesh was used.

4. CONCLUSIONS

CFD has proved capable of coping with real street canyon flow and pollutant dispersion. Regarding the turbulence models, all of them systematically underpredict the strength of the main vortex in four of the five experiments, with the RNG $k-\epsilon$ performing slightly better, while at the water channel experiment the standard $k-\epsilon$ gives the best results. RSM computations take much more time to perform and have convergence problems in some cases. The Reynolds Stress Models need further development.

5. ACKNOWLEDGEMENTS

This work was supported by the authorities of the municipality of Aghia Varvara Attikis, Greece.

6. REFERENCES

- Baik, J.J., Kim, J.J., 2002. On the escape of pollutants from urban street canyons, *Atmos. Environ.* 36, 527–536.
- Chan, T.L., Dong, G., Leung, C.W., Cheung, C.S., Hung, W.T., 2002. Validation of a two-dimensional pollutant dispersion model in an isolated street canyon. *Atmos. Environ.* 36, 861–872.
- DePaul, F.T., Sheih, C.M., 1986. Measurements of wind velocities in a street canyon. *Atmos. Environ.* 20 (3), 455–459.
- Fenger, J., 1999. Urban air quality. *Atmos. Environ.* 33, 4877–4900.
- Hassan, A.A., Crowther, J.M., 1998b. Modelling of fluid flow and pollutant dispersion in a street canyon. *Environmental Monitoring and Assessment* 52, 281–297.
- Hoydysh, W.G., Dabberdt, W.F., 1988. Kinematics and dispersion characteristics of flows in asymmetric street canyons. *Atmos. Environ.* 22 (12), 2677–2689.
- Huber, A.H., 1989. The influence of building width and orientation on plume dispersion in the wake of a building. *Atmos. Environ.* 23, No 10, 2109–2116.
- Hunter, L.J., Johnson, G.T., Watson, I.D., 1992. An investigation of three-dimensional characteristics of flow regimes within the urban canyon. *Atmos. Environ.* 26B, 425–432.
- Jeong, S.J., Andrews, M.J., 2002. Application of the $k-\epsilon$ turbulence model to the high Reynolds number skimming flow field of an urban street canyon. *Atmos. Environ.* 36, 1137–1145.
- Kovar-Pankus, A., Louka, P., Sini, J.-F., Savory, E., Czech, M., Abdelqari, A., Mestayer, P.G., Toy, N., 2002. Influence of geometry on the mean flow within urban street canyons – a comparison of wind tunnel experiments and numerical simulations. *Water, Air and Soil Pollution: Focus* 2, 365–380.
- Sahm, P., Louka, P., Ketzler, M., Guilloteau, E., Sini, J.-F., 2002. Intercomparison of numerical urban dispersion models – part I: street canyon and single building configurations. *Water, Air and Soil Pollution: Focus* 2, 587–601.
- Sini, J.-F., Anquetin, S., Mestayer, P.G., 1996. Pollutant dispersion and thermal effects in urban street canyons. *Atmos. Environ.* 30 (15), 2659–2677.
- Vardoulakis, S., Fisher, B.E.A., Pericleous, K., Gonzalez-Flesca, N., 2003. Modelling air quality in street canyons: a review. *Atmos. Environ.* 37, No. 2, 155–182.
- Walton, A., Cheng, A.Y.S., 2002. Large-eddy simulation of pollution dispersion in an urban street canyon – Part II: idealised canyon simulation. *Atmos. Environ.* 36, 3615–3627.

ADAPTATION OF PRESSURE BASED CFD SOLVERS TO URBAN HEAT ISLAND CONVECTION PROBLEM

Gergely Kristóf, Norbert Rácz, Miklós Balogh

Department of Fluid Mechanics, Budapest University of Technology and Economics, Budapest, Hungary

ABSTRACT

General purpose CFD solvers are frequently used in small scale urban pollution dispersion simulations involving no extensive vertical flow. Vertical flow, however, plays an important role in the formation of urban heat island induced country breeze, which has a great significance from the point of view of ventilation of big cities. Effects of atmospheric stratification must be taken into account in such simulation studies. A general purpose CFD software has been adapted to simulate atmospheric flow induced by urban heat island effect in order to take advantage of high flexibility in geometrical resolution and meshing. Compressibility and thermal stratification effects were taken into account by utilizing a novel system of transformations to the field variables and by adding the consequential source terms to the standard set of transport equations. Measured velocity and temperature profiles together with flow pattern visualisations from small scale laboratory experiments are used for validation of the mathematical model.

1. INTRODUCTION

Application of general purpose CFD solvers have many advantages such as: more accurate description of the surface, high flexibility in meshing, application of effective numerical techniques, easy implementation of model refinements, parallel computing. These highly developed codes would expect much more application in meteorology for micro-scale modelling and also in environmental research if the compressibility effects caused by vertical flows in the atmosphere could be included into the model. Motivation of the present model development came from a group of researchers dealing with urban climatology (Unger J., 2004), and we think that the results can be of benefits in several other areas of atmospheric simulation like modelling local winds or modelling dispersion of pollutants emitted by chimneys or cooling towers of power plants or modelling atmospheric gravity wave phenomena.

Most CFD solvers have compressible flow option, which means, that the air density is taken into account as a function of local pressure and temperature through the ideal gas law. This option, however, does not allow effective simulation of buoyancy driven atmospheric flow due to the severe limitation on the magnitude of time steps. In those cases when density depends only on temperature, ideal gas law with constant pressure, or Boussinesq approximation with constant thermal expansion coefficient can be used. Potential temperature formulation allows the application of incompressible gas models. As the potential temperature in standard atmosphere is a linear function of vertical coordinate, it leads to a parabolic vertical pressure profile and thus causes several order of magnitude difference between horizontal and vertical components of the pressure gradient vector, which can give rise to numerical instabilities in pressure based CFD solvers.

In meteorological models of local atmospheric circulations some variations of boundary layer equations with hydrostatic approximation to the vertical component of momentum equation are commonly used. Numerical solution is usually obtained by purpose developed solver (Yoshikado, 1992; Lu et al., 1997; Kurbatskii, 2001). If micro-scale details of the flow field, such as transport of pollutants in urban street canyons, are investigated then meso-scale models with nested CFD sub-models are usually employed. The drawback of this method is the interpolation of variables between grid interfaces with different resolution which is the source of numerical errors and model uncertainties (Sarma et al., 1999). Our purpose is to reformulate the mathematical model in a commonly used CFD solver in order for micro- and meso- scale flows in one common system to be analyzed, in such a way, that the micro structures could be studied by a simple local grid refinement process.

2. METHODOLOGY

The mathematical relation between the absolute physical quantities and the field variables used in the CFD solver are described by a set of transformation. The transformation formulae are based on the standard ICAO (Manual of the ICAO Standard Atmosphere, 1993) temperature and pressure profiles (Eq.1 and 2) and an approximate exponential function for the density profile which allows the simplification of some of the transformation expression (Eq.3).

$$\bar{T} = T_0 - \gamma z \quad (1) \quad \bar{p} = p_0 \left(\frac{T_0 - \gamma z}{T_0} \right)^{\frac{g}{R\gamma}} \quad (2) \quad \bar{\rho} = \rho_0 e^{-\zeta z} \quad (3)$$

z denotes the vertical coordinate, $\gamma = 0.65^\circ\text{C}/100\text{ m}$, $T_0 = 288.15\text{ K}$, $p_0 = 1.01325 \cdot 10^5\text{ Pa}$, $\rho_0 = 1.225\text{ kg/m}^3$, $g/(R\gamma) = 5.2553$, $\zeta = 10^{-4}\text{ m}^{-1}$. Note that, the above density profile approximates the standard profile within 0.4% error bound if $z < 4000\text{ m}$, but the error increasing rapidly at higher altitudes. We employ a transformation defined by (Eq.4-8).

$$T = \tilde{T} - T_0 + \bar{T} \quad (4) \quad p = \frac{\bar{p}}{\rho_0} \cdot \tilde{p} + \bar{p} = e^{-\zeta z} \cdot \tilde{p} + \bar{p} \quad (5) \quad \rho = \tilde{\rho} - \rho_0 + \bar{\rho} \quad (6)$$

$$z = -\frac{1}{\zeta} \text{Ln}(1 - \zeta z) \quad (7) \quad w = \frac{\rho_0}{\bar{\rho}} \tilde{w} = \tilde{w} e^{\zeta z} \quad (8) \quad \tilde{p} = \rho_0 - \rho_0 \beta(\tilde{T} - T_0) \quad (9)$$

in which, w is the vertical component of the velocity vector, T , p , ρ , z , w denotes absolute physical values and \tilde{T} , \tilde{p} , $\tilde{\rho}$, \tilde{z} , \tilde{w} are the transformed variables used in the simulation software. Unsteady variable density forms of continuity, momentum, and energy equations are solved by the simulation system with Boussinesq's approximation (Eq.9) to the density, in which, β is the cubic thermal heat expansion coefficient of air. In the simulation system \tilde{p} is used only for evaluating the buoyancy force in the vertical component of the momentum equation, in every other place ρ_0 is used instead. Turbulent transport is modeled by the Realizable k - ϵ turbulence model with full buoyancy effects (included in transport equations of both k and ϵ). Exact form of the governing equations can be referred from CFD literature and software manual therefore it is not cited here. Eq.7 and Eq.8 can be derived from the identity of stored mass in a dz high layer of air (Eq.10) and assuming the identity of vertical mass flux in real and transformed system (Eq.11)

$$\rho dz = \tilde{\rho} d\tilde{z} \cong \rho_0 d\tilde{z} \quad (10) \quad \rho w = \tilde{\rho} \tilde{w} \cong \rho_0 \tilde{w} \quad (11)$$

With this transformation the vertical extent of the atmosphere is "compressed" below a well defined limit ($1/\zeta$) therefore \tilde{z} cannot have values higher than $1/\zeta$ (see Eq.7). Conditions described in Eq.10 and Eq.11 ensures good approximation to the continuity and to the horizontal components of the momentum equation. Only the vertical component of pressure gradient needs correction. By assuming hydrostatic equilibrium at high altitudes, which is valid in atmospheric flows, it is possible to derive a source term for the vertical momentum equation which compensates for the vertical component of the pressure gradient:

$$S_w = -\rho_0 \beta g_z (\tilde{T} - T_0) \left(\frac{\rho_0^2}{\bar{\rho}^2} - 1 \right) - \frac{\tilde{p}}{\rho_0} \frac{\partial \tilde{p}}{\partial \tilde{z}} \frac{\rho_0^2}{\bar{\rho}^2} \quad (12)$$

$$S_w = -\rho_0 \beta g_z (\tilde{T} - T_0) \left((1 - \zeta \tilde{z})^{-2} - 1 \right) + \zeta \tilde{p} (1 - \zeta \tilde{z})^{-1} \quad (13)$$

Eq.12 allows the application of arbitrary equilibrium density profile, Eq.13 is valid only with density profile given by Eq.3.

The energy equation and the turbulent transport equations also need to be corrected by additional volume sources which are proportional to the difference between the magnitude of the equilibrium temperature gradient γ and the dry adiabatic temperature gradient $\Gamma = 0.976^\circ\text{C}/100\text{ m}$.

A user defined source term in the energy equation expresses the amount of heat introduced into unit volume of fluid in unit time therefore it has the dimension of W/m^3 . Temperature of vertical air flow follows the adiabatic gradient (Γ). The transformation applied to the temperature field variable (Eq.4) already includes a temperature gradient γ . Amount of heat corresponding to a temperature gradient $\Gamma - \gamma$ must be taken out from the vertical flow, therefore the necessary source term in the energy equation is:

$$S_T = -c_p \tilde{\rho} \tilde{w} (\Gamma - \gamma) \quad (14)$$

In k - ϵ models there is a production term for the turbulent kinetic energy which is calculated proportionally to the vertical component of the gradient of temperature \tilde{T} . This term represents the effect of buoyancy on turbulence and it should be zero if the thermal stratification is neutral, that is, Eq.15 is fulfilled by the absolute temperature. Temperature gradient can be expressed by the gradient of equilibrium temperature profile plus the gradient of transformed temperature (see. Eq.16).

$$\left. \frac{\partial T}{\partial z} \right|_{\text{stable}} = -\Gamma \quad (15)$$

$$\frac{\partial T}{\partial z} = \frac{\partial \tilde{T}}{\partial z} - \gamma \quad (16)$$

From Eq.15 and Eq.16 a source term described by Eq.17 for the turbulent kinetic energy can be derived, in which μ_t denotes the turbulent viscosity and Pr is the turbulent Prandtl number. Note that S_k is negative consequently the introduction of S_k into the model causes a damping effect to the turbulent intensity. Similar correction must be applied to the transport equation of ε (Eq.18).

$$S_k = -\beta g \frac{\mu_t}{Pr} (\Gamma - \gamma) \quad (17)$$

$$S_\varepsilon = -C_{1\varepsilon} C_{3\varepsilon} \frac{\varepsilon}{k} \beta g \frac{\mu_t}{Pr} (\Gamma - \gamma) \quad (18)$$

Here k is the turbulent kinetic energy, ε is the turbulent kinetic energy dissipation, $C_{1\varepsilon}$ and $C_{3\varepsilon}$ can be referred from the CFD literature or software documentation. Effect of Coriolis force can be taken into account either by using rotating frame of reference option or by some further user defined source terms.

3. RESULTS AND DISCUSSION

Reproducible measurement data are available mostly from laboratory experiments. Since laboratory scale experiments on atmospheric flow are based on approximate mathematical description themselves, only partial validation of the above mathematical model is possible on the basis of these data. As a first step experimental studies involving thermal convection in stably stratified medium are looked for.

Urban heat island circulation and also its interaction with sea breeze are investigated by (Cenedese 2003) in water tank with stable thermal stratification created by heated and cooled heat exchanger plates positioned at the top and the bottom of the tank. Thermal convection is generated by a thin layer $D=100$ mm diameter circular electric heater plate placed on the bottom of the tank. Velocity field has been recorded by PIV device at high spatial resolution in the horizontal symmetry plane along with temperature profile measurements above the heater plate.

Comparative CFD simulation has been carried out in FLUENT 6.2 simulation system after implementing source terms (Eq.13, 14, 17, 18) in the form of User Defined Function (UDF). A drawback of laboratory scale modeling is that the value of Reynolds number is several orders of magnitude lower than that of characterizing atmospheric scale flow. Due to the very weak turbulence k - ε model and the corresponding source terms (Eq.17-18) had to be switched off and Large Eddy Simulation (LES) method has been used instead. Variable density effects are not taken into account in the laboratory experiments, therefore source term (Eq.13) included in the vertical component of the momentum equation had to be switched off too, and so are the corresponding parts (Eq.5 and 7) of the transformation system. This way we have got a simplified version of the above mathematical model which still does have the capacity to describe low Reynolds number flow phenomena occurring in stratified liquid with the help of the most important volume source (Eq.14) included into the energy equation.

Results of the LES simulation in comparison of experimental data are plotted in Fig.1-3. x is horizontal z is vertical coordinate z_i denotes the mixing length, u is horizontal w is vertical velocity component U and W are velocity scales, temperature scale is $dT_m=(T_{axis}-T_a)_{z=0}$ in which T_a is the unperturbed (initial) temperature profile. Simulation results agrees well with experimental data both for velocity and temperature field.

4. CONCLUSIONS

General purpose CFD software has been adapted to atmospheric simulation problems involving stratification and compressibility effects. Modifications are formulated in a novel system of transformation together with some additional source terms to the governing equations which are implemented in the form of User Defined Functions in FLUENT simulation system. Simulation comparable to laboratory experiments aimed at the analyses of convection caused by urban heat island effect has been carried out by using a simplified version of the mathematical model. Results are in line with experimental observations both for velocity and temperature fields. Further validation is necessary to full scale atmospheric measurements.

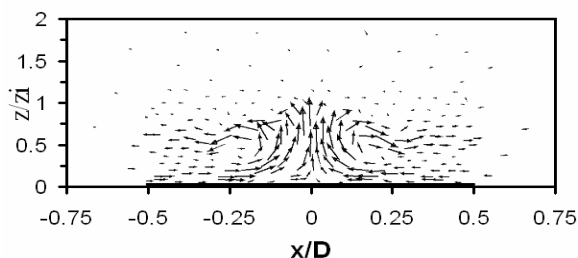


Figure 1. Computed flow field in the symmetry plane (time interval of averaging is 300 s)

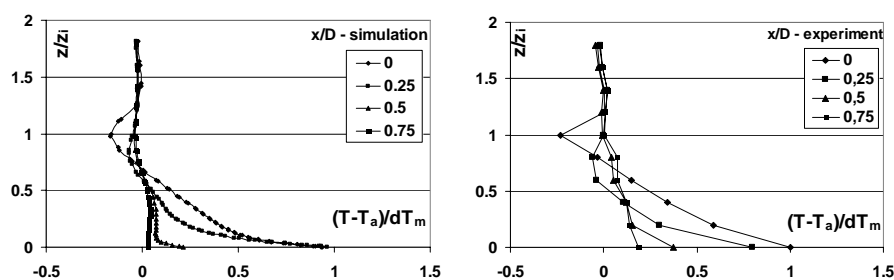


Figure 2. Dimensionless profiles of the temperature perturbation along the axis of the heater plate, LES results (left) and measured data (right)

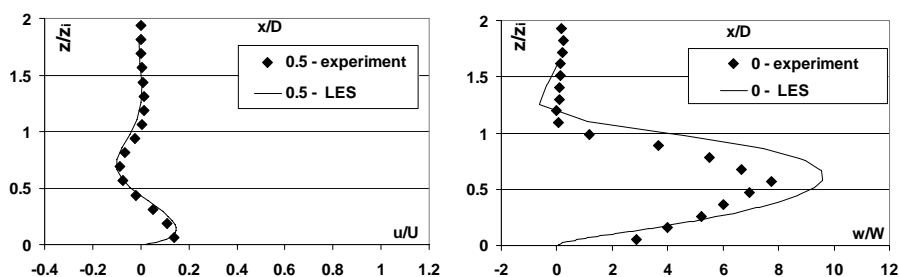


Figure 3. Dimensionless profiles of horizontal (left) and vertical (right) velocity components, symbols: measured data, solid line: LES result

5. ACKNOWLEDGEMENTS

This work has been supported by the Hungarian Research Fund under contract number OTKA T049573 and National Research and Development Program under contract number NKFP 3A/088/2004.

REFERENCES

- Cenedese, A. and Monti, P., 2003. Interaction between an Urban Heat Island and a Sea-Breeze Flow. A Laboratory Study. *J. Appl. Meteorol.* 42, 1569-1583.
- Kurbatskii, A.F., 2001. Computational modeling of turbulent penetrative convection above the urban heat island in a stably stratified environment. *J. Appl. Meteorol.*, 40, 1748-1761
- Lu, J., Arya, S.P., Snyder, W.H. and Lawson Jr, R.E., 1997. A laboratory study of the urban heat island in calm and stably stratified environment. Part II. Velocity field. *J. Appl. Meteorol.* 36, 1392-1402
- Manual of the ICAO Standard Atmosphere / Doc 7488, 1993.
- Sarma A., Ahmad N., Bacon D., Boybeyi Z., Dunn T., Hall M. and Lee P., 1999. Application of Adaptive Grid Refinement to Plume Modeling, Air Pollution VII, WIT Press, Southampton, 59-68.
- Unger J., 2004. Intra-urban relationship between surface geometry and urban heat island. review and new approach. *Climate Research* 27, 253-264
- Yoshikado, H. 1992. Numerical study of the daytime urban effect and its interaction with sea breeze. *J. Appl. Meteorol.* 31, 1146-1163

COMPARISON OF HOURLY AVERAGE CO CONCENTRATION FROM MONITORING AND CFD MODELLING IN A DEEP STREET CANYON

F. Murena and G. Favale

Dipartimento di Ingegneria Chimica - Università degli studi di Napoli "Federico II"
murena@unina.it

ABSTRACT

Hourly average CO concentrations in a real deep street canyon obtained by CFD simulations are reported and compared with data collected during a monitoring campaign. The canyon is $W = 5.8$ m wide, $H = 33$ m high (Aspect Ratio $AR = H/W \cong 5.7$) and $L = 315$ m long. Only one cross-road and a lateral road are present throughout the street length. Orientation of the street axis and hence of the traffic flow is in the direction $70^\circ - 250^\circ$ (i.e.; from E - NE to W - SW). Simulations were carried out assuming different configurations, starting from the ideal street canyon (2D simulations), to a quite real geometry where adjacent roads and cross-roads are considered (3D simulations).

1. INTRODUCTION

During last years the increase of urbanization in many cities caused a worsening in urban air quality. This problem is critical in many cities like Naples that are characterized by high population density particularly in their historical centres. Data reported in literature (Chan and Kwok 2000, Baik and Kim 2002, Vardoulakis et al. 2002, Tsai and Chen 2004) make reference to street canyons with aspect ratio ($AR = \text{height}/\text{width} < 1.7$). However, in historical centres very deep and narrow street canyons ($AR > 1.7$) are often present. Pollutant concentration in deep street canyons can reach very high value due to the limited efficiency of mass exchange with the surrounding atmosphere. In this study we report results referred to a real deep street canyon, via Nardones, situated in the historical centre of Naples. Via Nardones is situated few hundred meters from the seacoast line with its axis oriented from E-NE to W-SW and its geometry is: width $W=5.8$ m, average building height $H=33$ m ($AR \cong 5.7$) and length $L=315$ m (Figure 1). Only one cross-road and a lateral road are present throughout the street length and it is a one-way uphill street. Results of a one-week continuous monitoring campaign of carbon monoxide in this street canyon from 14 to 20 June 2006 are reported (Murena and Favale 2007). Data of the monitoring campaign are compared in this paper with results of 2D and 3D simulations carried out using the CFD programme FLUENT.

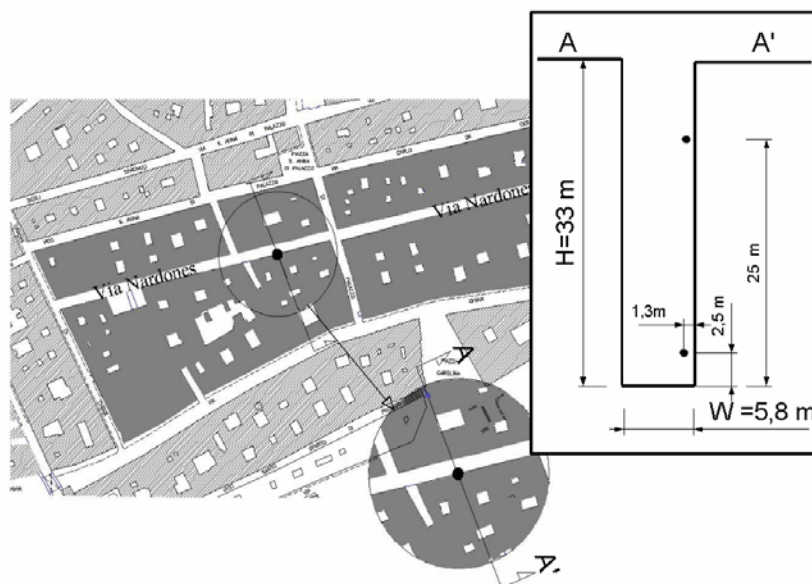


Figure 1 –Plan view of via Nardones and surroundings street (left), cross section of the street canyon (right)

2. METHODOLOGY

2D simulations were carried out assuming the street section in Fig. 1 and the wind direction orthogonal to the street axis. 3D simulations were carried out assuming two different schemes of the real geometry. In the first case we considered only via Nardones and its two parallel streets via Chiaia and via De Cesare (simplified model indicated in figures as FLUENT-S), in the second one we have considered also the

presence of the cross road and the lateral road (complete model indicated in figures as FLUENT-C). We adopted a unsteady RANS model with a $k-\varepsilon$ RNG turbulent closure method. Hourly average values of wind speed and wind direction measured by a permanent station sited at roof top level in the centre of Naples not far from via Nardones are reported in Figure 2. The wind direction is the one the wind is blowing from. The wind inflow velocity profile was approximated using a power law method:

$$v = v_r \left(\frac{z}{z_r} \right)^\alpha \quad (1)$$

where v_r is the reference velocity (Figure 2) measured at the reference height $z_r = 50$ m and $\alpha = 0.28$. The hourly CO vehicular emission rate in the street canyon (Figure 3) was obtained from manual measurements of traffic flow and using COPERT procedure. In CFD simulations the CO input flow was modelled assuming the road surface as an inflow surface from which a mixture of air and CO exits with a constant vertical velocity of 0.1 ms^{-1} in order to model the pollutant rise due to the buoyancy effect. The whole volume of via Nardones was spitted into six sub volumes where volume average values of CO concentration were evaluated. Three volumes are placed in the bottom part of via Nardones, from 0 to 4 meters and are positioned: one between the cross road and the lateral road. The others are placed at east and west sides. In correspondence the other three volumes were defined from 4 m to roof top level. Via Nardones was meshed using a uniform structured grid made by bricks all of the same dimension and the surrounding volume was meshed with an unstructured tetrahedral grid in order to treat the more complex geometry. All data reported make reference to a single day (15 June 2006) which was selected to carry out the comparison between experimental and modelling data.

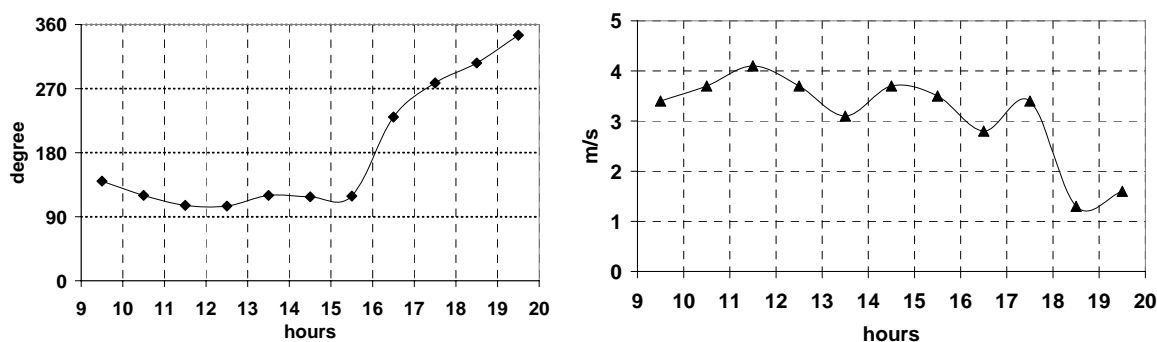


Figure 2 – Hourly average values of: wind direction (left) and wind velocity (right) measured at reference meteorological station (15 June 2006)

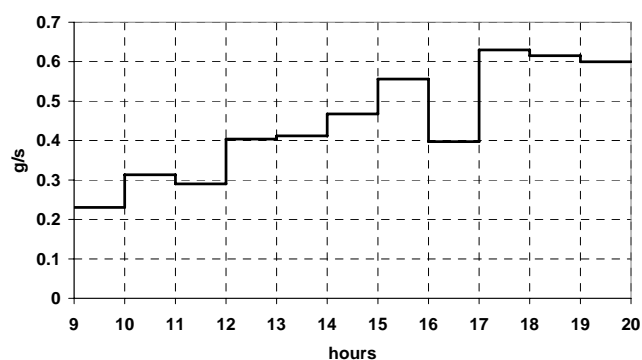


Figure 3 – Vehicular emission rate of carbon monoxide [g/s] as obtained by traffic flow measurements and COPERT procedure (15 June 2006)

3. RESULTS AND DISCUSSION

2D simulations were carried out preliminary but CO concentrations more than ten times higher than those measured were obtained. This result indicates that the 2D model is not apt in this case. Results obtained with 3D simulations show a good correlation with hourly average values measured as reported in Fig. 4 for both models (simplified and complete). In making the comparison it is necessary to remember that

concentration evaluated by modelling are average values in the central bottom volume (from 0 to 4 meter), while the monitoring data are representative of the sampling point at h=2.5 m inside the central bottom volume. Mean square error values reported in table 1 show that the complete model better correlates the measured values. Fig. 5 compares the patterns of the CO emission rate produced by the vehicles in the street canyon and the CO concentration level measured at h=2.5 m. As expected a relationship exists but only to a partial extent. In the same figures results obtained by the 3D models are also reported. It is quite evident in Fig. 5 that both models (FLUENT-S and FLUENT-C) are able to take in count other (meteorological) effects apart from emission rate that are responsible of the CO concentration level in the canyon in the range of hours considered. In particular the simplified model seems more able to follow the hourly variations as measured by the CO analyzer with respect to the complete model. The main discrepancy between the results of simplified model and monitoring data is the evaluation of the hourly average concentration between 15 and 16 hours. In this hour the model FLUENT-S evaluates a peak value while a bottom value was measured by the CO analyzer. On the contrary the complete model does not identify the peak at 13-14 and is not able to predict the increase of concentration in the afternoon from 16 to 18.

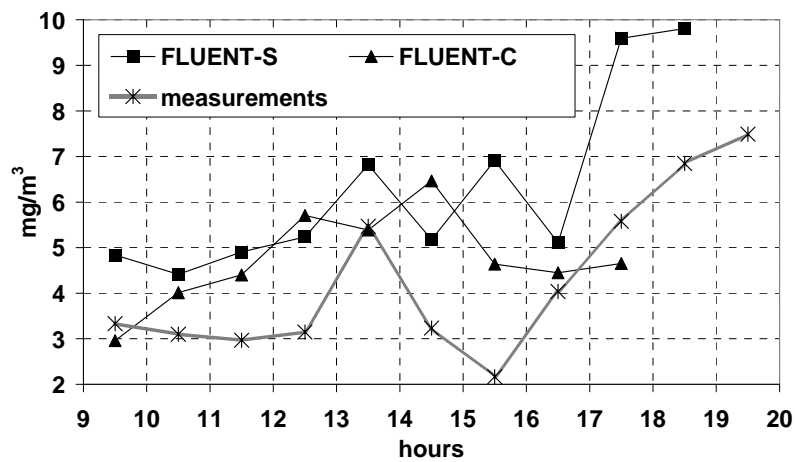


Figure 4 – Hourly average values of CO concentration measured by CO analyzer (x) and evaluated by simplified model (box) and complete model (triangle)

Table 1 – Mean square errors between easurements and model values.

	FLUENT-S	FLUENT-C
$\frac{1}{N} \sum_i^N e_i^2$	6,62	3.01

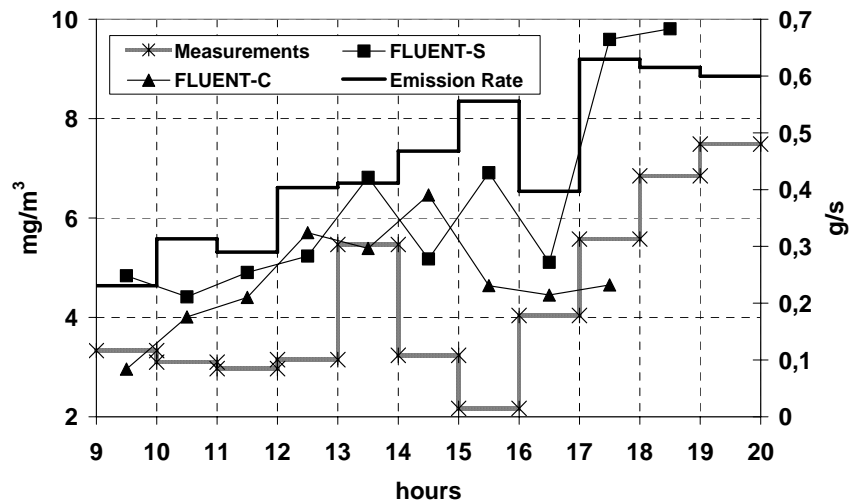


Figure 5 – Hourly average values of: CO emission rate (on the right scale), CO concentration measured by CO analyzer and CO concentration evaluated by modelling (on the left scale).

4. CONCLUSIONS

The 3D models developed are both able to predict the CO hourly average concentration with a reasonable good accuracy and much better with respect to the 2D model. Moreover the models are also quite able to follow the hourly variations taking in count both the variations of CO emission rate and of wind direction and velocity. A better description of the real geometry of the canyon and surrounding streets as developed in the “complete model” did not give, on the whole, a better result with respect to the “simplified model”. More work is necessary to understand how precise the description of the real geometry must be and to reduce the difference between concentration values measured from concentration values estimated by the CFD model.

5. REFERENCES

- Baik, J.J., Kim, J.J. 2002. On the escape of pollutants from urban street canyons. *Atmospheric Environment* 36, 527 - 536
- Chan, L.Y., Kwok, W.S. 2000. Vertical dispersion of suspended particulates in urban area of Hong Kong. *Atmospheric Environment* 34, 4403 - 4412
- Murena, F. and Favale, G. 2007. Continuous monitoring of carbon monoxide in a deep street canyon. *Atmospheric Environment* accepted for publication.
- Tsai, M.Y., Chen, K.S. 2004 Measurements and three-dimensional modelling of air pollutant dispersion in an Urban Street Canyon. *Atmospheric Environment* 38, 5911 – 5924.
- Vardoulakis, S., Gonzalez-Flesca, N., Fisher, B.E.A. 2002. Assessment of traffic-related air pollution in two street canyons in Paris: implications for exposure studies. *Atmospheric Environment* 36, 1025 – 1039

A MEASUREMENT CAMPAIGN IN A STREET CANYON IN HELSINKI AND COMPARISON OF RESULTS WITH PREDICTIONS OF THE CFD MODEL ADREA-HF

P. Neofytou^{*,a}, M. Haakana^b, A. Venetsanos^a, A. Kousa^c, J. Bartzis^a, J. Kukkonen^b

^a*Environmental Research Lab., INT-RP, NCSR Demokritos, Aghia Paraskevi, 15310 Athens, Greece*

^b*Finnish Meteorological Institute, Air Quality Research, Erik Palmelin aukio 1, P.O.Box 503, FI-00101 Helsinki, Finland*

^c*Helsinki Metropolitan Area Council, Opastinsilta 6 A, FIN-00520 Helsinki, Finland*

ABSTRACT

The current study utilises the NO_x concentration data measured from 1 January to 30 April in 2004 in a street canyon in Helsinki. During this period wind speed and direction measurements were also conducted on-site at the roof level. The computational fluid dynamics model ADREA-HF was used to compute the street concentrations and the results were compared with the measurements. The predictions for the selected cases agreed fairly well with the measured data, except for two cases. The main reasons for these disagreements are the negligence of traffic induced turbulence in the modelling, and an under-prediction of ventilation of urban background air from a crossing street. Numerical results illustrate the formation of the vortices in the canyon in terms of the wind direction and speed, and the influence of the characteristics of the flow fields on the concentration distributions.

1 INTRODUCTION

The Computational Fluid Dynamics (CFD) models are useful tools for evaluating the dispersion of pollution, and such models are especially required in urban areas, where buildings and other obstacles to dispersion have to be taken into account. The CFD methods offer the capability of allowing for the effects of the geometry of the surrounding buildings on the flow field, and subsequently, on the concentrations. The importance of accurately describing the geometry of an urban area for pollution dispersion predictions was prominent in the work by Chu *et al.* (2005) who used a Geographic Information System (GIS) software in order to extract the detailed coordinates and heights of the buildings of the area of interest. Parametric studies with respect to different wind speed and wind direction were carried out by Neofytou *et al.* (2006a) in order to study pollution dispersion in an urban area in Bremen, Germany by using the CFD code ADREA-HF.

The measurement campaign that was utilised in this study was preceded by campaigns and the related evaluation of the OSPM model by Kukkonen *et al.* (2001, 2003) in the same street canyon (Runeberg Street) in Helsinki. The numerical predictions were carried out using the CFD code ADREA-HF, which has also previously been used for environmental flow predictions (Neofytou *et al.* 2006a,b).

This study aims to gain insight into how accurately CFD models could be applied in order to evaluate dispersion in a street canyon. Another objective was to help local authorities that are responsible for the urban pollution control to understand the factors affecting air quality in urban environments. For a more detailed description of this study, the reader is referred to Neofytou *et al.* (2007).

2 METHODOLOGY

The measurement campaign was conducted in Runeberg St. in central Helsinki from 19 Feb 2003 to 31 Dec 2004. An overview of the measurement site is given here for readability; for a detailed description, the reader is referred to Kukkonen *et al.* (2001, 2003). The site is located in a street segment having almost uniform building structures over a distance of 175 m. The street level measurements were conducted from a sample intake located at a height of 4.0 m, above the middle of the pavement. The NO_x concentrations, and wind direction and speed data are available with the time resolution of one minute. The traffic volumes for each link in the studied area were obtained from a traffic demand modelling system developed by the Helsinki Metropolitan Area Council.

The methodology consisted in solving the transient, Reynolds averaged, mass and momentum 3D conservation equations for the mean flow and the mass fraction conservation equation for the pollutant dispersion, until steady state conditions were reached. We have constructed a computational domain that includes the geometry of all buildings in the area surrounding Runeberg Street, using actual coordinates provided by the Helsinki Metropolitan Area Council. The numerical grid has a higher spatial resolution within the Runeberg street canyon and near the measurement location, in order to be able to more accurately model the wind field and the spatial concentration distributions.

*Corresponding Author
email: panosn@ipta.demokritos.gr

According to the measured traffic flow data characteristic, less congested weekday daytime traffic in Runeberg Street is approximately 1200 vehicles/hour. The emissions were computed based on the national Finnish emission factors for vehicular traffic. The emission rate of NO_x that corresponds to the traffic volume of 1200 vehicles/hour was computed to be equal to 30.52 µg/m²/s. The total concentrations were subsequently evaluated by adding the measured average urban background concentrations to the values computed by the CFD model (that used the vehicular emissions in the street as input). We utilised the average measured urban background concentration of NO_x in daytime during the period from January to April, 2004, which was 55 µg/m³.

3 RESULTS AND DISCUSSION

3.1 Selection of the numerical receptor points and the evaluation of emissions

For the presentation of the numerical results, we have selected 16 receptor points; these can be classified in four groups, each of which contains four receptors. The receptors in each group have the same horizontal (*x* and *y*) coordinates, and the heights are 4, 10, 15 and 20 m (corresponding, e.g., to the locations from REF1 to REF4, respectively). The abbreviations used for the receptor point groups on the western and eastern sides of the street canyon are RWF and REF (W = western, E = eastern, F = façade of building).

Case	WS (m/s)	WD (deg)	Receptor points							
			Eastern side of the street canyon				Western side of the street canyon			
			REF1	REF2	REF3	REF4	RWF1	RWF2	RWF3	RWF4
Cases with a low wind speed										
1	1	6	393.9	157.5	62.5	14.4	367.8	169.3	72.3	18.6
2	1	186	391.5	168.4	73.0	21.8	364.1	157.8	67.3	19.8
3	1	96	414.2	284.4	227.1	141.2	24.5	16.6	14.8	11.3
4	1	276	14.5	10.8	9.7	7.0	264.2	182.0	156.7	84.5
Cases with a moderate wind speed										
5	3	6	123.3	48.2	19.1	4.6	124.4	58.7	25.6	6.7
6	3	186	127.4	55.4	24.6	7.7	115.7	49.7	21.2	6.4
7	3	96	137.3	93.6	74.1	46.4	8.0	5.2	4.6	3.5
8	3	276	4.2	3.1	2.8	2.0	82.2	56.5	48.8	27.0

Table 1. Predicted concentrations of NO_x (µg/m³) at the selected receptor points. The presented values include only the contribution of the emissions of traffic in Runeberg Street, but not the urban background concentrations.

All receptor points selected are located in the same vertical cross-section, which is perpendicular to the Runeberg Street. The location of the receptor point REF1 is equal to that of the air quality monitoring site in the street canyon. The horizontal distances of this location from the nearest crossing streets, Hesperian Street to the south, and Döbel Street to the north, are 52 and 40 m, respectively. All the selected receptor points are at a distance of 1.2 m from the adjacent building walls.

The computations included only the emissions originated from the vehicular traffic in Runeberg Street (measured urban background concentrations were subsequently added). The traffic emissions in Hesperian Street were evaluated to be on the average less than 10 % of those in Runeberg Street, and the emissions from Döbel Street are negligible.

3.2 Comparison of predicted and measured concentrations

The comparisons were carried out assuming various meteorological cases in terms of the roof level wind speeds and directions, as presented in Table 1. The computations were performed only for the NO_x concentrations; the ambient temperature and solar radiation do not therefore influence the results. The main objective was to select a wide variety of various conceivable flow conditions. We have addressed computed concentrations averaged within 15 minutes. The averaging period was selected to be fairly short (instead of the commonly applied hourly period), (i) in order to include the short-term temporal variations of concentrations, and (ii) in order to select more accurately the cases that corresponded to the selected wind speeds and directions used in the model computations.

Two groups of cases were defined; these correspond to the wind speeds of 1 and 3 m/s. The latter value is approximately the most frequently occurring wind speed at the site, and the low wind speed case represents more unfavourable cases in terms of air quality. Each wind speed group contains four cases that correspond

to the wind directions of 6, 186, 96, and 276°. The directions of 6° and 186° correspond to the wind directions parallel to the Runeberg Street, whereas the directions of 96° and 276° are perpendicular to the street.

The results of the comparison are presented in Figure 1. The observed NO_x concentrations are medians of the observed normalised concentrations. The predicted results were computed as the sum of ADREA-HF predictions and the average urban background concentration (55 µg/m³).

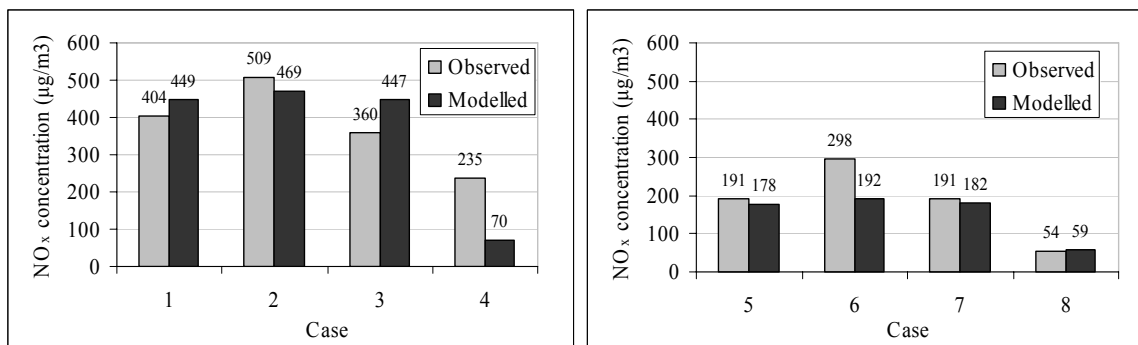


Figure 1. The predicted and observed NO_x concentrations at the receptor point REF1.

The predictions agree fairly well with the measured data, except for cases 4 and 6. In those cases, the measured NO_x concentrations were clearly under-predicted. Cases 4 and 8 represent windward flow with respect to the measurement station, and both the measured and predicted concentrations are therefore lower than for the other wind directions. The relative influence of traffic induced turbulence is largest in low wind speed conditions; and its effect on the concentrations at the street level is probably largest for windward flow conditions. The negligence of traffic induced turbulence in the ADREA-HF code is therefore expected to be the main reason for the under-prediction in case 4. In low wind speed conditions, it is also possible that a stationary vortex is not formed in reality, although it would be evident in the model computations; this would also most likely cause an under-prediction of concentrations by the model.

Cases 2 and 6 represent southerly flow parallel to the street canyon. The under-prediction of street level concentration by the model in case 6 could be caused by an under-prediction of ventilation of relatively more clean urban background air from the crossing Hesperian street. The relative effect of such a ventilation would be expected to be more pronounced for a stronger wind speed. There are also mature deciduous trees within this fairly wide boulevard; however, their effect was not included in the modelling.

3.3 Numerical results

We have investigated the flow fields and concentration distributions for cases 1 and 3 (Table 1) using numerical computations. These cases represent northerly and easterly wind directions, for 1m/s ambient wind velocity. Results for 3m/s ambient wind velocity are qualitatively similar although, as expected, the flow velocities are higher. Due to the nearly symmetric geometry of the street canyon, these cases are expected to illustrate fairly well the commonly occurring flow conditions within the canyon.

The concentration distributions for these cases at the height of the measurement point ($z=4\text{m}$) are presented in Figures 2a-b. The concentrations are higher for the cases with a parallel to the street canyon wind, compared with the corresponding case with a perpendicular wind direction. For perpendicular wind speeds, the increase of concentrations in the leeward side of the canyon is evident.

The horizontal flow fields for these cases at the height of the measurement point ($z=4\text{m}$) are presented in Figures 2c-d. As expected, the horizontal flow velocities are substantially higher for the case with parallel to canyon wind direction, compared to the case with a perpendicular wind. Clearly, the street level air flow in the crossing Hesperian Street is substantially stronger for easterly winds, compared with northerly winds; this tends to increase pollutant dispersion in the vicinity of the crossing of the Hesperian and Runeberg Streets. This effect can also be seen in the horizontal concentration distributions (Fig. 2a-b).

Figures 2e-f show the flow velocity in a vertical plane that contains the receptor points. There is a clear vortex structure for the easterly wind cases; this is the reason for the increased leeward concentrations within the canyon (e.g., Fig. 2a-b). For the perpendicular to canyon wind direction, the vertical velocity component

is substantially increased, compared with the case with parallel to canyon winds. Clearly, the vertical air flow plays a crucial role in the dispersion and advection of pollution; the street level concentrations are therefore higher for parallel to canyon winds, compared with perpendicular winds.

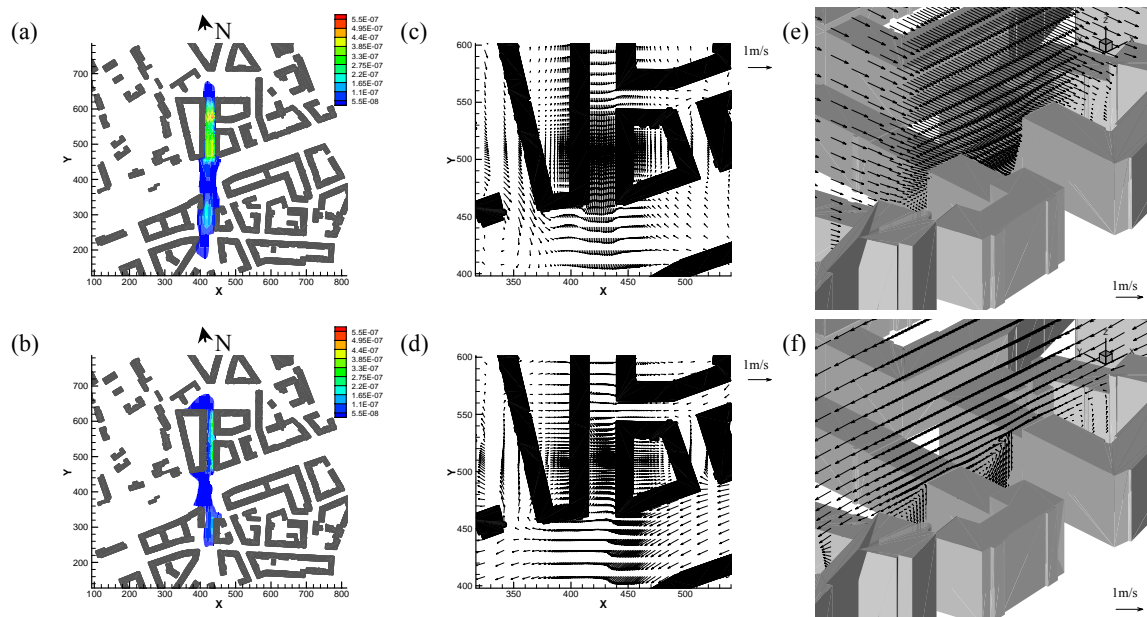


Figure 2. Predicted horizontal distribution of the concentrations of NO_x ($\mu\text{g}/\text{m}^3$) at the height of 4 m for cases (a) 1, (b) 3; Predicted horizontal flow field at the height of 4 m for cases (c) 1, (d) 3; Predicted flow field in a vertical cross-section as a diagonal view that contains the measurement point for cases (e) 1, (f) 3.

4 CONCLUSIONS

This study has utilised the NO_x data from a measuring campaign that was conducted in a street canyon (Runeberg St.) in Helsinki in 2003 – 2004. The predictions regarding 15 min average concentrations agreed with the measured data within $< 25\%$, except for two cases, in which the measured NO_x concentrations were under-predicted. Numerical results were also presented for various example cases; these illustrate the formation of the vortices in the canyon in terms of the wind direction, and their influences on the concentration distributions. The concentrations were higher for the cases with a parallel to the street canyon wind, compared with the corresponding cases with a perpendicular wind direction, irrespective of the wind speed. The main reason for this difference is that the vortex flow structure causes an increased advection and dispersion of street level pollution.

5 ACKNOWLEDGEMENTS

The financial support from the European Union under the contract EVK4-CT-2002-00083 (the OSCAR project) is gratefully acknowledged.

6 REFERENCES

- Chu A.K.M., Kwok R.C.W., Yu K.N., 2005. Study of pollution dispersion in urban areas using Computational Fluid Dynamics (CFD) and Geographic Information System (GIS). *Environ. Modell. Softw.* 20, 273-277.
- Kukkonen J., Valkonen E., Walden J., Koskentalo T., Aarnio P., Karppinen A., Bercowicz R., Kartastenpää R., 2001. A measurement campaign in a street canyon in Helsinki and comparison of results with predictions of the OSPM model. *Atmos. Environ.* 35, 231-243.
- Kukkonen J., Partanen L., Karppinen A., Walden J., Kartastenpää R., Aarnio P., Koskentalo T., Bercowicz R., 2003. Evaluation of the OSPM model combined with an urban background model against the data measured in 1997 in Runeberg street, Helsinki. *Atmos. Environ.* 37, 1101-1112.
- Neofytou P., Venetsanos A.G., Rafailidis S., Bartzis J.G., 2006a. Numerical Investigation of the Pollution Dispersion in an Urban Street-Canyon. *Environ. Modell. Softw.* 21, 525-531.
- Neofytou P., Venetsanos A.G., Vlachogiannis D., Bartzis J.G., Scaperdas A., 2006b. CFD Simulations of the Wind Environment around an Airport Terminal Building. *Environ. Modell. Softw.* 21, 520-524.
- Neofytou P., Haakana M., Venetsanos A., Kousa A., Bartzis J., Kukkonen J., 2007. Computational Fluid Dynamics modelling of the pollution dispersion and comparison with measurements in a street canyon in Helsinki. *Environ. Model. Assess.* (accepted).

LOCAL SCALE NUMERICAL SIMULATION OF AN EXTREME SO₂ POLLUTION EPISODE IN BULGARIA

Prodanova M.¹⁾, Perez J.²⁾, Syrakov D.¹⁾, San Jose R.²⁾, Ganev K.³⁾, Miloshev N.³⁾

¹⁾ National Institute of Meteorology and Hydrology, Bulgarian Academy of Sciences, Sofia 1784, Bulgaria

²⁾ Technical University of Madrid, Computer Science School, 28660 Madrid, Spain

³⁾ Geophysical Institute, Bulgarian Academy of Sciences, Sofia 1111, Bulgaria

ABSTRACT

The US EPA Model-3 system (MM5/SMOKE/CMAQ) is applied for simulation and analysis of an extreme SO₂ episode in the city of Stara Zagora caused possibly by the neighboring thermal power plants (TPPs). A downscaling from horizontal resolution of 81 to 1 km is applied. NCEP Global Analysis Data with resolution 1°×1° is used as meteorological input to MM5. Official SO_x emission inventory for “Maritza-Iztok” TPPs for 2005 is input to SMOKE to produce detailed space/time distribution of the emissions from elevated point sources (SMOKE’s module ELEVPOINT), based on the ambient air characteristics provided by the MM5 calculations. The results of simulations are presented and analyzed in details. They show particularly reasonable from physical point of view behavior, but the calculations do not match the observational data. The reason for this failure is discussed and comparison with the results of similar simulations carried out by other authors is made.

1. INTRODUCTION

Several industrial hot spots exist in Bulgaria and detailed study of every one of them is worth to be done, but often incidents with high pollution levels over an usually relatively clean populated areas cause big political and community concern. Stara Zagora is one of the biggest cities in Bulgaria (300 000 inhabitants) located in the middle of the country. In the summer of 2004 and 2005 some very high level SO₂ pollution events happened thus causing big public complains and even political and judicial consequences. For the moment appropriate monitoring and forecasting system does not exist, there; only ambient air concentrations are measured in several points that is sufficient neither to predict nor even to explain the cases. As far as the mathematical modeling is alternative and supplementing tool according to the EU Framework Directive on Air Quality (96/62/ES) and its daughter directives (see, EC, 1998, EC, 1999, EP, 2002), an attempt to simulate one of these events (July 8-11, 2005) was made, applying one of the most comprehensive modeling tools, mainly the US EPA Model-3 system.

2. DESCRIPTION OF THE POLLUTION EPISODE

Four days, one after another, very high SO₂ concentrations were observed in the afternoon hours over Stara Zagora, leading to appearance of mist and visibility decrease. The concentrations were about and over the alert threshold of 350 µg/m³. Keeping in mind that the high SO₂ pollution covered an area of several square kilometers, it is easy to estimate that tones of sulphur were released over the town. As far as all this happened in summertime and the domestic heating could be not the reason for such pollution, it was supposed that a possible source might be the three thermal power plants (TPPs) disposed at 40 km southeast of the town.

“Maritza-Iztok” TPPs were built in early 70s around a big lignite coal field exploited by open-pit mining. The coals have high sulphur content and this is the reason these TPPs to be the main sulphur polluters not only in Bulgaria but in all southeastern Europe. The emission parameters of these plants are given in Table 1. The total SO_x emission, estimated by the experts of Bulgarian National Statistical Institute, where the official emission reports to EMEP are elaborated, is about 700 000 tones, i.e. about 2000 tones daily. In the last column of Table 1, the percentage from the total Bulgarian SO_x emission is displayed.

Table 1. Emission parameters of “Maritza-Iztok” TPPs

TPP	Latitude	Longitude	Stack					SO _x annual emission, Mg	%
			Nr	Height m	Diameter m	Temperature °C	Flow Nm ³ /h		
Maritza-Iztok 1	25.91	42.16	1	150	6	192	2116000	60139	6
Maritza-Iztok 2	26.08	42.23	1	325	12	192	5400000	310714	50
			2	325	10	178	2900000	173572	
Maritza-Iztok 3	26.01	42.14	1	325	12	192	5150000	156938	16
Total emitted								701363	72

The configuration of Stara Zagora and “Maritza-Iztok” TPPs is given in Fig. 1, together with the position of the measuring stations. In the town itself an air quality monitoring station supplied by automatic gas analyzers is operating continuously. Another monitoring station supplied by DOAS installation is

operating in Mogila village, several kilometers southeast of the town. Other two sampling points are operating in Radnevo and Galabovo – small towns near TPPs.

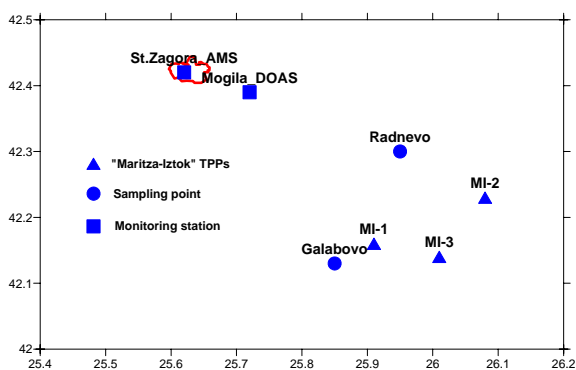


Fig.1. Configuration of polluters and receivers in the region of Stara Zagora

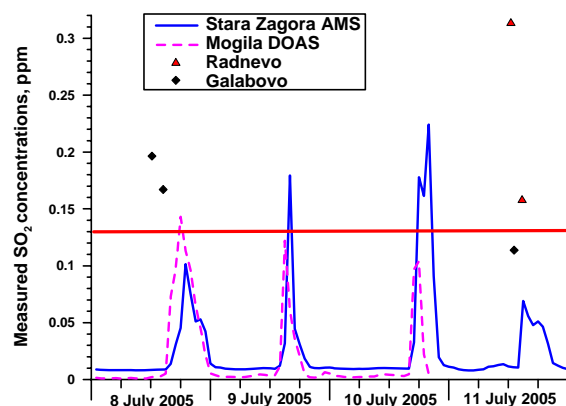


Fig.2. Measured SO₂ concentrations

In Fig. 2 the measured SO₂ concentrations are displayed. The straight line shows the alert threshold for SO₂ ($350 \mu\text{g}/\text{m}^3 = 0.131 \text{ ppm}$). In the sampling points only observed data above and near these values are shown. It is clearly seen that during the entire period on a background of low SO₂ concentration (under 10 ppb) a sharp rises in concentration appear in the afternoon hours. On the base of physical considerations three possible mechanisms can explain this behavior in case it is due to the TPPs:

1. In a stable PBL during night and morning hours the plume from high stacks is keeping high SO₂ concentrations aloft some tens of kilometers from the sources. If a steady flow exists from southeast, such concentrations will exist over the town. The development of convective turbulence in the afternoon hours would drag this pollution to the ground (fumigation). In the evening, the PBL gets stable and pollution does not influence the surface (see, Hurley and Physick, 1991, Palau et al., 2005 and their reference).

2. Meandering of the plume and respective changes of wind direction in the PBL.
3. Combination of both mechanisms.

It is quite interesting that, in spite of availability of such powerful SO_x pollution source in the vicinity of this big town, the pollution episodes are quite rare – several times a year. The reason can be that the synoptic situations favorable for such episodes are rare. In the indicated period, a high pressure system is located southwest of British Isles and moves over the Great Britain, covering the most part of the continent. A low shallow depression initially centered over France moves eastward and remains blocked on the Balkan Peninsula region. The airflow over Bulgaria is from southwest, strong at upper levels (500 hPa), weakening and more southerly at lower levels (700, 850 hPa), changing to westerly at surface. All this means that low and unstable winds are prevailing over the region during the episode.

3. US EPA MODEL-3 SYSTEM

In the frame of the EC 5thFP project BULAIR (<http://www.meteo.bg/bulair>) the Model-3 system of US EPA was recognized as one of the best and up-to-the-science air quality modeling tools. It continues to be developed intensively by a big community of scientists. Its important advantages are that it is free downloadable and can be run on contemporary PCs. In the same time, this is a tool of large flexibility with a range of options and possibilities to be used for different applications/purposes on a range of different regions (nesting capabilities). In the frame of BULAIR, several tasks on regional and local scale were solved making use of this system.

In the system, **MM5** - the 5th generation PSU/NCAR Meso-meteorological Model (Dudhia, 1993, Grell et al., 1994) – is used as meteorological pre-processor, **SMOKE** - the Sparse Matrix Operator Kernel Emissions Modeling System (CEP, 2003) – is used as emission pre-processor, and **CMAQ** - the Community Multiscale Air Quality System (Byun et al., 1998, Byun and Ching, 1999) – is the Chemical Transport Model.

4. COMPUTATIONAL DOMAINS

For this local task meteorological data set from **NCEP Global Analysis Data** for 2005 is exploited (<http://dss.ucar.edu/datasets/ds083.2/>). As far as the space resolution of this data is 1°×1° (i.e. ~100 km) the MM5 nesting capabilities are used for downscaling to 1 km step for a domain around Stara Zagora. The MM5 preprocessing program TERRAIN is used to define five domains with 81, 27, 9, 3 and 1 km horizontal resolution (37×37, 55×55, 46×55, 37×37 and 55×55 grid points, respectively). These five nested domains (referred as *D1*–*D5*) are so chosen that the domain with finest resolution (*D5*) is centered in the middle of the distance between TPPs and the town of Stara Zagora. Lambert conformal conic projection, with true latitudes

at 30°N and 60°N and central point with coordinates 42.30N and 25.85E are chosen. Together with grids definition TERRAIN specifies the raw topographic, vegetative, and soil type data.

5. MM5 SIMULATIONS

In addition to the supplementary information (land use, relief, etc.), CMAQ needs two kinds of input information – meteorology and emissions. MM5 is used here to provide CMAQ with meteorological fields.

For this simulation, MM5 is run firstly on the both rough grids (*D1* and *D2*) simultaneously with “two-way nesting” mode on. Then, after extracting initial and boundary conditions from the resulting fields for *D2*, MM5 is run on the finer *D3-D5* grids as completely separate simulations with “one-way nesting” mode on. Four-dimensional data assimilation (Stauffer and Seaman, 1990) is applied to the external domain *D1* nudging the model results towards the NCEP data. A 23-level vertical structure is chosen.

The first 1 kilometer of the atmosphere, the so called Atmospheric/Planetary Boundary Layer (ABL/PBL), where the dispersion of pollutants mainly occurs, is resolved by 8 levels that seem to be a good presentation. It is complex and difficult task to model PBL in details (in time and space) over non-homogeneous terrain. MM5 provides optionally a number of different PBL and other parameterization schemes. The choice of appropriate scheme is usually made by validation – comparison of model results with the observed air temperature, humidity and wind data. Here, in absence of such data, one of the most comprehensive PBL scheme, namely the **MRF**-scheme, is applied.

The MM5 simulations started at 12:00 of July 7, 2005, and continued up to 00:00 of July 12, 2005. The first 12 hours were added to avoid the spin-up effects. The main impression from the analysis of the wind fields is that during the period calm and non-oriented winds prevail. All this breaks the first hypothetical mechanism able to explain the observed concentration behavior.

The CMAQ preprocessing routine MCIP is used for preparing the CMAQ input from MM5 output.

6. EMISSION INPUT TO CMAQ

Taking into account the behavior of measured SO₂ concentrations shown in Fig 2, it was decided to neglect all diffuse SO_x sources in the region that create the background concentration, and to consider the three TPPs as the only sources of SO_x pollution. This also permitted to run CMAQ over the two inner domains only. The emission input files were constructed by using SMOKE, version 2.0. The purpose was to convert the annually emission inventory data to the resolution needed by the air quality model. CMAQ typically requires emission data on an hourly basis, for each model grid cell, model layer, and for each model species. Consequently, the emission processing involves transforming the emission inventory through temporal allocation, chemical speciation, and spatial allocation. In this case, SMOKE produces detailed space/time distribution of the emissions from elevated point sources (SMOKE's module ELEVPOINT) for each of the TPP stacks as already described in Table 1.

7. CMAQ MODEL RESULTS AND DISCUSSION

The considerations in the previous paragraph allow using zero initial and boundary conditions, set for the 3-km domain only. The nesting capabilities of CMAQ produce such conditions for the finest 1-km domain.

CMAQ is run from 8 to 11 July 2005 day by day, having the final moment concentration fields of the previous day as initial condition for the next day.

In the very beginning of the exercise a relatively rough 6-layer vertical structure of CMAQ was set. Further it was improved by setting up 14 levels, 8 of which in PBL. Gaseous Carbon Bound IV (CB-4) chemical mechanism was chosen for these calculations.

The CMAQ calculated concentration fields for different hours of each day of the period are visualized and analyzed. In Fig. 3, graphs for two afternoon hours from the period are shown. The analysis of all results shows that, in spite of the numerous runs with different parameters, the calculated concentrations in the points with measurements **do not follow the observations**. It must be mentioned, however, that pollution spots near Stara Zagora can be observed every afternoon, but they hardly cover the city.

As a whole, the calculated SO₂ concentration fields have a reasonable behavior from physical point of view. In night hours, in a relatively stable PBL, the pollution released from elevated sources keeps aloft and the whole 1-km domain is not polluted at all. In the day hours, the fast development of turbulent mixing drains the pollution to the surface at distances not far from the stacks, thus forming well expressed plumes with very high concentrations. This is quite reasonable for summer time and is discussed by many authors (Palau et al., 2005, Hurley and Physick, 1991, Luhar, 2002, Luhar and Young, 2002, and others). All they experienced the same problems trying to compare model results for high stacks with observation data.

This behavior of the calculated fields shows that the second physical hypothesis discussed above is possibly in force here. A suitable direction of the wind from TPPs to the town of Stara Zagora is observed each afternoon. These flows form pollution spots in different places around the town, but not over it. In some cases, deviation of the wind direction by several degrees or change of the wind speed by several m/s could

form spots over the town in the right periods. Small changes in the PBL height and turbulent mixing could lead to the same results. Here emerge all difficulties, faced when trying to model local scale phenomena in complex conditions. According to the author's opinion, the main shortcomings come from the MM5 simulations. In spite of being up-to-the-science modeling tool, MM5 is a **model** of the reality and as every model has its limitations. The reality can be (and often is) much more complicated than any model, which is obviously the case here.

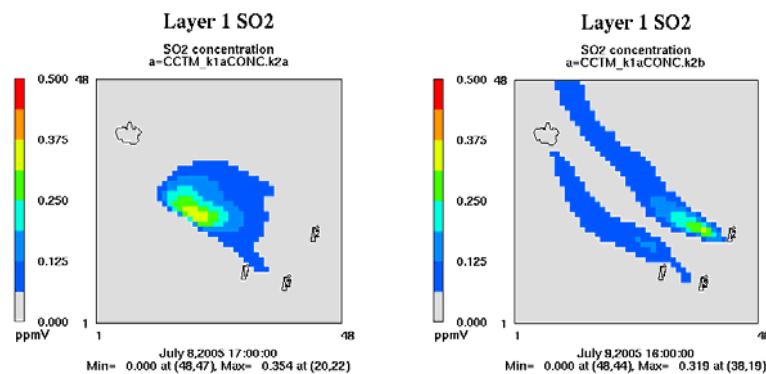


Fig. 4. Examples of SO₂ concentration fields in the period of simulation, 1-km resolution

8. CONCLUSIONS

The applied MM5/SMOKE/CMAQ model system is quite complex and needs validation for each stage of simulation. As no data are available for the vertical structure of the atmosphere and the surface data are not sufficient, the choice of parameterization schemes is based on literature recommendations. The MRF-scheme is known to predict correctly the PBL height and surface temperature and the surface wind in most of the cases (but evidently not in our case).

In general, we conclude that the modeling exercise was reasonable. At this stage it cannot explain quantitatively the observed SO₂ episode in the summer of 2005. For further development validation data for the meteorological model are necessary. In a state of no validation data, numerical experiments can continue in several directions as: increase of models' levels, other parameterization schemes, etc.

9. ACKNOWLEDGEMENTS

This study was made under the financial support of European Commission through the 6thFP Network of Excellence ACCENT (Contract Nr. GOCE-CT-2002-500337) and Integrated Project QUANTIFY (Contract Nr. GOG-003893). Gratitude is due to Cost Action 728 as well.

10. REFERENCE

- Byun, D., Ching, J. (1999) Science Algorithms of the EPA Models-3 Community Multiscale Air Quality (CMAQ) Modeling System. *EPA Report 600/R-99/030*, Washington DC. <http://www.epa.gov/asmdnerl/models3/doc/science/science.html>.
- Byun, D., J. Young, G. Gipson, J. Godowitch, F.S. Binkowski, S. Roselle, B. Benjey, J. Pleim, J. Ching, J. Novak, C. Coats, T. Odman, A. Hanna, K. Alapaty, R. Mathur, J. McHenry, U. Shankar, S. Fine, A. Xiu, and C. Jang, (1998) Description of the Models-3 Community Multiscale Air Quality (CMAQ) Modeling System, *10th Joint Conference on the Applications of Air Pollution Meteorology with the A&WMA, 11-16 January 1998, Phoenix, Arizona*, 264-268.
- CEP (2003) Sparse Matrix Operator Kernel Emission (SMOKE) Modeling System, University of Carolina, Carolina Environmental Programs, Research Triangle Park, North Carolina.
- Dudhia, J. (1993) A non-hydrostatic version of the Penn State/NCAR Mesoscale Model: validation tests and simulation of an Atlantic cyclone and cold front. *Mon. Wea. Rev.* **121**, pp.1493-1513.
- EC (1998) Amended draft of the daughter directive for ozone, *Directorate XI – Environment, Nuclear Safety and Civil Protection*, European Commission, Brussels.
- EC (1999) Ozone position paper, *Directorate XI – Environment, Nuclear Safety and Civil Protection*, European Commission, Brussels.
- EP (2002) Directive 2002/3/EC of the European Parliament and the Council of 12 February 2002 relating to ozone in ambient air. *Official Journal of the European Communities*, **L67**, 9.3.2002, pp. 14-30.
- Grell, G.A., J. Dudhia, and D.R. Stauffer, 1994: A description of the Fifth Generation Penn State/NCAR Mesoscale Model (MM5). *NCAR Technical Note*, NCAR TN-398-STR, 138 pp.
- Hurley, P. and Physick, W. (1991): A lagrangian particle model of fumigation by breakdown of the nocturnal inversion, *Atmospheric Environment*, **25A**(7), 1313–1325.
- Luhar, A. K. (2002): The influence of vertical wind direction shear on dispersion in the convective boundary layer, and its incorporation in coastal fumigation models, *Boundary-Layer Meteorology*, **102**, 1–38, 2002.
- Luhar, A. K. and Young, S. A. (2002): Dispersion moments of fumigating plumes-LIDAR estimates and model simulations. *Boundary-Layer Meteorology*, **104**(3), 411–444.
- Palau, J., Perez-Landa, G., Melia, J., Segarra, D., Millan, M. (2005) A study of dispersion in complex terrain under winter conditions using high-resolution mesoscale and Lagrangian particle models, *Atmospheric Chemistry and Physics Discussion*, **5**, 11965–12030.
- Stauffer, D.R. and N.L. Seaman (1990) Use of four-dimensional data assimilation in a limited area mesoscale model. Part I: Experiments with synoptic data. *Mon. Wea. Rev.* **118**, pp.1250-1277.